AN ABSTRACT OF THE THESIS OF

Abdallah Al-Shehri for the degree of Doctor of Philosophy in Electrical Engineering presented on January 11, 1985.

Title: Capacitive Coupling Compensation Facilitating Single-Pole Switching on Six-Phase Transmission Lines.

Abstract approved: Redacted for privacy

Gerald C. Alexander

In this research, a novel shunt compensation scheme design procedure is developed for unbalanced, untransposed n-phase transmission lines. The main function of the scheme is to reduce the effect of the capacitive coupling on untransposed transmission lines to levels where successful single-pole switching is assured. The analysis procedure is carried out for six-phase transmission lines, but it could be applied to any n-phase system.

In the first part of the research, the arc characteristics for various gap lengths are investigated. The results of the investigation are utilized in developing the transmission line gap recovery characteristics. Equations that express the capacitively-coupled secondary arc current and recovery voltage in terms of line constants and the compensation scheme element values are derived. A digital computer is used to find the optimum compensation element values using these equations. Two

existing transmission line data are utilized as a demonstration of the adequacy of the shunt compensation in reducing the secondary arc current and the recovery voltage. The performance of the compensation scheme under various line conditions is verified by simulating the line and the compensation bank using the Electromagnetic Transient digital computer program.

The results indicate that without the shunt compensation the single-pole switching application to EHV six-phase transmission lines will not be successful. When the shunt compensation scheme is used, the magnitude and rate of rise of the recovery voltage, and the secondary arc current are reduced by more than 50% of their uncompensated values. These results indicate that single-pole switching application to the compensated lines is expected to be successful.

Capacitive Coupling Compensation Facilitating Single-Pole Switching on Six-Phase Transmission Lines.

by

Abdallah M. Al-Shehri

A THESIS

submitted to

Oregon State University

in partial fulfillment of
the requirements for the
degree of

Doctor of Philosophy

Completed January 11, 1985

Commencement June, 1985

APPROVED:

Redacted for privacy

Professor of Electrical Engineering in charge of major

Redacted for privacy

Head of Department of Electrical Engineering

Redacted for privacy

Dean of Graduate School

Date thesis is presented January 11, 1985

Typed by Sarah R. Lillie for Abdallah Al-Shehri

ACKNOWLEDGEMENTS

A deep depth of gratitude is due to Prof. G.C. Alexander the major advisor, for his invaluable guidance and encouragement throughout this work.

I wish also to express my sincere appreciation to the other committee members Prof. J.F. Engle, Prof. J.L. Saugen, Prof. P.C. Magnusson, and Prof. K.H. Funk for their guidance and encouragements.

I would like to thank Prof. H.K. Lauw of the Department of Electrical and Computer Engineering, O.S.U. for his invaluable help in getting access to, and using the Electromagnetic Transient Program (EMTP). My great thanks also for Mr. John Walker, Dr. Scott Meyer, and Dr. T.H. Liu, BPA, Portland, for their assitance in using the EMTP.

TABLE OF CONTENTS

List of Figures

List of Tables

CAPACITIVE COUPLING COMPENSATION FACILITATING SINGLE-POLE SWITCHING ON SIX-PHASE TRANSMISSION LINES

I INTRODUCTION

Investigations by Venkata, et. al. [1], Stewart and Wilson [2,3], and Stewart and Grant [4] have indicated that six-phase transmission is not only feasible but also offers increased transmission capabilities for the same right of way. It becomes more attractive as right-of-way utilization and acquisition problems continue to grow and transmission capacity and economy increase in importance [5]. The benefits of six-phase transmission arise from the smaller voltage between adjacent phases. For example, a three-phase 138 KV phase-to-ground corresponds to 230 KV between the phases; for six-phase, the same 138 KV phase-to-ground corresponds to 138 KV between the phases. Therefore, it becomes easier to insulate one phase from another, and the spacings between the conductors can be smaller.

Six-phase transmission line may also have the following advantages over a three-phase double-circuit line with the same line-to-ground voltage: reduced conductor gradients, lower audible noise levels, lower radio interference levels, and better public acceptance; since it will have smaller size and a lower voltage level. Thus, the net result is that, for a given phase-to-ground volt-

age, a smaller line can be used to transmit a larger amount of power at a better line performance. The only disadvantages of a six-phase system over a three-phase double circuit with the same line-to-ground voltage appear to be: some substation and central system changes that might be needed, system unbalance that might exist due to the fact that it is impractical to fully transpose six-phase transmission lines, and problems in coordination with three-phase lines and systems.

Because of the growing interest in six-phase transmission, several papers [1-14] have reported on different aspects of this new power technology; viz. feasibility, fault analysis, modeling, interconnection with three-phase systems, etc. The application of single-pole switching (SPS) to six-phase transmission lines has not, apparently, been investigated. Using SPS on six-phase transmission lines provides a great opportunity for improvement of stability. The reason for this is the fact that about 93% of the faults on high voltage transmission lines without overhead ground wires are of the single-line-to-ground (SLG) type and that most of these are transitory [15]. Hence, the transmission ability of such lines could be rated by their stability limits for SLG faults, provided that such faults could be successfully cleared and closed by SPS. If SPS is applied to six-phase trans-

mission lines, it would still be possible to transmit about 75% of the system rated power during a SLG fault [16]. Thus, a great gain in the system stability margin is achieved. In addition to improving the dynamic stability in a transmission system, SPS has the following benefits [17]:

1. It reduces the risk of cascading trip-outs for higher order multiple contingency trip-outs.
2. It reduces the reliance on non localized complex stability control.
3. It reduces the cumulative fatigue in the generator-prime-mover shaft caused by the pulsating torque that occurs with high-speed multi-pole reclosure.
4. In some cases, the improved reliability with SPS would permit higher loadings or deter transmission additions.

In SPS the circuit breakers open at both ends of the faulted phase to clear the fault. The opened phase, however, is coupled capacitively and inductively to the sound phases which are still energized at normal system voltage and carrying load current. This coupling, if not compensated, can maintain the secondary arc in the path of the primary fault current and prevent successful single-pole reclosing. The secondary arc is inherently unstable and will eventually be extinguished [16]. How-

ever, for the preservation of the system stability it must be extinguished within 30 cycles [18]. The arc extinction time depends on several factors of which the most important are the secondary arc current and the recovery voltage. The secondary arc current is that which exists after isolating the faulted conductor by opening the appropriate circuit breaker poles. It is much smaller than the primary fault current which exists before opening the circuit breakers. The recovery voltage is the voltage across the fault path after extinction of the secondary fault arc and before reclosure of the circuit breakers [16]. Both the secondary arc current and the recovery voltage have two components corresponding to the two types of coupling mentioned above. The results of studies performed on three-phase systems indicate that the capacitive coupling is the more important [16]. To compensate for the capacitive coupling and therefore to ensure successful SPS on transmission lines, special schemes have been suggested for three-phase systems [19-22]. Knudson [19], and Kimbark [20] introduced a method of reactor compensation for transposed three-phase systems that seems to offer the possibility of reducing the arc current and voltage by neutralizing the capacitive coupling of the line. The proposed scheme was composed of a four-legged reactor bank. Kimbark [16] also inves-

tigated the application of the compensation reactor bank to long three-phase, double-circuit transmission lines. The investigation results revealed that satisfactory reduction in the line capacitive coupling could be achieved using the reactor scheme. In all these investigations, fully transposed, balanced, transmission lines were assumed and the symmetrical component analysis was utilized.

The main subject of this research is to develop a design procedure for designing a shunt compensation scheme that will minimize the capacitive coupling on six-phase transmission lines and hence will assure successful SPS application in the case of a SLG fault. Usually, six-phase transmission lines are not balanced. Not only that, but if six-phase transmission lines are fully transposed, they lose their main advantage; that is, the lower voltage between the phases. Thus, the six-phase transmission lines cannot be transposed; and the simplification assumptions and analysis methods that were used for three-phase transmission lines analysis cannot be applied for six-phase analysis. It is very difficult to analyze untransposed six-phase transmission lines. The complex inductive and capacitive coupling in the line makes it necessary to use a digital computer if reasonably accurate results are to be achieved.

The first part of this research is devoted to the determination of the transmission line secondary arc characteristics. This is not an easy task because not much data could be found on this subject. For this reason, the short gap and long gap arc characteristics are investigated and their data are extrapolated and utilized together with the available transmission line gap arc data to determine the characteristics of the latter.

In the second part of the research, a new method for designing a shunt compensation scheme for six-phase transmission lines is presented. The lumped equivalent capacitive circuit of the transmission line is utilized to express the secondary arc current and the recovery voltage of the line in terms of the line capacitance and the compensation scheme element values. A digital computer program is written to solve the formed current and voltage expressions and to search for the compensation scheme element values that will minimize the capacitive components of the secondary arc current and the recovery voltage. To investigate the effect of the magnetic coupling and to test the performance of the designed compensation scheme, the transmission line together with the scheme are simulated on a digital computer.

Two existing transmission line data are utilized to demonstrate the accuracy of the design procedure and

to confirm the predicted improvement in the line overall performance when the compensation scheme is used. Primary results indicate that using the shunt compensation scheme to reduce the capacitive coupling on six-phase transmission lines will make it possible to use SPS, which is otherwise impossible, on such lines. The results also indicated that an all-inductive compensation bank cannot effectively compensate unbalanced six-phase transmission lines when the unbalance is large. The best compensation scheme for such lines was found to be a reactor bank of tree form with a capacitive neutral. The design procedure was developed in a manner that allows the user to easily test both schemes for any given line parameters; and hence, enables him to judge which one is suitable for that particular line.

II LITERATURE REVIEW

This study can be visualized as comprising two fields of power engineering:

a - Six-Phase Transmission Systems.

b - Single-Pole Switching Techniques.

In order to have a clear idea of what dissertation-related work has been done, it is essential to examine topics related to the above two fields.

2.1 Six-Phase Transmission Systems

Six-Phase transmission has been studied as early as 1971. Most of the early studies were devoted to the analysis and simulation techniques of polyphase transmission systems [6,7]. None of the published six-phase studies has suggested building complete six-phase systems including six-phase substations. It seems that future power systems will continue to be three-phase AC systems with an occasional six-phase link connecting two points. Three-phase-to-six-phase transformers will be needed to connect the six-phase transmission lines to the three-phase systems while all generation will remain three phase. Single-phase transformers or three-phase-to-six-phase transformers can be used to make the connection from three-phase to six-phase systems. fig (1).

Detailed six-phase fault analyses were reported

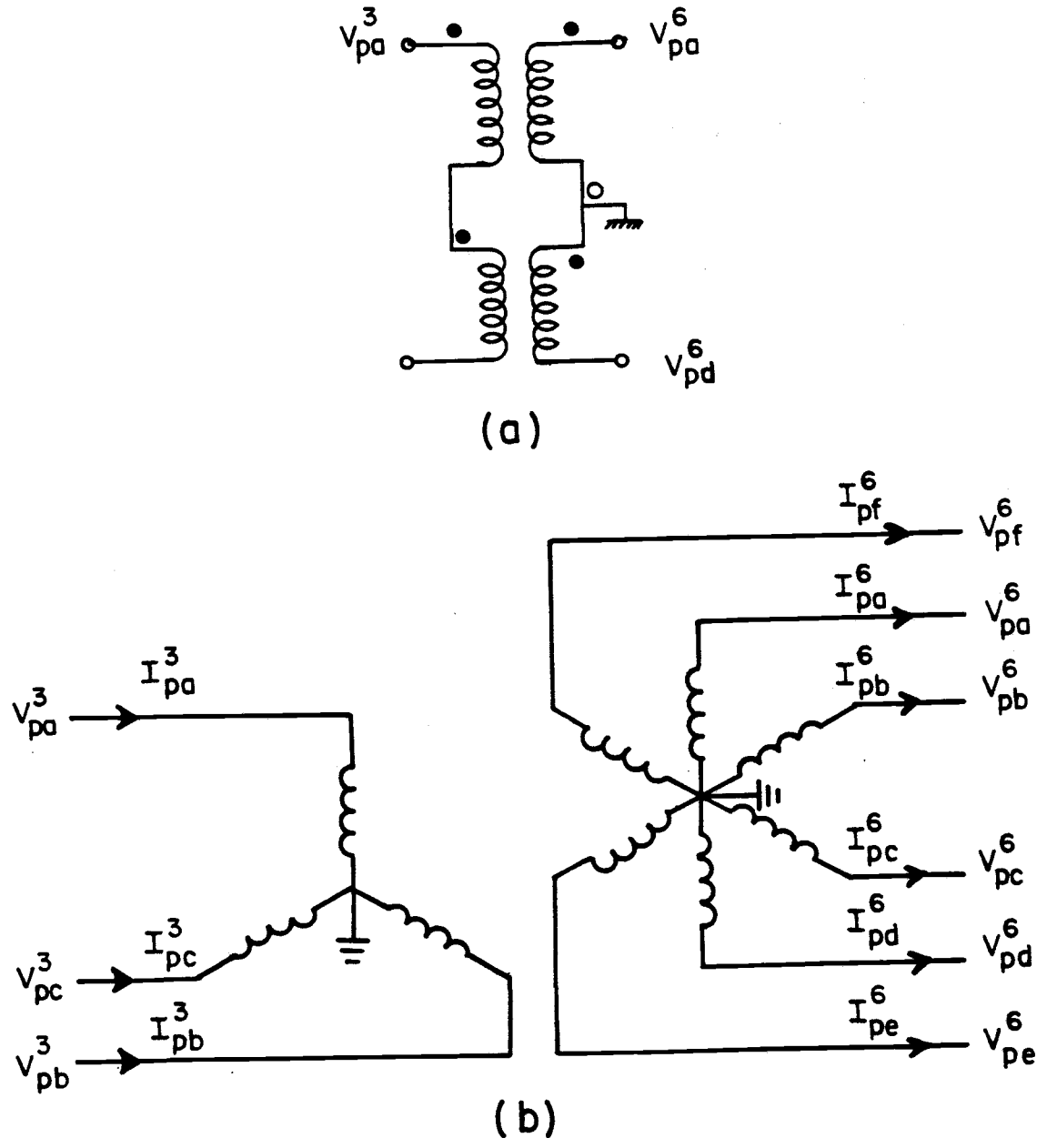

Fig(1) Three-phase-to-six-phase transformers.

a - single-phase transformers used to make three-phase to six-phase connection.

b - Single core three-phase-to-six-phase transformers.

by Bhatt, et. al. in 1977 [8], and Venkata, et. al. in 1982 [5]. A balanced, fully transposed, system was assumed and the symmetrical component theory for six-phase systems was developed. A variety of fault types that could arise on six-phase lines were discussed. The analytical results were presented for all types of significant faults that could occur on a six-phase transmission system.

In 1977 Venkata, and Bhatt [1] performed an economic analysis of six-phase power transmission systems. They developed an economical model and applied it to a 138 KV three-phase/six-phase transmission system. The results were compared with that for an equivalent 138 KV three-phase system. The relative results indicated that the six-phase transmission system concept was economically feasible.

In 1978 a feasibility analysis of high-phase order transmission was conducted by Stewart and Wilson [2]. They concluded that high-phase order lines exhibit line current unbalance characteristics comparable to or better than the three-phase counterparts. It was found that the radio and audible noise were reduced with phase order while ground level electric fields increased with phase order and may be a limiting design parameter at EHV levels. The lower noise level is due to the reduction

in the conductor surface gradient and, hence, the reduction in the corona loss. In moderately heavy rain, the line had 2046 watts of corona loss per conductor when energized as double circuit three-phase as opposed to 338 watts when energized as six-phase with the same phase--ground voltage [11]. Fault overvoltages for six-phase systems can be slightly higher than for a comparable three-phase system while the rate of rise of recovery voltage during fault clearing is less on six-phase systems than for three-phase systems with comparable equivalent short circuit MVA. Terminal insulation levels were found to be slightly higher for six-phase than for three-phase systems.

In 1979 Willems [9], analyzed the interconnection of three-phase and polyphase power systems. He showed that the interconnected three-phase and six-phase power systems could be analyzed either by replacing the six--phase part by an equivalent three-phase element or by replacing the three-phase part by an equivalent six-phase element. Several types of three-phase-to-six-phase transformer connections were analyzed. Special attention was given to the model of the transformers with respect to three-phase and six-phase symmetrical components. Equivalent admittance, impedance, and ABCD parameter models of interconnected three-phase and six-phase

elements were derived.

A study in 1980 by Pearan, Al-Nema, and Zynal [10] was devoted to the diagonalization of the six-phase power transmission system impedance matrix by a real transformation which was a generalization of the alpha-beta-zero transformation. All types of unbalanced short circuits were considered and emphasis was laid upon developing the connections of the component networks for each type of fault.

In 1982 Tiwari, and Singh, Indian Institute of Technology, India, [12] presented a paper in which the various mathematical representations of polyphase components; transmission lines, transformers, and loads suitable for balanced as well as unbalanced network analysis were developed. Employing one of the proposed modeling schemes, the impact of the addition of polyphase lines in an existing three-phase network was investigated for load flow analysis. A study carried out on a test system revealed that when more and more six-phase lines were added in place of existing three-phase (double-circuit) networks, the performance of the overall system was improved in terms of better voltage regulation and transmission efficiency in addition to increased transmission capability.

In 1981, and 1982 the U.S. Department of Energy

[4,11] sponsored a project to construct six and twelve phase transmission line sections and to develop experimental and analytical data for application of high phase order transmission. Variations studied included system operating voltage; insulator and tower designs; system short circuit capacity; circuit breaker closing characteristics with and without surge suppression resistors; line length and parameters; multiple of three-phase and single-phase switching; energization with and without trapped charge; effect of transformers and effect of faults. The tests results confirmed that calculation methods developed for six-phase from three-phase accurately predict noise levels, field strengths, and mechanical behavior of high-phase order.

In 1983 a method of suppressing fault currents and voltage rise in a six-phase power transmission system was proposed by Onogi, et. al. [14]. The main idea of the method was to use transformers with tertiary windings. The windings were connected in series on both the primary and the secondary sides. The neutral was solidly grounded. The two tertiary windings were cross connected through an impedance (Z), so that the summation over the two emf's in the loop composed of the windings became zero in normal operating conditions. The design required the use of two single-phase transformers with

the same number of turns or a three-legged single-phase transformer, fig(2). The fault analysis showed that the fault current at the sending end single line-to-ground (SLG) fault in the proposed six-phase system became approximately half that in the conventional double circuit system.

It is important to point out that most of the six-phase analysis techniques were developed assuming balanced, fully transposed lines where the phase impedance matrix had only two distinct terms; the self and the mutual terms. The primary benefits of six-phase occur because of the reduced voltages between the adjacent conductors due to the sixty degree electrical angle between adjacent phases. If complete conductor transpositions were used, these benefits would be lost. Therefore, if the advantages of high phase order are to be exploited, the best which can be accomplished is a roll transposition where each phase retains its relationship to all others. For six-phase lines, this results in a circulant matrix of four distinct terms, the self and three distinct mutuals [23]. This roll transposition does diagonalize the symmetrical component impedance matrix so that the system is balanced. The full transposition assumption generates an error in the calculations of about $\pm$ 13% [5].

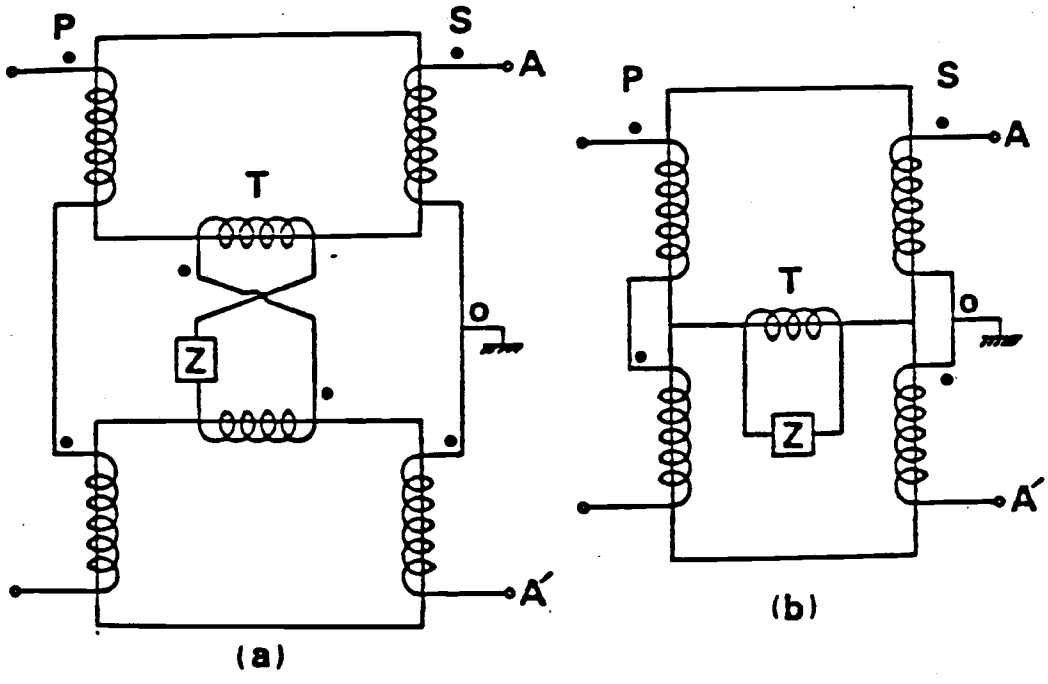

Fig(2) Connection diagrams of the transformers proposed to suppress fault current in a six-phase transmission system.

[Reproduced from reference [14]]

2.2 Single-Pole Switching

2.2.1 General Discussion

The primary condition for using SPS as a means to improve the dynamic stability in a transmission system is that the secondary arc be extinguished within a fraction of a second [19]. The secondary arc current is maintained by the capacitive and inductive coupling between the faulted conductor and the unfaulted conductors which are still energized at approximately normal circuit voltage and carrying load current. Of the two types of coupling, the capacitive coupling is the more important [20]. Its importance increases with increase of circuit voltage. The inductive coupling is proportional to the length of the line and its loading [16]. The possibility of arc extinction is decided by two important factors:

1: The magnitude and rate of rise of the recovery voltage

2: The magnitude of the current to be interrupted, i.e. the current in the secondary arc.

Many studies have been performed to investigate the application of single-pole switching to three-phase single-circuit and double-circuit transmission lines. In 1941 Trainor, Hubson, and Muller, [24], performed extensive field tests on the system of the Public Service

Company of Indiana, Inc. The tests were primarily intended to check the functioning of the relays and reclosing equipment. Oscillographs were stationed at several places along the line to record various quantities including phase currents, phase voltages, and residual currents. The results indicated that on high voltage systems where most transmission line faults were SLG faults in nature, single-pole reclosing provided higher transient power limits than three-pole reclosing. This permitted the transmission of more power over given line sections, and permitted slower speeds of reclosure on very high voltage systems where adequate time allowance for arc clearing was important. It was also, mentioned that the advantages of SPS over three-pole switching were minimized if the transmitted power was kept low enough so that no outages occurred for self-clearing three-phase faults; although there was still the advantage of less shock to the system during the more common single-phase and two-phase fault conditions.

2.2.2 Schemes to Reduce Secondary Arc Dead Time

A method by which the recovery voltage and the secondary arc current of balanced three-phase transmission lines could be reduced was presented for the first time by Knudson [19] in 1962, and Kimbark [20] in 1964. The

main idea of the method was to neutralize the capacitive coupling between the faulted line and the sound phases, using a lumped shunt inductive reactance equal and opposite to the capacitive reactance. The proposed scheme was analogous to the use of a Peterson coil. However, the new scheme would neutralize the capacitance between the phases, amounting to the difference between the positive sequence and zero sequence capacitances, that is, (C_1-C_0), while the Peterson coil neutralizes the capacitance to ground, $3C_0$. Because of imperfect tuning, losses or harmonics, the fault current does not become zero. However, the neutralized current is only 10% to 20% of the unneutralized, capacitively-fed fault current [20]. Knudson also showed that the secondary arc current and the recovery voltage were related mainly through the system's Thevenin equivalent impedance at the fault point.

Peterson, and Dravid [21] in 1967 presented a method of nullifying the capacitive coupling effect for SPS in EHV transmission. The method required the addition of a capacitor, connected across the terminals of each breaker pole, proportional to the parameters of the particular line being switched. Each phase required a capacitance which is essentially $(C_1-C_0)/3$. This provides a current through the fault path of $I_f \underline{/180^o}$, where I_f is the fault current.

In 1976 Kimbark [16] investigated the application of the shunt compensation reactor to 500KV three-phase, double circuit lines. He assumed a balanced transmission line system and used three-phase, symmetrical component analysis. The compensation scheme that was used is shown in fig(38). Because of the unbalance in the phase-to-phase capacitances, it is not possible to compensate a long untransposed line by use of a symmetrical circuit of inductors. To circumvent this problem Kimbark suggested elimination of it by addition of a lumped capacitance of proper value connected between the two outer conductors.

Means by which the reactive component of the secondary arc current could be reduced was investigated by Kimbark [16] using a digital computer. The first method was to discharge the disconnected line by grounding it at both ends. The results indicated that the recovery voltage dropped appreciably but the secondary arc current increased. Thus, single-pole reclosure was unsuccessful. The most promising method for reducing the magnetic coupling was to provide a switch at the midpoint of each of the six conductors. Upon occurrence of a fault, the faulted conductor would first be disconnected at the two terminals and would then be sectionalized by the appropriate midpoint switches. More reduction of recovery

voltage and of residual fault current than those obtained by division of disconnected conductors into two sections could be obtained by division into a greater number of sections. This, of course, requires more switches and would result in lower reliability of operation as well as increased complexity of switch controls.

In 1978 Shperling, Fakheri, and Ware [22] developed a modified four-legged reactive compensation scheme for single-pole switching on untransposed, three-phase, transmission lines. The new scheme was to be used in conjunction with a conventional four-legged reactor, developed by Kimbark and Knudson, at the other end. The modified reactor bank included four low-cost switches whose operations were coordinated with the line breakers. The modified reactor scheme, with associated neutral switch positions for various phase-to-ground faults, is shown in fig(3).

The primary advantage of this scheme is the reduced level of the secondary arc current on unbalanced, untransposed lines compared to that achieved through the use of a four-legged reactor scheme which is designed for balanced systems. The major disadvantage of the proposed method is the reactor switching that is required immediately following single-phase fault clearing. The implementation of this scheme requires extensive additional

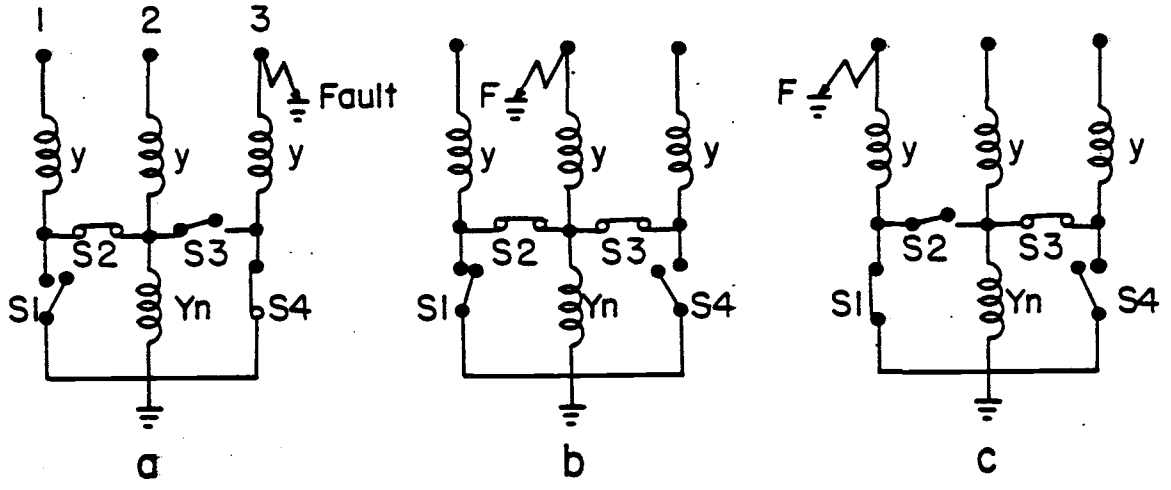

Fig(3) Modified 4-legged reactor bank. Switch positions for various phase-to-ground faults.

relaying for the system.

In 1981 Hasibar, Legate, Brunke, and Peterson [17] investigated the application of high-speed grounding switches (HSGS) to 500 KV single-pole switched lines of the BPA system. They indicated that this method afforded significant economic advantages over the four-legged reactor scheme for 500 KV lines that do not require shunt reactors. For lines on which shunt reactors are to be used for voltage control, a four-legged reactor bank should be considered for SPS. Voltages and currents that the ground switch would be required to interrupt were given for various conditions. Field test results on 122 miles, 500 KV transmission line showed successful application of the HSGS to extinguish the secondary arc.

2.2.3 Field Tests and Digital Analyses of SPS

In 1968 a digital analysis of single-pole switching on EHV lines was performed by Shipley, et. al. [25]. The results indicated that the most economical shunt compensation reactor installation for three-phase systems would be a four-legged reactor bank located at the middle of the line. It showed also that it was undesirable to compensate the line 100% because a small variation in the reactance of the reactors when the compensation is near 100% can cause overvoltages. Calculations made

when the line was compensated near 100% indicated that if a phase-to-ground reactor at the sending end was changed by 2.6% the voltage at the sending end would rise from 49.1 KV to 590 KV. The effect of transposition was also investigated. The results indicated that transposing the lines decreased the recovery voltage and the secondary arc current by a factor of about 25%.

In 1971 Edwards, et. al. [18] verified the results mentioned above for three-phase, fully transposed, 500 KV, 93 miles long transmission lines. The results indicated that for that particular line, without the compensation reactors, single-pole tripping and reclosing within one-half second was unsuccessful. It was shown that with the reactors out, the secondary arc current was greater than 20 amps. The extinction occurred too late and hence the fault arc restruck when the first circuit breaker reclosed. With the compensation reactors connected to the system, the secondary arc current was less than 20 amps, the recovery voltage was less than 59 KV, and the extinction occurred in less than ten cycles. The neutral reactor had a value of 588 ohms and a ten-second rating of 117.5 amps.

In 1974 Balser, and Krause [26] studied the system transients with transposed and untransposed lines in the case of single-pole switching. The system tested

by Edwards et. al. [18] was simulated on a hybrid computer and the results obtained were verified by comparing them with the field test data for the transposed line case. The source was simulated as a balanced set of constant three-phase voltages behind transient reactance X_d'. For the transposed lines the maximum recovery voltage was approximately 10% of the prefault line-to-neutral voltage. The steady state recovery voltage was about 6%. For the untransposed lines the transient recovery voltage reached 35% of the prefault voltage. The steady state recovery voltage was 26%. With the lines untransposed, the neutral reactor value was varied over a wide range but no significant change in the recovery voltage was observed. The effect of unbalanced shunt reactors connected to the outer conductors and the one connected to the middle one was tested. The results indicated that this unbalance had a little effect on the transient and steady state recovery voltages.

In 1977 Lambert, et. al. [27] investigated the effect of transposition schemes, power flow, and other system conditions on the magnitude and characteristics of the secondary arc current of a three-phase, 500 KV, 493 mile long transmission system. The investigation was carried out using a digital computer. The results shown in fig(4) indicate that the secondary arc current was not very

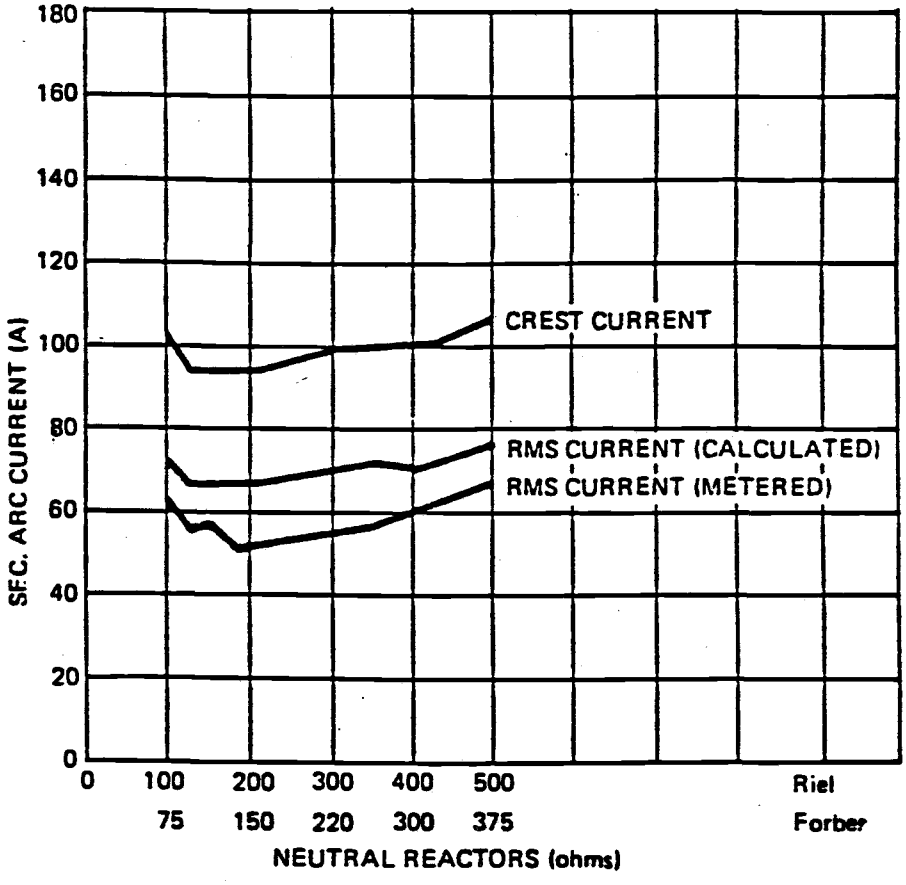

Fig(4) Effect of neutral reactor on secondary arc current with 1000 MW load flow.

[Reproduced from reference [27]]

sensitive to neutral reactor ohmic value. Figure(5) shows the effect of power flow on the secondary arc current. Since the interphase electrostatic coupling was effectively 100% compensated, the secondary arc current was principally due to inductive coupling. With zero power flow the secondary arc current was a result of inductive coupling due to var flow along the line. Fault location also had a significant effect on the magnitude of the secondary arc current. Figure(6) shows the current as a function of fault location with 1000 MW of power flow. The results indicate that the currents are higher with faults located near the line ends. The effect of transposition was also studied. The three transposition types shown in fig(7) were considered. The highest secondary arc current along the line for different conditions is shown in table(1). It is obvious that the most effective transposition type was type 3 which provided one complete transposition of the line. It was observed that the secondary arc current, the recovery voltage, and the sustained and transient overvoltages were significantly less for the transposed than for the untransposed models. The transient and sustained overvoltages resulting from single phase reclosing were significantly affected by the magnitude of the prefault load being transferred. This is shown in fig(8). It was also observed

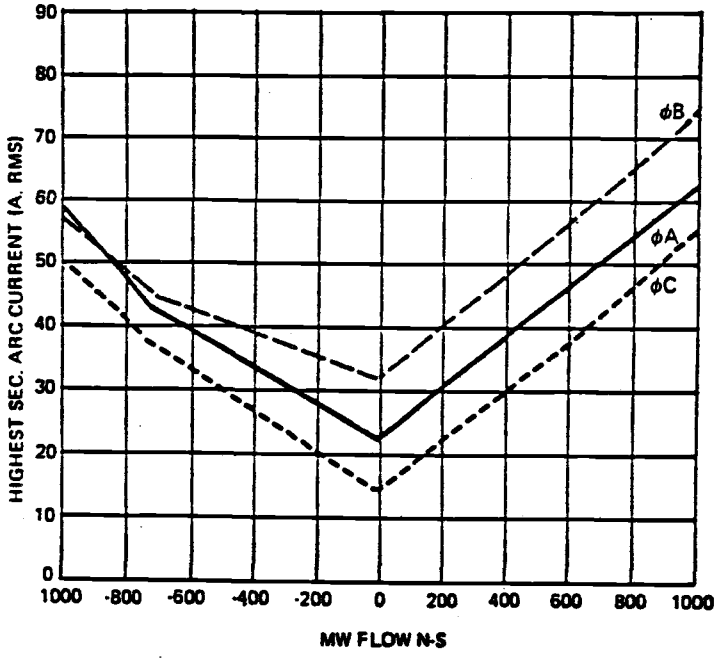

Fig(5) Effect of power flow on secondary arc current.

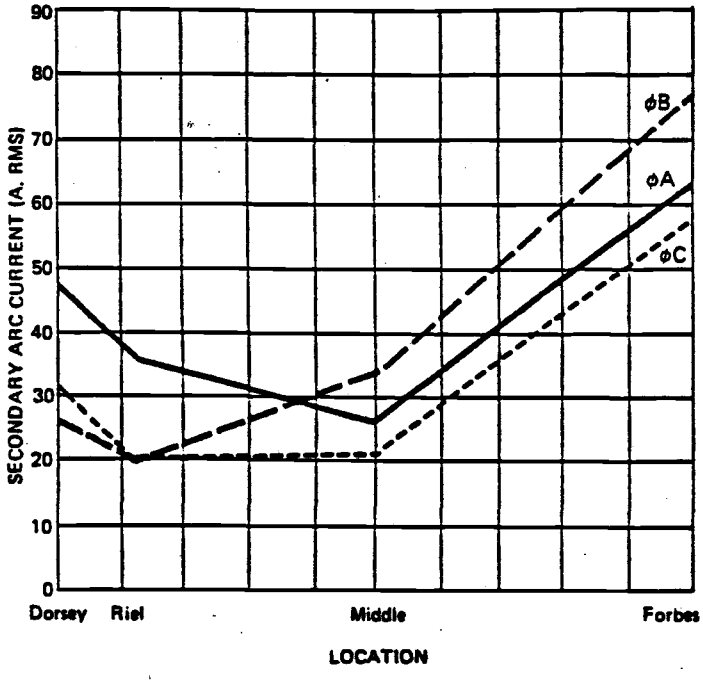

Fig(6) Effect of fault location on secondary arc current (1000 MW).

[Reproduced from reference [27]]

Line Configuration –

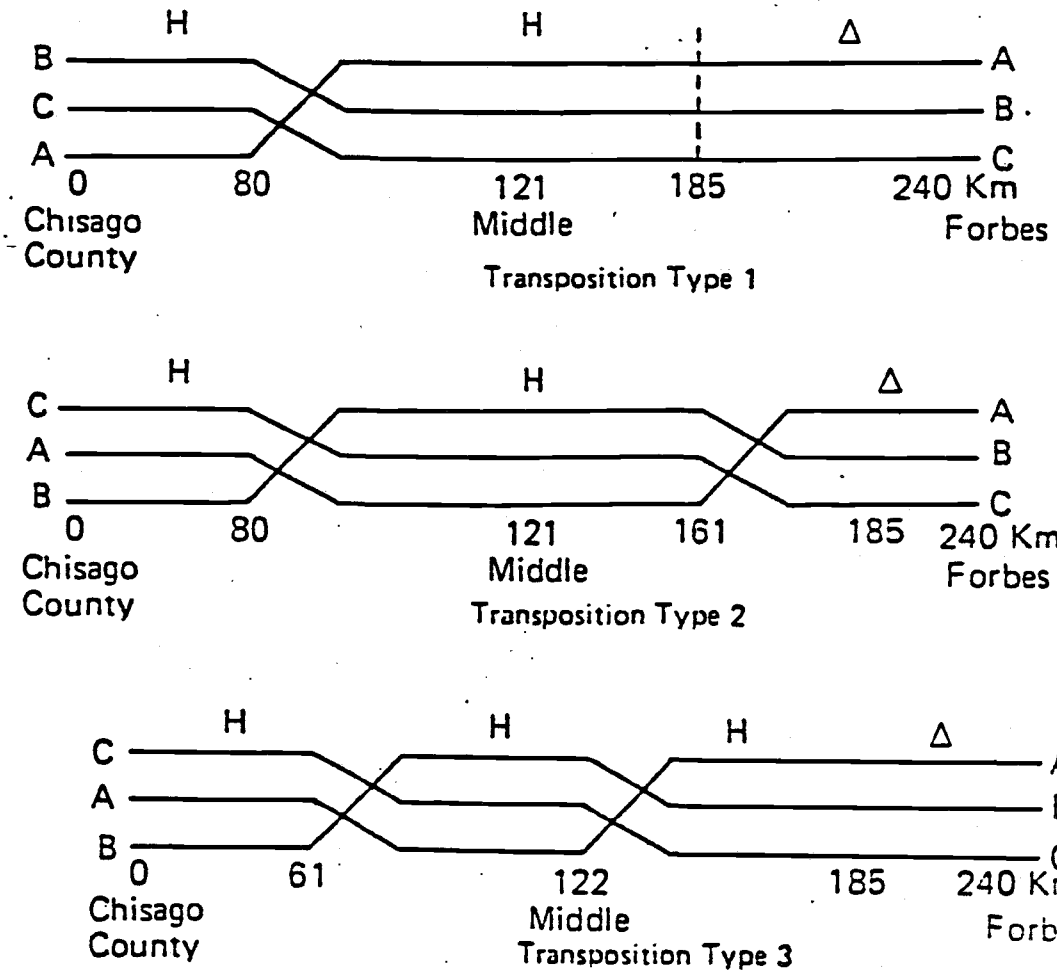

Fig(7) Transposition types

Table(1) Effect of Transpositions on Secondary Arc Current (Digital Results)

[Reproduced from reference [27]]

Transposition Type	Pre-fault Line Flow	Highest Secondary Arc Current (A)		
		Chisago	Middle	Forbes
	(A)			
1	0	16.4	15.5	16.0
1	1091 S-N	39.1	15.5	35.0
2	0	9.5	9.4	9.4
2	1091 S-N	32.4	11.3	31.3
2	1091 S-N	31.0	8.0	29.8
3	0	3.4	2.7	2.9
3	1096 S-N	18.9	3.0	16.6
3	1095 S-N	18.1	3.9	17.9

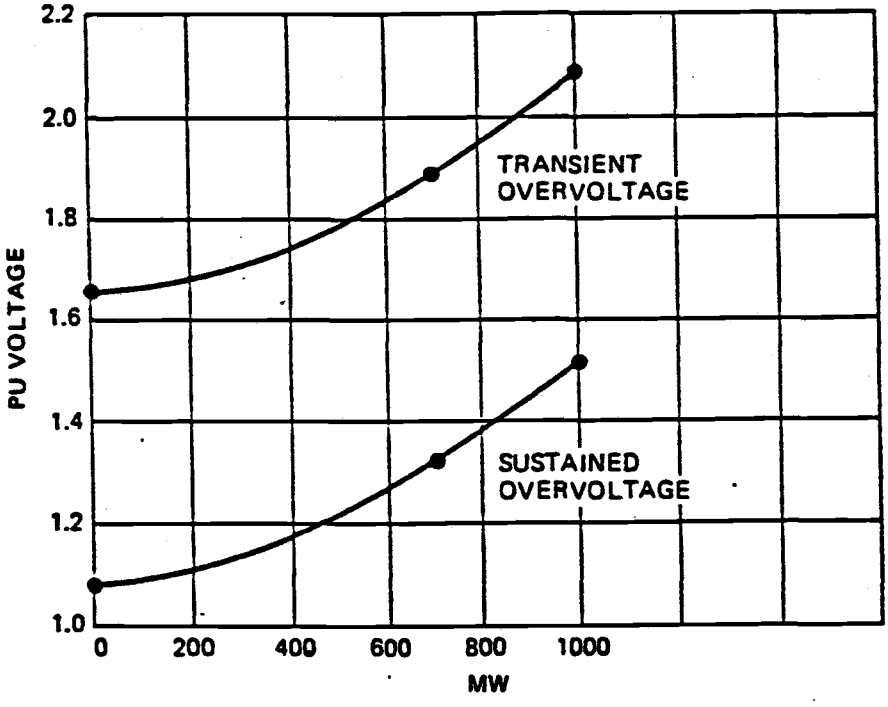

Fig(8) Overvoltages as a function of pre-fault power flow.

[Reproduced from reference [27]]

that the three-phase energizing overvoltages were influenced by the existence of the neutral reactor. The transient overvoltages were higher when the neutral reactor was present.

In 1979 Shperling, and Fakheri [28] developed a method to optimize the neutral reactor values in order to minimize the secondary arc current for different arrangements of the modified and simple four-legged reactors. A modified four-legged reactor bank in conjunction with a simple four-legged bank was considered as a base case. The modified four-legged bank's application was analyzed for SPS on relatively short lines where only one shunt reactor bank was required. In addition, their application was extended to lines which were compensated by three shunt reactor banks. The SPS parameters were obtained and analyzed for the various reactor arrangements using, as an example, a large range of 765 KV lines. The optimum neutral reactances as well as the secondary arc current, recovery voltage, and neutral reactor voltages were presented as functions of the compensation factor. The secondary arc current and the recovery voltage did not exceed 13 amps and 14% of normal voltage, respectively, for optimum neutral reactor values.

The results of Transient Network Analyzer (TNA) and digital computer studies to evaluate secondary arc

current harmonics during SPS of two planned 500 KV systems were reported in 1980 by Kappenman, et. al. [29]. These studies showed that the third and fifth harmonics of the power frequency of a relatively high magnitude can appear in the secondary arc current for certain fault locations. The source of these harmonics was shown to be in the transformer magnetizing current amplified by long-line effects. Field tests to verify the existence of these harmonics and filters to control them were proposed.

In 1981 staged fault tests were performed by Shperling, Fakheri, Shih, and Ware [30] to test SPS compensation schemes for untransposed transmission lines. The performance of the compensation schemes for untransposed lines was analyzed and their effectiveness was confirmed by staged fault tests on a 765 KV system. A large range of single phase switching parameters was simulated during the tests by intentional variations of the secondary arc current and the recovery voltage on the opened phase. The results demonstrated the applicability of high speed single pole reclosing on EHV transmission lines.

In 1982 Kappenman, et. al. [31] reported the results of staged fault tests on a three-phase, 528 km, 500 KV line using SPS. Three-phase shunt reactors were located

at three substations along the line. The reactor bank sizes were 225, 300, and 150 MVARs. These reactors provided the line with 73% shunt compensation. The neutral reactor sizes were 425, 325, and 1250 ohms. The results indicated that the secondary arc time (time from last breaker to open to initial secondary arc extinction) was found to be dependent on the amount of DC offset in the primary fault current. It was found that the arc recovery voltages, with an initial rate of rise of 3-4 KV/ms, did not result in restriking of the secondary arc. After arc extinction the recovery voltage across the arc path reached peak values from 30 KV to 61 KV under normal switching conditions.

III SECONDARY ARC CHARACTERISTICS

3.1 General Discussion

Knowledge of the secondary arc characteristics of power systems is of fundamental importance in determining and improving the system performance, particularly under single-pole switching conditions. It helps in determining the system stability limits, the permissible reclosing times for the circuit breakers, and the performance of the compensation schemes. The conditions under which arc extinction and reignition occur determine the size of the compensation reactors needed to assure successful secondary arc extinction and the magnitude and characteristics of the system transient voltages; and hence, the required insulation levels of the system.

The secondary arc is inherently unstable; that is, given sufficient time the arc will self extinguish. Extinction of the secondary arc depends upon the outcome of a kind of race between two contending factors, one depending principally on the arc space alone and the other on the external circuit alone. The first is measured by the rate at which the arc space recovers its dielectric strength as a result of the disappearance of ions throughout the whole or certain portions of the arc space. This factor depends upon the magnitude of

the arc current, the length of the arc path, the wind velocity, and perhaps on other factors. The second factor is measured by the rate of buildup and magnitude of the voltage applied to the arc terminals by the external circuit and tending to reignite the arc [32]. If the peak magnitude or the rate of rise of the recovery voltage is greater than the dielectric strength of the arc path, then a dielectric reignition of the arc path will occur.

3.2 Short Gap Arcs

Many studies have been performed to investigate the mechanism of extinguishing secondary arcs. Most of them were experimental works performed on short gaps; that is, less than one centimeter. Results of these studies indicated that the lower the secondary arc current was, the higher the reignition voltage and the shorter the time required for the arc to self-extinguish, fig(9) [33]. The abrupt drop in the reignition voltage and the increase in the burning voltage happened at the transition from the "field" type to the thermionic type of the arc cathode. This type of transition is a characteristic of short gaps.

Arc reignition in short gaps can take place via two types of breakdowns associated with the two types of arc cathodes mentioned above. The first is field

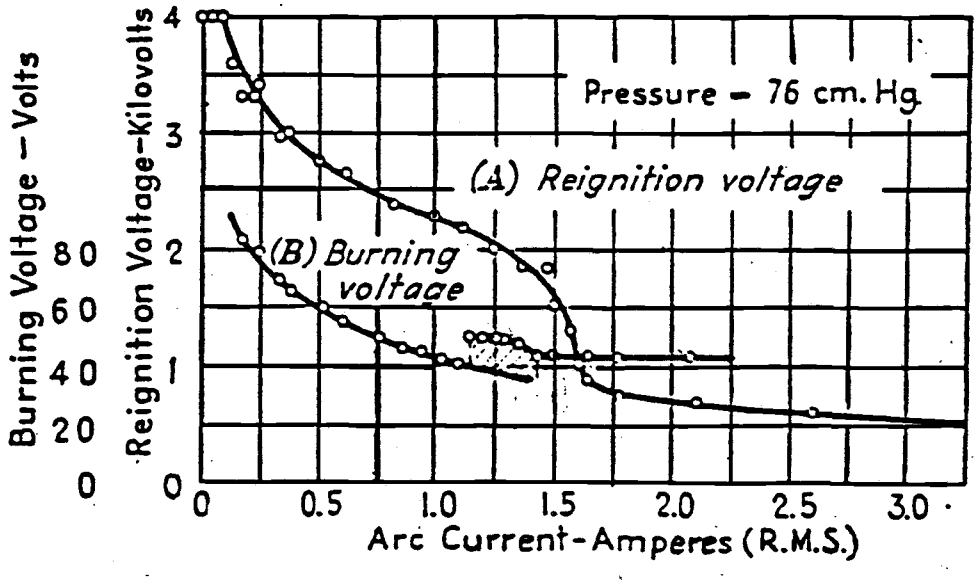

Fig(9) A-C. Carbon-arc characteristics in air (pure graphite electordes, gap = 1.mm.)

[Reproduced from reference [33]]

(spark) breakdown which always occurs in the final stages of recovery when the free charge is negligible and the gas density in the arc path is lower than the pre-arc value. The second is thermal breakdown which, on the other hand, occurs in the immediate post-arc period when the free charge concentration is high and the gas density is low. Under these conditions of high electrical conductivity, any voltage applied to the gap produces immediate current conduction and energy input. If this energy input produces increased temperature and thermal ionization, and hence a reduction in resistivity, a cumulative growth of current may occur if the energy input is maintained at a value greater than the transient losses. Such a current growth will terminate in an arc reignition. It is not possible to specify a precise instant during the recovery at which the transition from thermal to spark breakdown will occur, because the processes are controlled in a complex fashion by the relative importance of free charge, electric field configuration, and losses [34].

In short gaps the electrodes, by virtue of their heat content and capacity, affect the recovery of the arc space appreciably. This effect is marked by changes which can occur in the space-charge regions close to the electrode surfaces. Thus, after an arc interruption,

it is possible for the cathode space charge to be removed in less than one microsecond by surface recombination [34]. This leads to the formation of a deionized cathode layer where practically all the dielectric strength of the arc resides. The deionized layer under normal pressure can withstand electric gradients of the order of 10 to 100 KV/cm. [32]. The formation of this layer immediately after the arc interruption is an important characteristic of short gaps.

In 1954 Kelham [35] presented reignition-voltage/time curves for different conditions of electrode material, gas, gap length, arc current, arc duration, and reignition polarity with gas pressure at or near atmospheric. Figure(10) shows the reignition-voltage/time characteristics in air for polished copper, polished tungsten, mild steel, aluminum and graphite electrodes using arc of 20 amp amplitude and 27 millisecond duration. The electrodes are 3/8" in diameter, and the gap length is 1 cm. The effect of the electrode material on the reignition voltage is depicted in fig(10). For instance, arcs between polishedcopper and polished tungsten electrodes in air, for currents of 20 amps, require a reignition voltage of 355 volts within 3 microseconds after arc interruption. Aluminum, on the other hand, shows a low initial reignition voltage of only about 50 volts, but the reigni-

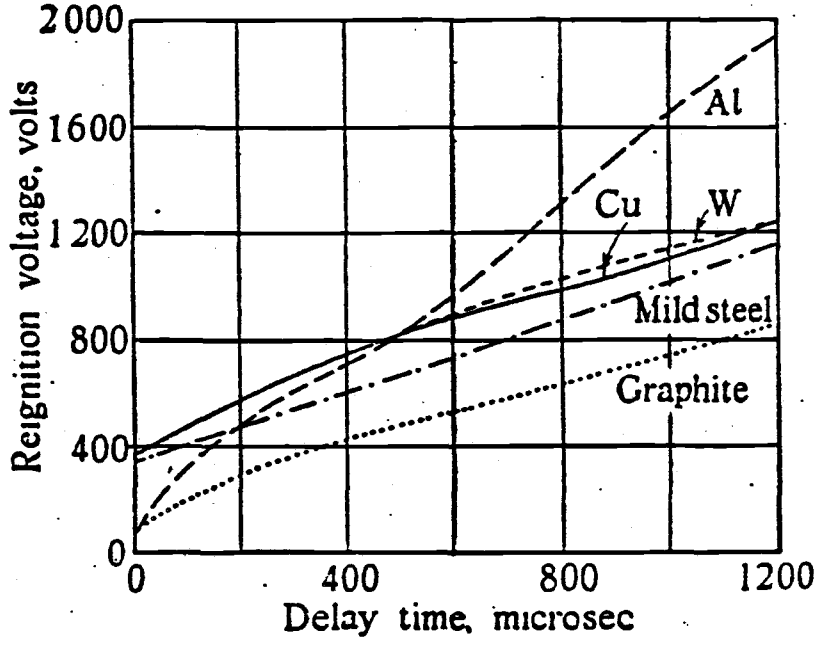

Fig(10) Reignition-voltage/time characteristics in air for 20 amp arcs.

[Reproduced from reference [35]]

tion voltage subsequently increases with delay time at approximately double the rate for the other electrode types. Effect of the gap length on reignition voltage was also investigated by Crawford, and Edels in 1960 [34]. The results indicated that the reignition voltage was proportional to the gap length for short gaps, fig(11).

3.3 Long Gap Arcs

The above results apply only to short arc gaps where most of the recovered dielectric strength resides in the deionized layer next to the cathode. For long arcs the situation is different. Thus, during the extinction period of the long arc, the larger part of the recovered dielectric strength resides in the space away from the cathode layer. In a long arc, the ionization disappears in a relatively gradual manner during the extinction period. The ions in the arc space are continually lost in two principal ways: one, by direct recombination of ions of opposite signs within the space, and the other by diffusion assisted by electric fields, air blast, or other means [32]. If the space is to maintain its conductivity these losses of ions must be made up by some ionizing agent. The ionization agents are directly dependent on the impressed electric field and the degree

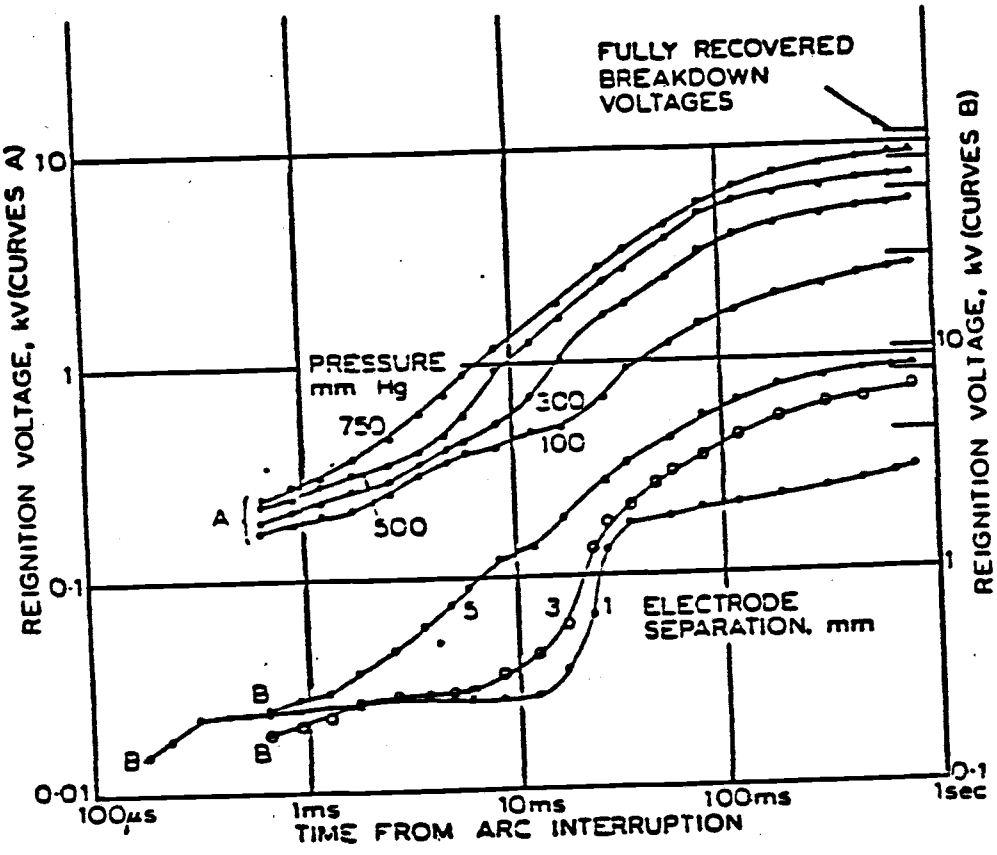

Fig(11) Reignition voltage characteristics for air.
Variation of pressure and electrode separation

Arc-current = 20 amp.
Duration = 100 millisec.
Electrodes: carbon 4mm diameter.
A. 5 mm electrode separation.
B. 750 mm Hg pressure.

[Reproduced from reference [34]]

of ionization of the space. There is a particular electric gradient for which the ionizing agents are just sufficiently intense to make up the ionization which is being lost in the arc space, and hence, to help the conductivity of the space to maintain itself. If a smaller gradient is impressed the space conductivity will diminish. If a larger gradient is impressed the space conductivity will increase. The critical gradient at which the conductivity of the space just maintains itself is called breakdown gradient [32].

In 1949 a test technique was developed for studying the rates of dielectic recovery of large air gaps by McCann, Conner, and Ellis [36]. Results were presented showing the rate of dielectric recovery for 3,6, and 11 inch standard rod gaps for power frequency fault currents up to 700 amps, one-half cycle duration, in air, fig(12). They stated that it was difficult to vary any parameter without causing appreciable changes in one or more of the others. Thus, it was difficult to accurately reproduce any test conditions, therefore, so many tests were required to get enough points so that the effect of variations in the test conditions could be eliminated by using an average value. Each point on the curves in fig(12) was the result of 70 to 150 actual tests.

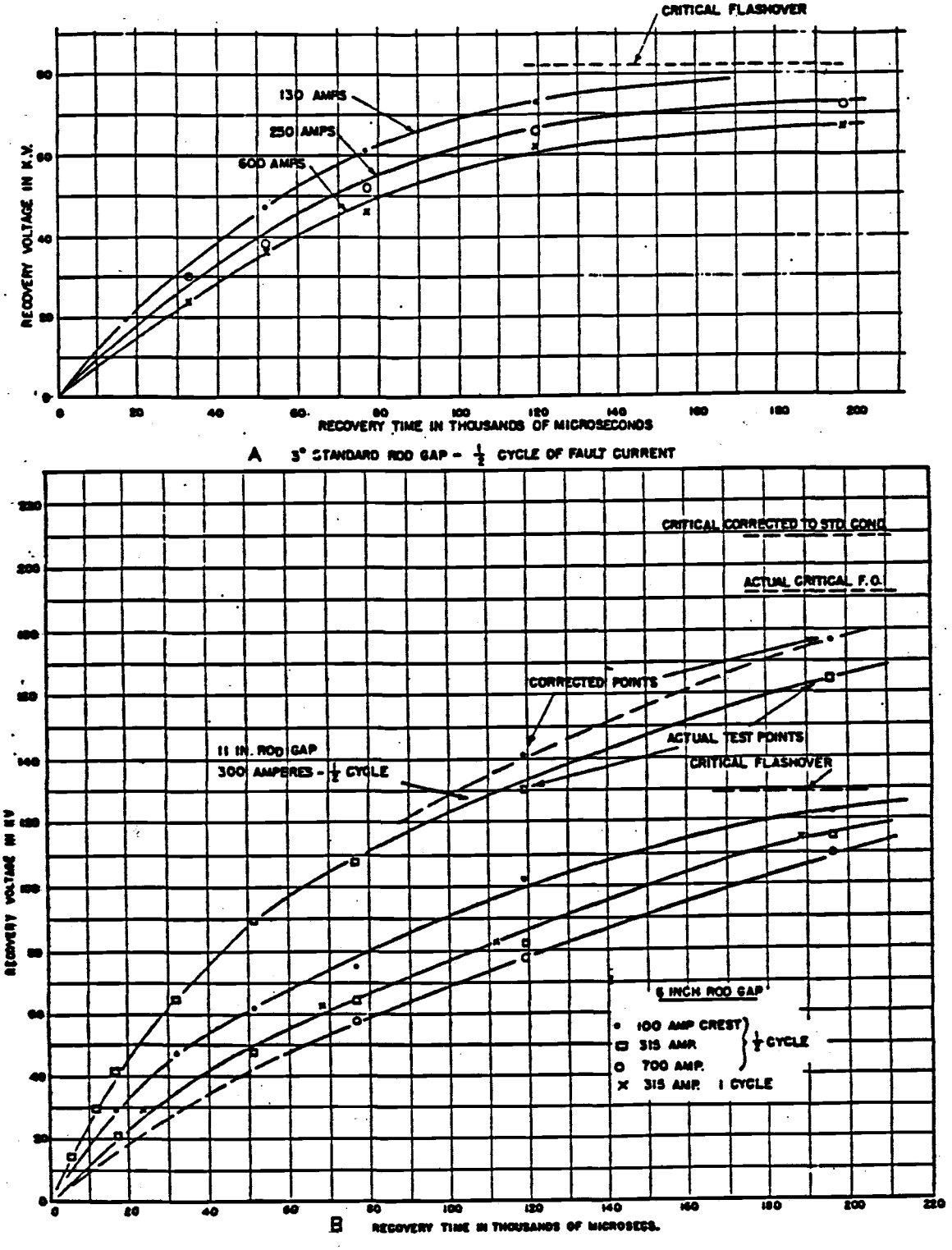

Fig(12) Dielectric-recovery curves obtained with two generator tests

A. Three-inch standard rod gaps B. Six-and eleven-inch gaps.

[Reproduced from reference [36]]

Comparison of the three-inch and six-inch gap data in fig(12) shows that the relative rate of recovery of the three-inch gap is more rapid than that for the six--inch gap. Also, the critical breakdown strength of the three-inch gap is greater than for the six-inch gap. This is due mainly to electrode cooling effect in the three-inch gap case. for gaps of six inches or more this effect is not appreciable as shown by the comparison between the six-inch and the eleven-inch gap curves. The eleven-inch gap data are proportionately higher than the six-inch gap data. It thus appears that data obtained from these gaps can be extrapolated to larger gap spacings. The six and eleven inch gap data show that for fault current of 100 to 700 amps time intervals of .05 to .08 sec. are required for the insulation to recover to one half of its original strength.

3.4 Transmission Line Arcs

The valuable data mentioned above are valid for short and relatively long gaps. However, due to the complexity of the phenomena and the difficulty of performing significant tests on much longer gaps these data cannot be directly applied to transmission line arcs except to the circuit breaker arc or to small gaps where electrode effects dominate. Moreover, these data do

not lead to a formulation of an interruption theory nor is there a formula to extend them to longer gaps. However, this bulk of data gives a qualitative view of the relationships between factors affecting the secondary arc in general. They seem to suggest that the smaller the peak magnitude and rate of rise of the recovery voltage are, the higher the probability of arc extinction will be. Data obtained from transmission line arcs support this observation.

The first data on SPS obtained from tests on typical transmission systems was reported in 1941 by Trainer, Hobson, and Muller [24]. Table(2) gives approximate data of the minimum reclosing time permissible without reestablishment of the arc. These figures are to be taken as typical of expected results under average conditions. The reclosing time was measured from the time the breaker trip coil was energized until the breaker had opened, and the contacts were again closed [24].

Knudson [19] stated that, for a 230 KV, 300 mile, three-phase transmission system, an arc current of 19 amps and a recovery voltage of 19 KV appear to be critical according to tests carried out in Sweden. He, also, mentioned that tests showed that a secondary arc over a 400 KV insulator string was likely to be maintained if the recovery voltage equaled 22 KV and the secondary

Table(2) Typical Arc Deionizing Times

[Reproduced from reference [24]]

Nominal System Voltage (KV)	Deionizing Time for 95% of Faults (Cycles on 60-Cycle Basis)	Minimum Permissible Reclosing Time With Eight-Cycle Breakers	Minimum Permissible Reclosing Time With Five-Cycle Breakers
23	4	12	9
46	5	13	10
69	6	14	11
115	8.5	16.5	13.5
138	10	18	15
161	13	21	18
230	18	26	23

arc current equaled 34 amps when the line length was of the order of 400 km or more.

Kimbark [20] mentioned that information on the unneutralized secondary arc currents indicated that with 0.4 second dead time, there was high probability of successful reclosure if the secondary arc current did not exceed 20 amps.

Sturton, discussor of reference [16], stated that his experience regarding single line to ground faults was that for:

i) Dead time less than 0.3 sec., reclosing would probably be unsuccessful, even if secondary arc went out in 50-100 msec., since there was a real and apparently fairly long time required for build up of the dielectric strength of the air around the arc path - unless there was a substantial wind.

ii) Dead time greater than 0.3 sec., but less than 0.5 sec., reclosing might not be successful.

iii) Dead time greater than 0.5 sec., secondary arc and dielectric strength would not interfer with successful reclose.

The results of staged fault tests, performed to test SPS compensation schemes for untransposed, 765 KV, transmission lines, indicated that in 22 tests the secon-

dary arc current was less than 40 amps (rms) and the arc lasted no longer than 60 ms. [30]. In one test with a 38 amps (rms) current the arc extinguished in 160 ms. after the circuit breaker cleared the faulted phase. The arc extinction time was practically independent of the current magnitude. In four tests with the 60 Hz component of the secondary arc current larger than 45 amps (rms) the arc did not extinguish in 30 cycles and single pole reclosings were unsuccessful.

It was also, mentioned that the tests proved that the rate of rise and the steady state of the recovery voltage depend mainly on line and reactor parameters [30]. Parameters such as fault initiation angle and primary fault and secondary arc burning times did not affect the recovery voltage to a significant extent. Thus, for instance, fig(13) shows the peak voltages in each half cycle versus time from the moment of arc extinction in two similar tests with compensation reactors connected at both ends of the line. Despite the fact that the arc extinction time in these two tests was different (60 ms. and 160 ms.) the rate of rise of the recovery voltage was practically the same.

Lee, from New Brunswick Electric Power Commission, Canada, discussor of reference [30], indicated that TNA studies, for a 317 km, 345 KV, transposed line, showed

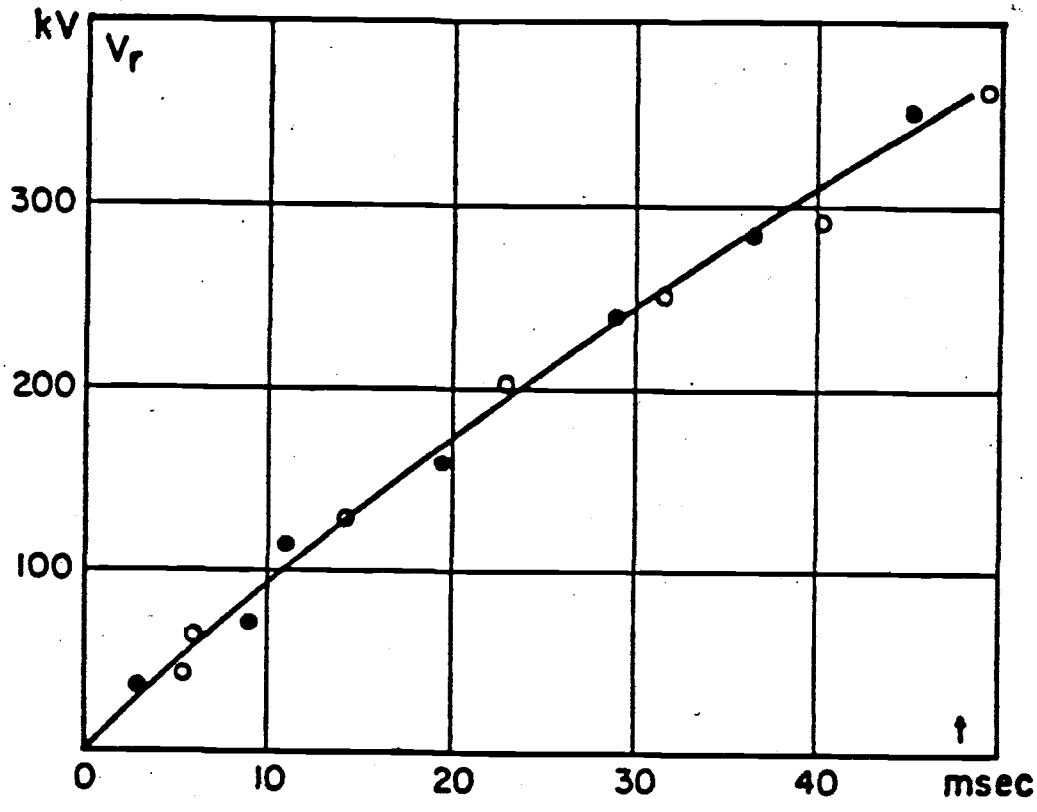

Fig(13) Rate of rise of the recovery voltage. Fault on the middle phase. Neutral reactors of 400 Ohms at Kammer and 150 Ohms at Marysville. 60 Hz component of the secondary arc current equals 53 A.

Arc extinction time
o - 60 msec
o - 160 msec

[Reproduced from Reference [30]]

that the line had secondary arc current in the range of 21.7 to 40 amps and recovery voltage of 52 KV to 94 KV peak. The line was not compensated and the dead time was set at 41.5 cycles. The line experienced three SPS operations during 16 months period without having any unsuccessful reclosings.

Variation of the steady state recovery voltage (V_r) and of secondary arc current (I_s) with line length for 500 KV lines is shown in fig(14). These results were taken from computer simulations for the standard 500 KV single-circuit transmission line design [17].

The results obtained by Kimbark [16], using digital computer analysis to test the performance of compensation reactors, are shown in table (3) [16]. The tested system was a three-phase, double circuit, 735 KV (rms) phase-to-phase, 200 miles, stacked configuration. The lines were assumed fully transposed.

In the first series of tests, the receiving-end voltage was in phase with the sending-end voltage for simulating no-load conditions. In the second series, 50% series compensation was inserted at the midpoint of the line, and the delivered power was increased to 6.64 GW by making the phase difference between sending-end and receiving-end voltages equal to 34^{o}. Shunt compensation, including capacitor between like phases to balance

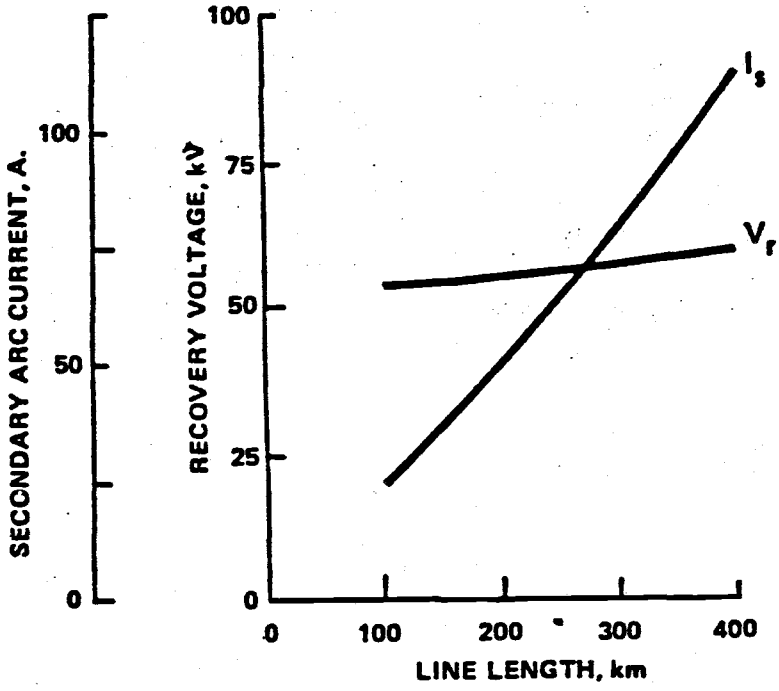

Fig(14) Recovery voltage and secondary arc current versus line length for a SLG fault (no load)

[Reproduced from reference [17]]

Table(3) Residual Fault Currents and Recovery Voltages of SLG Fault and of Simultaneous SLG Faults on Same Phase of Both Circuits of Double-Circuit 735-kV 200-Mile Line Represented by Six Pi Sections

[Reproduced from reference [16]]

Test Series	Shunt Circuit	Compensation Degree h_1	Line Load (GW)	Fault on Conductors	Recovery Voltage (kV)	Residual Fault Current (A)	Thevenin's Impedance (kilohms)	Remarks
	None	0.0	None	ag or bg	79.5	116.	0.685	
1	Tree	0.7	None	cg	3.48	1.78	1.96	
	Tree	0.9	None	bg	5.56	1.02	5.45	
	None	0.	6.64	bg	89.7	134.	0.669	
	Tree	0.6	6.64	bg	62.9	44.5	1.41	50% series
	Tree	0.7	6.64	bg	65.9	35.2	1.87	Compen-
2	Tree	0.7	6.64	adg	60.3	32.2	1.87	sation
	Tree	0.9	6.64	bg	89.3	17.2	5.19	at mid-
	Tree	0.9	6.64	adg	69.2	13.2	5.25	point.
	None	0.	6.64	bg	78.7	57.4	1.37	Faulted Conductor
3	Tree	0.6	6.64	bg	41.4	14.1	2.94	Sectional-
	Tree	0.7	6.64	bg	41.2	10.9	3.78	ized at
	Tree	0.9	6.64	cg	112.	10.6	10.6	midpoint of line.

the system, was connected at both ends. With no compensation, the secondary arc current and the recovery voltage were increased by 13 to 19%. This shows that the shunt capacitive coupling is more important than the series inductive coupling at a load of 6.64 GW. With shunt compensation, the recovery voltages were reduced from 0 to 30%, depending on the degree of compensation, but the residual fault current was reduced more, by 67 to 90%. However, some of these currents were still as high as 32 to 44 amps. Since the shunt coupling was neutralized, these currents were caused almost entirely by series inductive coupling [16].

In the third series of tests the effect of sectionalizing the disconnected conductor upon secondary arc current and recovery voltage of a SLG fault was tested. The results are shown in the lower part of table(3). Comparing the results of the third series of tests with the results of the second shows clearly that more reduction of secondary arc current and of recovery voltage than those obtained by division of disconnected conductors into two sections could be obtained by division into a greater number of sections.

The results of another digital computer analysis of SPS on EHV lines are shown in tables (4), (5), and (6) for points on the line diagram in fig(15) [25].

Table(4) Effect of Transpositions on Secondary Arc current and coupling voltages (Line is uncompensated)
[Reproduced from reference [25]]

	Untransposed		Transposed	
Point	Coupling Voltage (kV, rms)	Secondary Arc Current (A, rms)	Coupling Voltage (kV, rms)	Secondary Arc Current (A, rms)
1	63.8	41.1	50.7	33.0
2	38.0	24.3	27.2	17.5
3	26.8	17.1	18.0	11.5
4	19.8	12.7	20.2	13.1
5	30.6	19.8	42.1	27.3

Table(5) Effect of Nominal 100% Reactor Compensation on Secondary Arc Currents and Coupling Voltages

[Reproduced from reference [25]]

	Reactors at Sending End		Reactors at Midpoint		Reactors at Each End	
Point	Coupling Voltage (Kv, rms)	Secondary Arc Current (A, rms)	Coupling Voltage (Kv, rms)	Secondary Arc Current (A, rms)	Coupling Voltage (Kv, rms)	Secondary Arc Current (A, rms)
1	1512	20.5	82.4	0.47	616	3.9
2	1504	19.8	67.3	0.39	621	3.9
3	1496	19.5	65.6	0.38	625	3.9
4	1485	19.2	67.7	0.39	629	3.9
5	1461	18.8	86.1	0.50	640	4.0

Table(6) Effect of Additional Transpositions on Secondary Arc Currents and Coupling Voltages.

[Reproduced from reference [25]]

Point	Reactors at Each End Coupling Voltage (kV,rms)	Reactors at Each End Secondary Arc Current (A,rms)	Reactors at Midpoint Coupling Voltage (kV,rms)	Reactors at Midpoint Secondary Arc Current (A,rms)
1	49.1	0.31	68.2	0.42
2	20.2	0.13	38.7	0.24
3	4.8	0.03	23.1	0.15
4	10.6	0.07	7.5	0.05
5	40.0	0.25	22.6	0.14

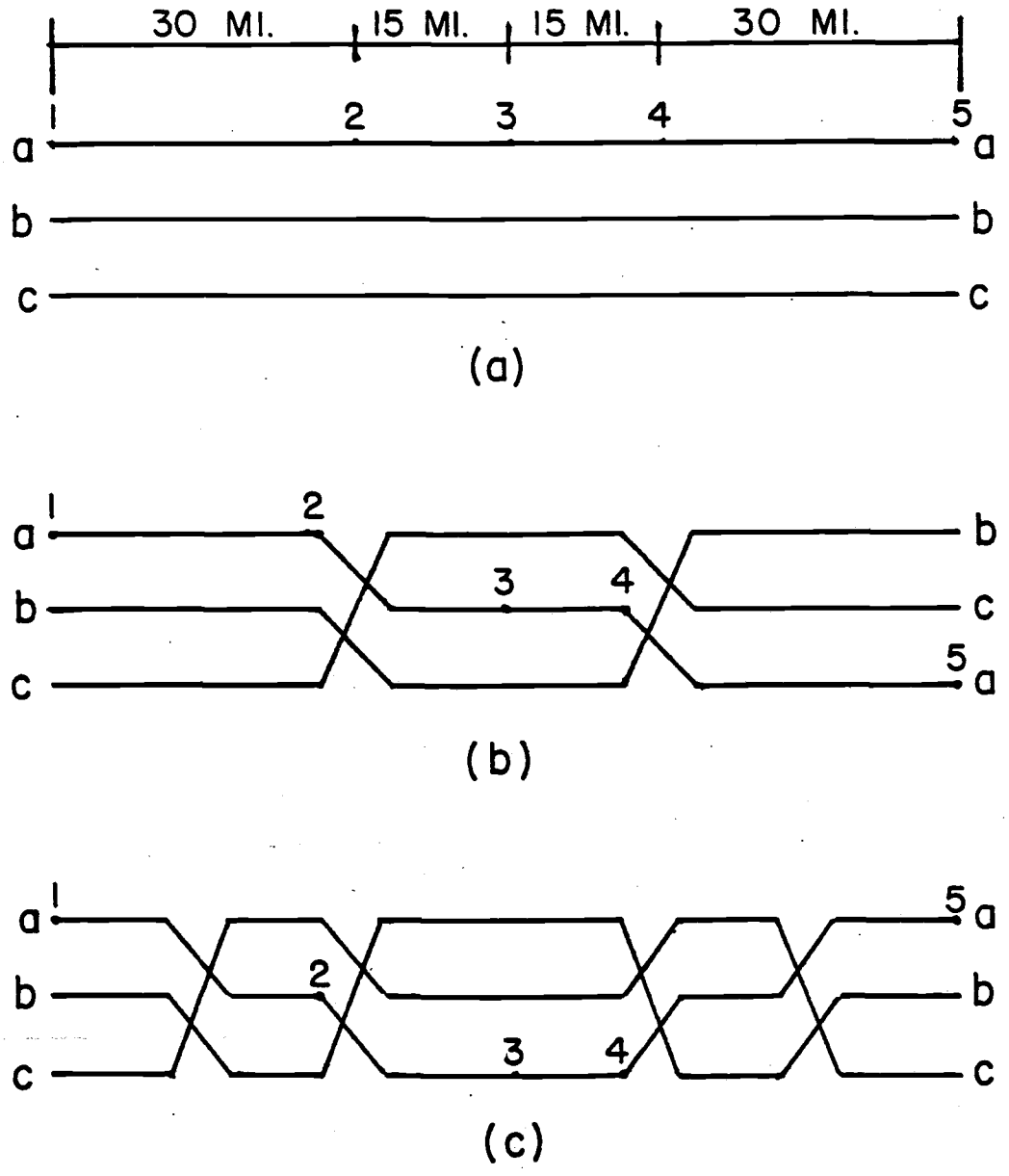

Fig(15) Methods of transposition and points at which voltages and currents were calculated.

[Reproduced from reference [25]]

Table (4) shows a comparison between the secondary arc current and the recovery voltage for an untransposed line and for a line transposed as in fig(15b). There is no reactor compensation in either case. Table(5) shows the effect of the compensation reactor arrangements. The line istransposed as in fig(15b). The results indicate that with reactors at the sending end only, or with reactors at each end, the recovery voltages are extremely high. This is due to series resonance which is caused by improper transpositions [25]. Table (6) shows the effect of tranposing the line as in fig(15c). The results indicate that the distribution of voltages along the open conductor is fairly symmetrical for the case with reactors at each end. The distribution is not symmetrical with reactors at the middle, because the presence of the reactors introduces a discontinuity in the line [25].

Some of staged fault test results for a three-phase, fully transposed, 500 KV, 93 mile long transmission system are shown in figs(16), and (17) [18]. Secondary arc current of 12.5 amps and recovery voltage of 59 KV are shown in fig(16). Single-pole reclosing was successful. In fig(17) the secondary arc current is 22.5 amps. Single-pole reclosing was unsuccessful.

Gillies, and Perry, from BPA , discussors of refer-

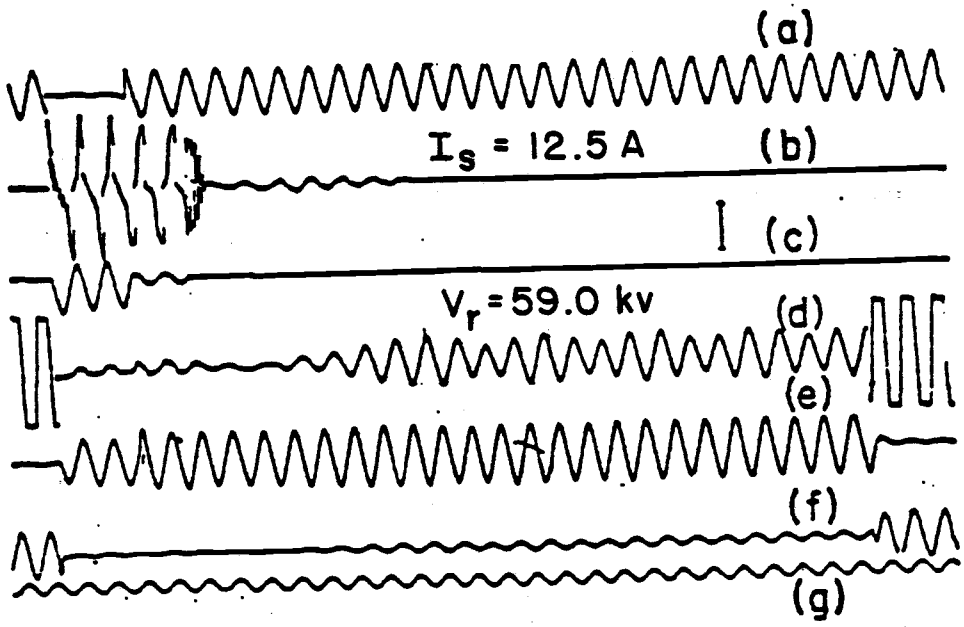

Fig(16) Oscillogram record at Davidson for a C-Phase--to-ground fault at Davidson. Generation 945 MW, Voltage 517 kV.

(a) 500-kV Bus-C-phase-to-Neutral Voltage (Capacitance Divider). (b) Secondary Arc Current. (c) Total Fault Current. (d) Expanded Recovery Voltage-Line (5 times Trace f). (e) Recovery Voltage, C-phase Breaker (Capacitance Dividers). (f) Paradise Line-C-Phase Voltage (Capacitance Divider). (g) 60-Hz Timing Wave.

[Reproduced from reference [18]]

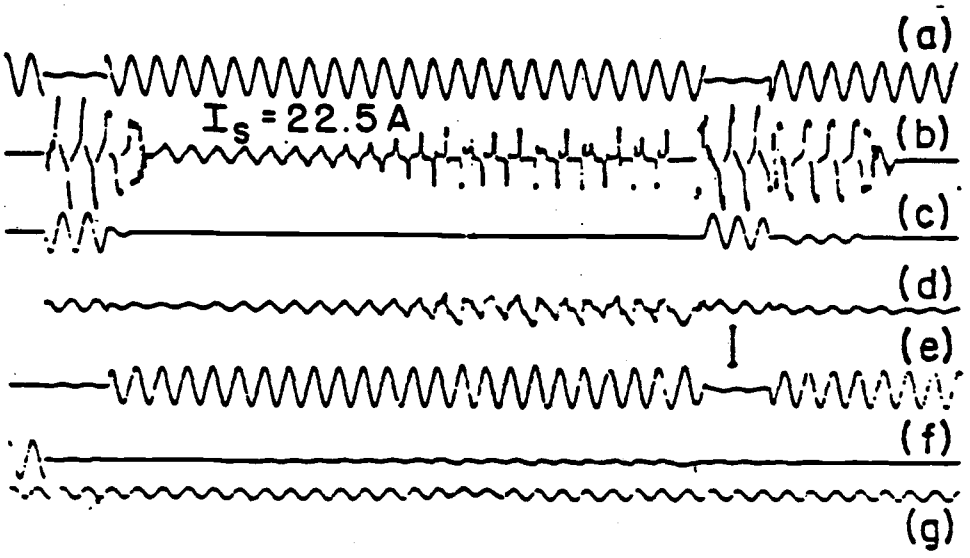

Fig(17) Oscillogram record at Davidson for a C-phase-to-ground fault at Davidson - reactors out.

(a) 500-kV Bus-C-phase-to-Neutral Voltage (Capacitance Divider). (b) Secondary Arc Current. (c) Total Fault Current. (d) Expanded Recovery Voltage-Line (5 times Trace f). (e) Recovery Voltage, C-phase Breaker (Capacitance Dividers). (f) Paradise Line-C-Phase Voltage (Capacitance Divider). (g) 60-Hz Timing Wave.

[Reproduced from reference [18]]

ence [37], mentioned that single-pole reclosing tests on BPA 500 KV lines indicated about 45 KV recovery voltage at 40 amps as about the limit for successful single pole reclosure. In reference [27] the authors stated that at the more likely power flow levels on a 500 KV line the secondary arc currents were below 70 amps (rms) and satisfactory performance of SPS was expected.

3.5 Conclusions

The theoretical and experimental results mentioned above demonstrate that the magnitude and rate of rise of the recovery voltage, the arc current, and the gap length are the most important factors in deciding whether an arc will self-extinguish or not. These four factors act simultaneously in an interactive manner. For a certain gap length, the higher the arc current, the lower the recovery voltage is; and as the gap length increases, the recovery voltage increases. The results also show that in short arc gaps, the gap terminal conditions are important but the effect of the weather conditions on the arc characteristics is minimal. For long gaps the terminal effects have no impact on the arc recovery; but, as the gap length increases, the importance of the weather condition effect increases. Consequently, it is impossible to extrapolate short gap data to long gaps.

However, the qualitative behavior of the arc voltage and the arc current in the short gap provides an indication of the current and voltage behavior in the long gap.

There has been a generally accepted idea that when the arc current is flowing, the arc resistance is negligible or zero; and when the arc is interrupted at current zero, the current comes to zero and no appreciable current flows thereafter. Thus, the arc resistance becomes infinite. This assumption is a simplification that might be acceptable only when considering worst case conditions. From the usual arc voltage and current characteristic for stable conditions, it is evident that the effective resistance of the arc path is a variable and increases rapidly as the current approaches zero. This can be seen in fig(9). The results mentioned above also show that if the arc resistance increases more rapidly than the voltage across the arc the arc will extinguish. Thus, the arc extinction, as mentioned above, can be considered as a race between the dielectric strength of the arc path and the arc recovery voltage. It is important, however, to remember that a current is still flowing during the time of the voltage rise, and the two are not independent, since the current that flows retards the deionization and increase of resistance,

and also modifies the rate of rise of the recovery voltage. Hence, the characteristic of the arc during the ionization-deionization process time can be expected to follow one of the three schemes shown in fig(18). Curve A represents the characteristic of an arc equilibrium when the current and voltage increase slowly; so that the ionizing activity just balances the deionizing activity. Curve B shows the characteristic of an arc where the voltage is increasing faster than the arc resistance. In this case the current will increase and the ionization process will be faster than the deionization. Thus, the possibility of an arc restrike is great. The third case is shown by curve C where the voltage is lower for a given current value than for a stable condition of the same arc. In this case the deionization process is faster than the ionization process and the arc current will decrease slowly. In this case the arc extinction is possible.

Because of the complexity of the interactions that take place in the arc space during the ionization-deionization process, and because of the strong dependence between the parameters affecting such processes, it is almost impossible to reproduce any single test, especially in the case of long-gap arcs. Hence, to develop a formula that will exactly predict the characteristic of an arc

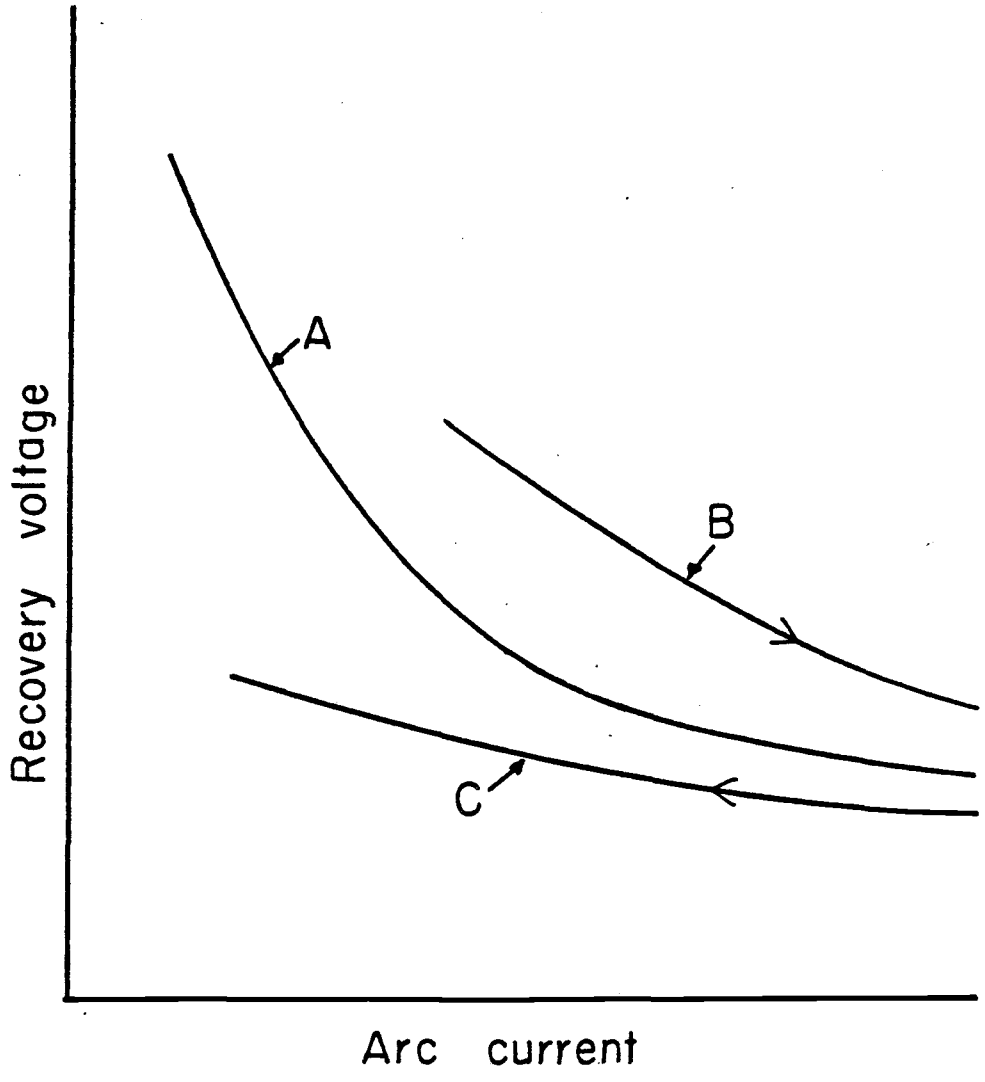

Fig(18) Arc Characteristics

does not seem conceivable. For this reason most of the theoretical and experimental studies done up to date on the extinction of long gap arcs have been aimed at establishing worst case limits on the controllable parameters. In between these limits the expectation of an arc extinction is very high. For a certain arc length, the only controllable parameters are the recovery voltage and the arc current.

In short arc gaps, a maximum voltage gradient of 10 to 40 KV/cm was observed [33,34,35]. Most of this voltage is, of course, in the small deionized layer near the electrode surface. As the arc current increases, the voltage drops, fig(9). As the gap length increases, the voltage increases but not with the same proportion. Figure(12) shows that the three-inch gap has about twice the proportionate rate of recovery as the six-inch gap. This is probably due to the electrode effect. For gaps of six inches or more, this effect should not be appreciable. The six-inch and eleven-inch gaps [36], shown in fig(12), show quite similar rates of recovery. They have nearly the same proportionality factor at all points. It thus appears evident that data obtained from gaps of these lengths can be extrapolated to larger gap spacings under the same conditions. For much longer gaps, such as transmission line gaps, the effects of

wind and other weather conditions are important; and, at the same time, difficult to estimate. Hence, such extrapolation will result in accurate results so long as the arc lengths and conditions are not very different.

In transmission line gaps, the arc phenomenon is very complicated. It is almost impossible to reproduce any test results. Thus, enough data to visualize the relationship between the various factors affecting the arc recovery cannot be obtained. However, it is expected that the transmission line arc characteristic will be qualitatively similar to those observed in short and long gaps. That is, the recovery voltage is directly proportional to the gap length, and inversely proportional to the arc current. Also, the arc resistance is variable. It increases more rapidly as the current approaches zero. When the voltage is rising, the arc current is not zero and the arc resistance is not infinite. If the arc voltage is maintained below the arc space breakdown voltage at all times an arc extinction will be possible. Also, as the arc current increases, the ionized path area increases; and a longer time will be needed for the arc dielectric strength to build up. The rate of increase of the arc area and the gradient of the arc voltage decrease as the current increases as can be seen from fig(12). Hence, the time required

for the arc dielectric to recover and for the arc to self extinguish is a function of the arc voltage, arc current, and arc length, table(2) and fig(12).

The theoretical and staged fault test results mentioned above for transmission line arcs show a wide range of variations. For instance, the results in figs(16), and (17) indicate that, for a 500 KV transmission line, an arc current of 22 amps and a recovery voltage of 59 KV are about the limits for the arc to self extinguish within 30 cycles. In reference (39) it was mentioned that for a 500 KV line, an arc current of 40 amps at a recovery voltage of 59 KV was extinguishable. Kimbark [20] stated that a 20 amp arc current was the limit for an arc to self extinguish. He showed that for a 735 KV transmission system the recovery voltage was 89.3 KV for an arc current of 17.2 amps, table (3). This, of course, implies that this arc will self extinguish. On the other hand, the results of staged fault tests on 765 KV transmission lines indicated that 40 amp current extinguished within 60 ms. while a 45 amp current did not extinguish within 30 cycles. Also, Knudson mentioned that the results of tests carried out for 230 KV transmission lines indicated that a current of 19 amps and a recovery voltage of 19 KV appeared to be critical limits. These results seem to suggest that the 20 amp

limit on the secondary arc current suggested by Kimbark appears to be a very conservative figure. A more realistic criterion would seem to be that for circuits of 230 KV or less, a recovery voltage of less than 10% of normal circuit voltage and an arc current of 20 amps are acceptable limits for the arc to extinguish within 30 cycles. For circuits of higher voltages, currents of up to 40 amps at recovery voltages of about 10% of circuit voltage will be tolerable and the arc will extinguish within the permissable reclosing time of 30 cycles. It is important to emphasize that, as mentioned above, these are the extreme limits. The recovery voltage is the open circuit voltage across the arc and the current is the short circuit current through the arc. In practice these limits will not be reached. When the voltage rises, the current is not zero and the arc resistance is not infinite; and when the current is flowing, the arc resistance varies with voltage, current, and time, and the voltage across and the current through such arcs will always be less than these limits.

IV COMPENSATION SCHEME DESIGN

4.1 Primary Analysis

4.1.1 General Discussion

The main purpose of the compensation scheme to be designed is to reduce the secondary arc current and the magnitude and the rate of rise of recovery voltage on the disconnected phase. These three quantities must be reduced to levels where it is possible to extinguish the secondary arc in a short time (<30 cycles) and, hence, to assure successful single pole reclosure. To which degree each of the three factors is important for successful interruption is not known [19]. But, if it is known that arc extinction will occur at certain conditions, it can be concluded that it will occur at all conditions which involve at the same time reduced values of all the three factors mentioned above.

The main function of the proposed compensation scheme is to minimize the capacitive coupling between the faulted conductor and the sound phases by neutralizing the interline capcitances. The inductive coupling is not affected by the shunt compensation reactors. However, the inductive coupling, as mentioned above, contributes only about 10% of the total line coupling under normal conditions [16,20]. Thus, its effect is not too great, but it must

be taken into account during the compensation design stage. The secondary arc current and recovery voltage limits mentioned in chapter (3) were suggested on the basis of staged fault test results and on the single-pole switching performance data reported for transmission systems in operation. These data, of course, include both capacitive and magnetic coupling effects. Hence, when designing the shunt compensation reactors, the maximum secondary arc current and recovery voltage due to the capacitive coupling must be kept below the above stated limits so as to leave a safety margin to account for the inductive coupling. In other words, the designed compensation scheme should reduce the capacitive secondary arc current and recovery voltage to values at least 10% less than the limits stated above. That is, the capacitive component of the secondary arc current must not exceed 18 amps for circuits rated less than 230 KV, and 35 amps for circuits of greater than 230 KV rated voltage. The capacitively coupled recovery voltage should be less than 9% of normal circuit voltage.

The third important factor in deciding whether an arc will self extinguish or not is the rate of rise of recovery voltage. This factor depends strongly on the magnitude of the secondary arc current. Test data for various neutral reactors showed direct dependency between

the recovery voltage rate of rise K_r(KV/ms.) and the secondary arc current I_s(amps rms). The dependency was described by $K_r=0.2I_s$ [30]. Thus, any reduction in the secondary arc current will be enhanced by more reduction in the rate of rise of the recovery voltage. For secondary arc currents of less than 40 amps, the recovery voltage rate of rise is less than 8 KV/ms. Comparing this figure with the staged fault test results shown in fig(13) for a 765 KV system indicates that a successful single-pole reclosure within 160 ms. or less after arc extinction can be achieved.

An important aspect of six-phase transmission lines to be mentioned here is the transposition. In most of the three-phase transmission line studies cited in chapter (2), full line transposition was assumed to simplify the analysis. This assumption results in equality of all the off diagonal terms of the impedance matrix. If six-phase transmission lines are fully transposed the main advantage of six-phase systems is lost; that is, the low voltage between adjacent phases no longer holds over some sections of the line. Moreover, if full transposition of six-phase transmission lines is to be implemented, fifteen transposition sections are needed, which requires many expensive interchanges of conductor position. A transposition scheme that seems practical

for six-phase systems is "rolling", where the six conductors are rolled one position at a time. The conductors keep their relative positions with respect to each other. With this type of transposition, the off diagonal terms of the impedance matrix are no longer identical. The symmetrical component impedance matrix remains diagonal however, and therefore balanced currents cause only balanced voltage drops [38]. In this study no transposition is assumed.

4.1.2 Application of the Three-Phase Compensation Design Procedure to Six-Phase Transmission Lines

The procedure developed by Kimbark [16] for design of the shunt compensation reactors for three-phase double-circuit transmission lines is repeated here for six-phase transmission lines to show that it cannot be applied for unbalanced systems. Two symmetrical polyphase circuits that might be used for the shunt inductive compensation of a six-phase, all of tree form, are shown in fig(38). The most suitable circuit for compensating a six-phase line appears to be that shown in part(b). None of these compensating circuits, however, has more than three different values of reactances, while there are at least four different values of capacitances to be compensated, fig(39). This suggests a connection

of lumped capacitors between opposite phases, A and A' for example, which adds to the distributed shunt capacitances between the opposite phases, to raise them to equality with the capacitances between non-opposite phases. For short lines, the connection of the lumped capacitors between the conductors may balance the line capacitance to a certain degree. For long lines, due to the distributed nature of the line capacitance, the line effective capacitance as seen at the fault varies depending on the fault location. Hence, the lumped capacitors will help in balancing the line effective capacitance at their connection point, but the farther the fault is from that point, the larger the error in calculating the effective capacitance will be; and consequently the unbalance in the system capacitance will still be large. For primary analysis, this error might be tolerable if the line is not too long.

The phasor diagram of the six-phase symmetrical sequences is shown in fig(19). Taking line 'a' as the faulted line, the interline and ground capacitances are as shown in fig(39). To simplify the analysis, the lines are assumed to lie on the corners of a hexagonal. Applying voltages to the mesh circuit in fig(39), applied

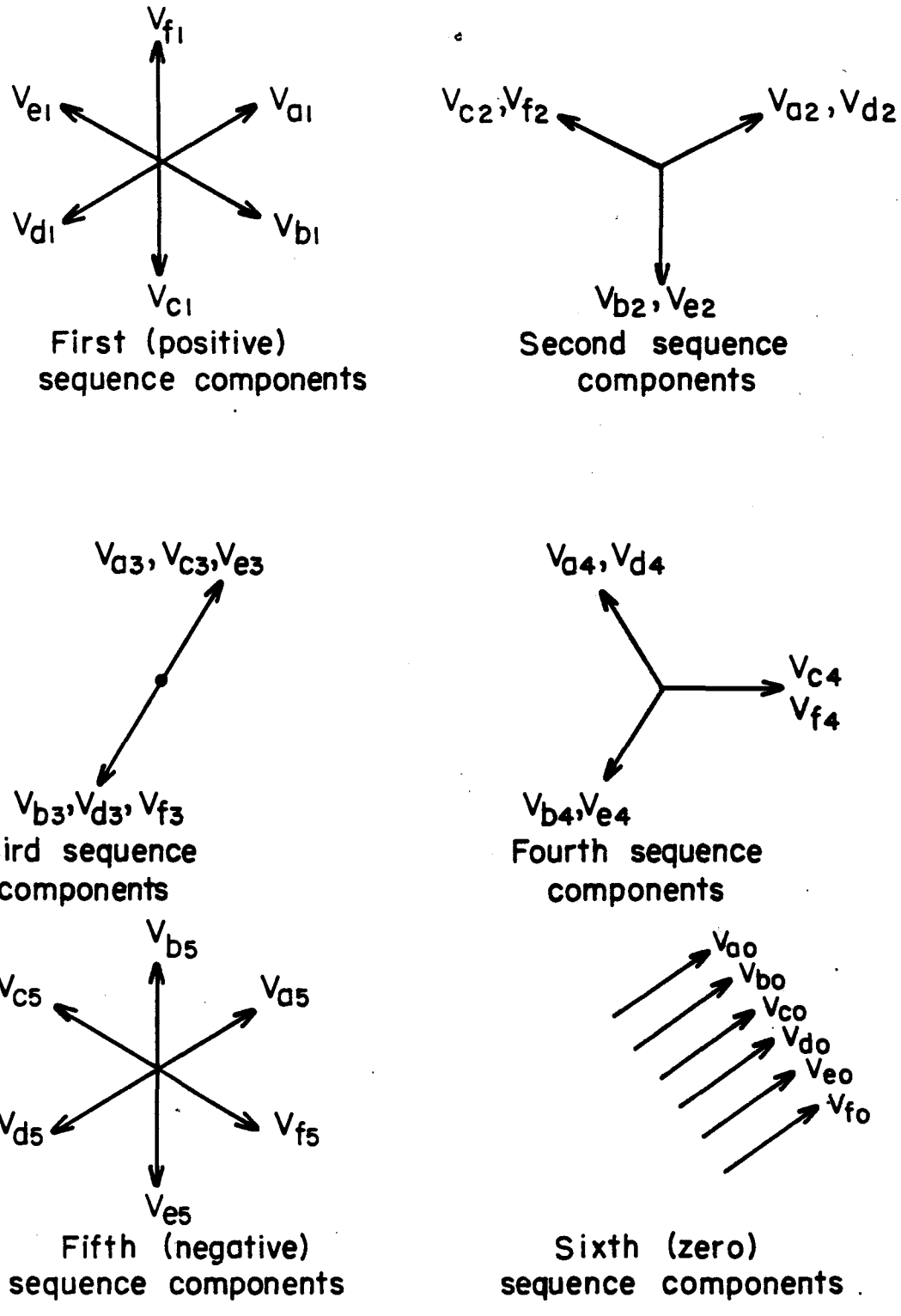

Fig(19) Six-balanced sets of symmetrical components of six unbalanced voltage phasors.

from conductor to ground, yields:

$$I_a=V_aB_{cg}+[2V_a-V_b-V_f]B_{ch} + [2V_a-V_c-V_e]B_{ci}+[V_a-V_d]B_{cj} \quad (4.1)$$

Substituting a set of voltages of one sequence, fig(19), into equation (4.1) yields the following results:

1- For zero sequence, there are equal voltages V_o from every phase to ground. Hence, there is no current in any branch except that from 'a' to ground. Hence:

$$B_{co}=B_{cg} \quad (4.2)$$

2- For positive and fifth sequences the expression is:

$$B_{c1}=B_{cg}+B_{ch}+3B_{ci}+2B_{cj}=B_{c5} \quad (4.3)$$

3- For negative and fourth sequences:

$$B_{c2}=B_{cg}+B_{ch}+3B_{ci}=B_{c4} \quad (4.4)$$

4- For third sequence:

$$B_{c3}=B_{cg}+B_{ch}+2B_{cj} \quad (4.5)$$

where $B_{ck}=wC_k=2\pi fC_k$

The procedure for finding the symmetrical components of the inductive reactances of a shunt tree circuit is the dual of the procedure of the procedure for finding the symmetrical components of shunt capacitive susceptances. A set of currents of a single sequence is impressed on each terminal instead of a voltage, the resulting branch currents and voltage drops are found by inspection,

and drops are summed from phase to ground. Using fig(38b) the results are:

$$X_{L0}=X_p + 2X_m + 6X_n \qquad \text{i}$$
$$X_{L1}=X_p \qquad =X_{L5} \qquad \text{ii} \qquad (4.6)$$
$$X_{L2}=X_p+2X_m \qquad =X_{L4} \qquad \text{iii}$$
$$X_{L3}=X_p \qquad \text{iv}$$

Where the reactances of the compensation reactor's upper branches are assumed all equal. Since there are four capacitance values to be compensated and only three reactance values are present, as mentioned above, it is possible to add a lumped capacitor in parallel with C_j to make $C_j=C_i$. Equations (4.3) through (4.5) become:

$$\begin{vmatrix} \overline{B}_{c_1} \\ B_{c_2} \\ B_{c_3} \end{vmatrix} = \begin{vmatrix} \overline{1} & 1 & \overline{5} \\ 1 & 3 & 3 \\ 1 & 4 & 2 \end{vmatrix} * \begin{vmatrix} \overline{B}_{cg} \\ B_{ch} \\ B_{ci} \end{vmatrix} \qquad (4.7)$$

To calculate the susceptances of the transmission line physical cpacitances B_{cg}, B_{ch}, and B_{ci}, it is necessary to find the inverse of the coefficient matrix in equation (4.7). Unfortunately this coefficient matrix is singular. Hence, a solution of equation (4.7) cannot be found. Thus, this method cannot be used for the analysis of six-phase systems. The main reason for this difficulty is that the method works only for balanced systems. The six-phase system is untransposed and, hence, unbal-

anced. Therefore, symmetrical components analysis is not applicable and Kimbark's compensation design procedure cannot be implemented in the case of six-phase untransposed transmission lines.

4.2 New Design Procedure

4.2.1 Compensation Bank Analysis

Untransposed six-phase transmission lines are usually unbalanced. If they are to be compensated with a shunt compensation bank, one of two options is to be used. Either the shunt compensation bank must be similarly unbalanced or the unbalance of the transmission line shunt capacitive impedances be balanced by adding shunt lumped capacitors. In the first option, only shunt compensation banks are needed. In the latter option a shunt compensation bank and a capacitive bank are needed at each compensation point. When more than one shunt compensation bank is required to compensate a line, the addition of a similar number of capacitive banks seems to be cumbersome. In this research the first option is implemented. The main disadvantage of using unbalanced compensation scheme is the calculation complications. The symmetrical component theory is not applicable and the computations become very lengthy and difficult. However, with the computer at our disposal, this problem is minimal.

The most common configuration of six-phase transmission lines is the stack type as shown in fig(20). The line impedances and capacitances are calculated using the EMTP Line Constants subroutine. The calculation

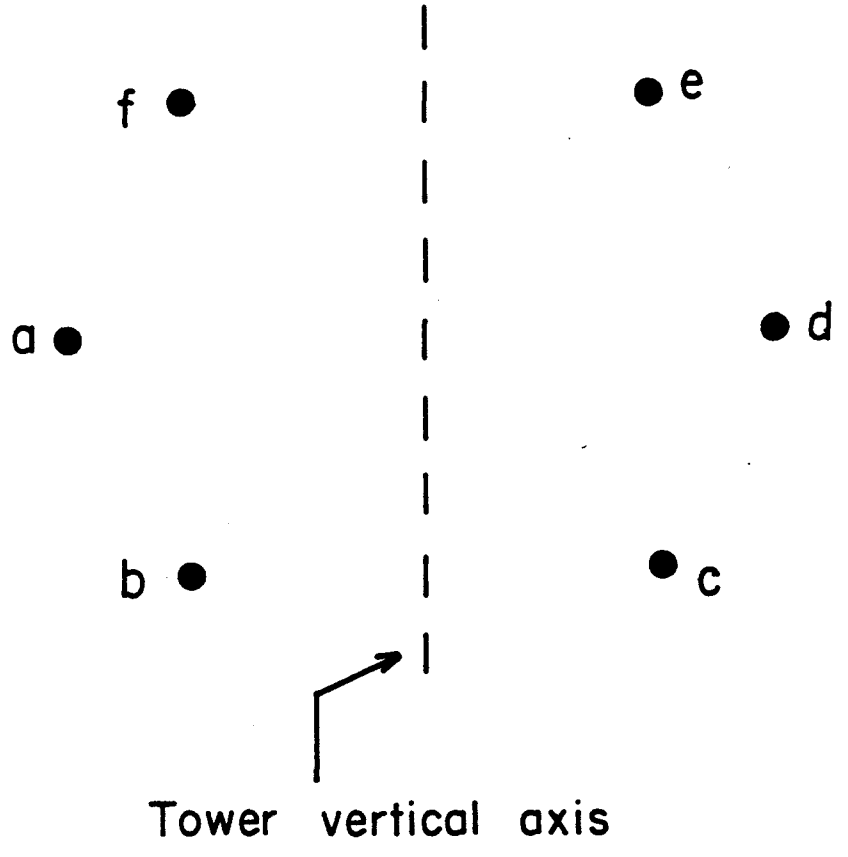

Fig(20) Common six-phase conductor arrangement on tower.

procedure is shown in appendix B. The ground effect is taken into account using Carson's equations [39]. The conductors usually have symmetry about the vertical axis of the tower. The symmetry is reflected into the impedance and capacitance matrices. For the configuration in fig(20), the lines at a certain level above ground have the same impedance and capacitance elements. The capacitance and impedance matrices can be visualized as consisting of three distinct groups of elements. Each group corresponds to a pair of lines at a certain level. The largest unbalance exists between the upper two and the lower two conductors. Thus, when designing a compensation scheme for the transmission lines, all lines symmetrical about the tower vertical axis at a certain level above ground are to be treated the same.

The scheme used to compensate six-phase transmission lines is similar to the one used for compensating three--phase double circuit transmission lines, shown in fig(38b), with some modifications to take into account the unbalance in the line capacitances. It has three different admittance values for the upper six branches, Y_p, Y_{p1}, and Y_{p2}, in addition to the middle and neutral reactors. Thus, a total of five parameters are available and can be varied independently to obtain an optimum compensation scheme for the line. The reason for grouping

the upper six branches into three variable values is to match the three distinct level groups of the transmission lines. The modified compensation reactor bank is shown in fig(21).

4.2.2 Compensation Bank Calculations

The transmission line capacitance matrix is calculated using the EMTP with the ground effect taken into account. The ground wire effect can be included or excluded from the calculations without much extra effort. If line 'a', for instance, is chosen as the faulted line, the line-to-ground and line-to-line equivalent capacitances in addition to the new compensation reactors are connected as shown in fig(22). The lines are assumed to be arranged as in fig(21). It is important to note that the reactors are connected directly to the line equivalent lumped capacitances, and the whole analysis is to be carried out in the real time domain.

Since the compensation reactors and the line capacitors are all in parallel it is easier to work with admittances y rather than impedances. In this analysis y is used to represent an inductive susceptance while y' represents capacitive susceptance. The voltages on the sound phases are assumed to be at normal operating levels. Hence, each phase voltage can be represented

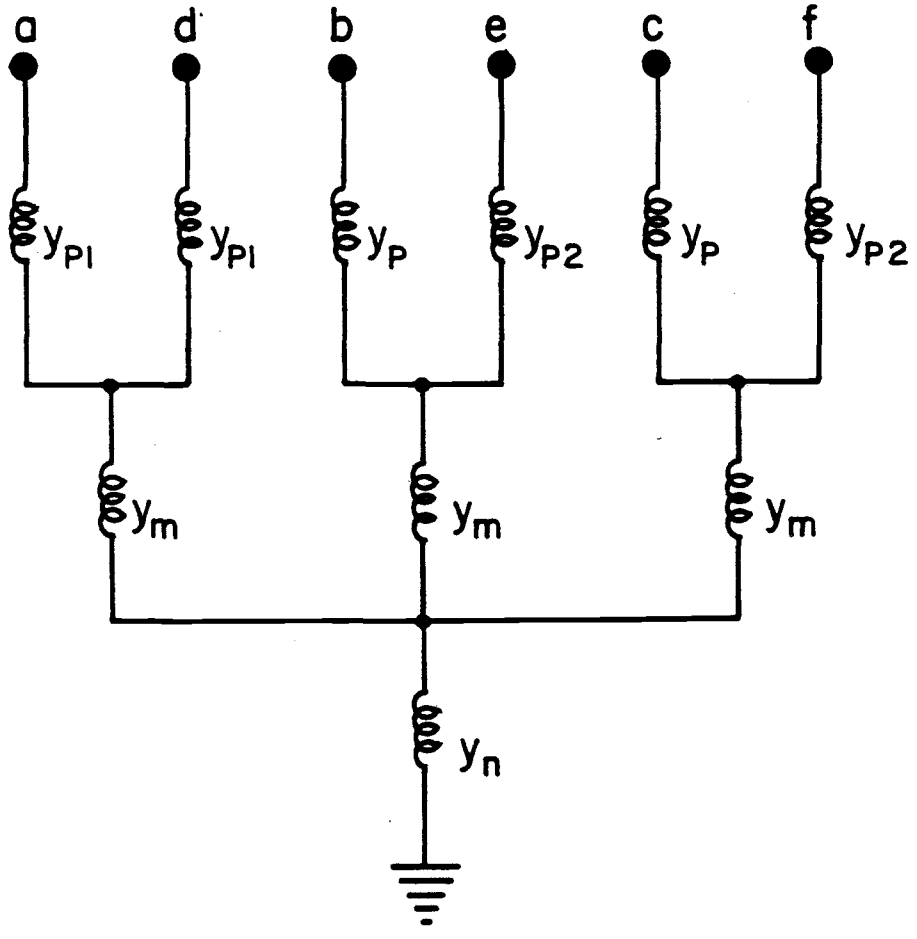

Fig(21) Compensation reactor bank, with different values for upper branch reactors, to be used for compensating six-phase transmission lines.

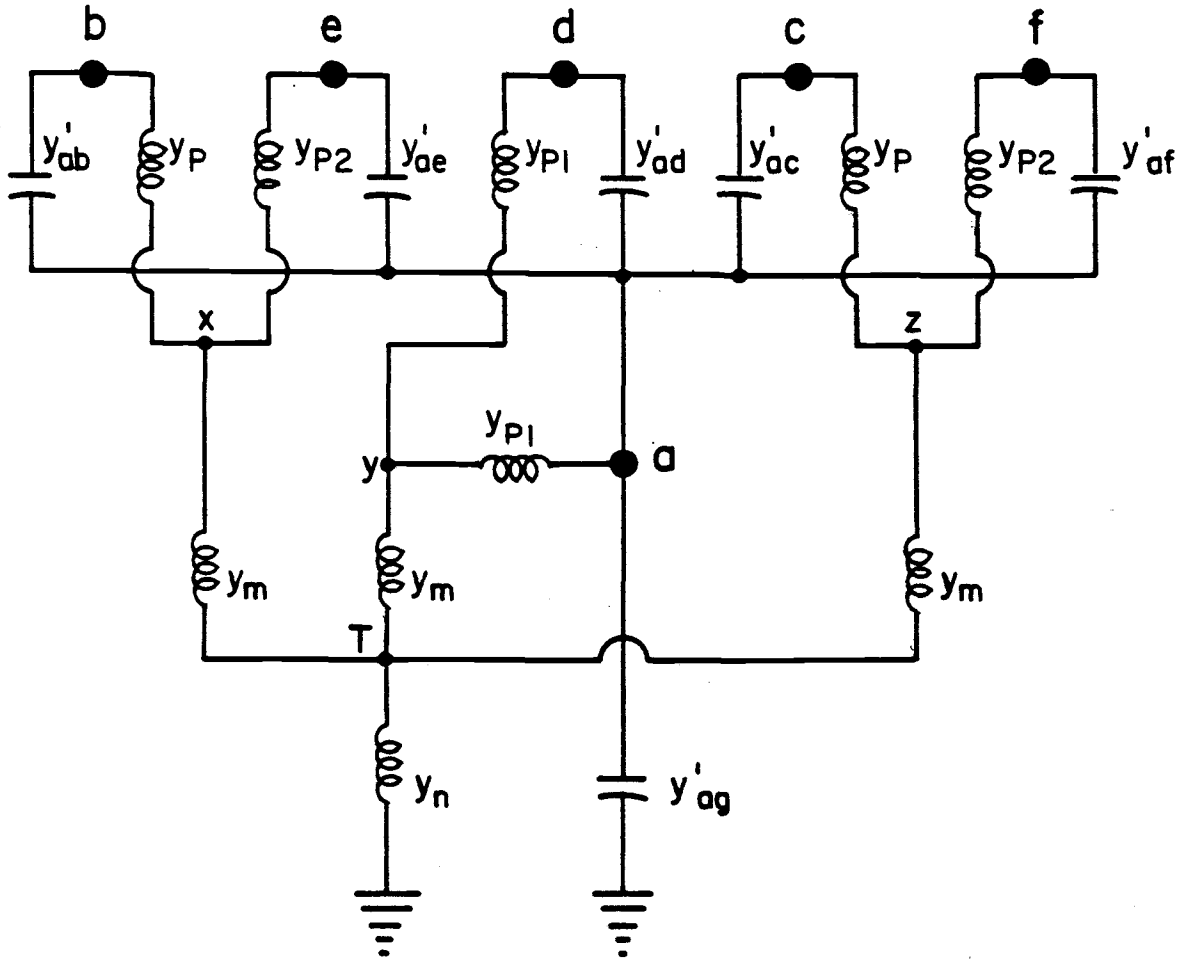

Fig(22) Compensation reactor bank connections to the transmission lines equivalent capacitive susceptances for line 'a' disconnected.

by a phasor of the form:

$$V_k = |V|\underline{/\theta_k} = M\underline{/\theta_k} \qquad (4.8)$$

Where θ_k = 0, 60, 120, ...and k represents any one of the sound phases.

Applying nodal analysis to the circuit in fig(22) yields:

at node a:

$$(V_b-V_a)Y'_{ab}+(V_c-V_a)Y'_{ac}+(V_d-V_a)Y'_{ad}+(V_e-V_a)Y'_{ae}$$

$$+(V_f-V_a)Y'_{af}+(V_y-V_a)Y_{p1}-V_aY'_{ag} = 0 \qquad (4.9)$$

at node y:

$$(V_d-V_y)Y_{p1}+(V_a-V_y)Y_{p1}+(V_T-V_y)Y_m = 0 \qquad (4.10)$$

at node x:

$$(V_b-V_x)Y_p+(V_e-V_x)Y_{p2}+(V_T-V_x)Y_m = 0 \qquad (4.11)$$

at node z:

$$(V_c-V_z)Y_p+(V_f-V_z)Y_{p2}+(V_T-V_z)Y_m = 0 \qquad (4.12)$$

at node T:

$$(V_x-V_T)Y_m+(V_y-V_T)Y_m+(V_z-V_T)Y_m-V_TY_n = 0 \qquad (4.13)$$

In equations (4.9) through (4.13) the unknown voltage V_a represents the capcitively induced voltage on the disconnected line when the transmission system is compensated. The arc current is assumed to be extinguished and hence the arc resistance is infinite. Thus, V_a is equal to the recovery voltage across the arc path. By arranging and grouping sim-

ilar terms, equations (4.9) through (4.13) can be written in matrix form:

$$\begin{vmatrix} Y_{ra} & -Y_{p_1} & 0 & 0 & 0 \\ -Y_{p_1} & Y_{s_1} & 0 & 0 & -Y_m \\ 0 & 0 & Y_{s_2} & 0 & -Y_m \\ 0 & 0 & 0 & Y_{s_2} & -Y_m \\ 0 & -Y_m & -Y_m & -Y_m & Y_q \end{vmatrix} \begin{vmatrix} V_a \\ V_m \\ V_x \\ V_z \\ V_T \end{vmatrix} = \begin{vmatrix} I_a \\ I_{ya} \\ I_{xa} \\ I_{za} \\ 0 \end{vmatrix} \qquad (4.14)$$

where:

$$Y_{ra} = Y'_{ag}+Y'_{ab}+Y'_{ac}+Y'_{ad}+Y'_{ae}+Y'_{af}+Y_{p_1} \qquad (4.15)$$

$$Y_{s_1} = 2Y_{p_1}+Y_m \qquad (4.16)$$

$$Y_{s_2} = Y_p + Y_{p_2} + Y_m \qquad (4.17)$$

$$Y_q = 3Y_m+Y_n \qquad (4.18)$$

$$I_a = V_b Y'_{ab}+V_c Y'_{ac}+V_d Y'_{ad}+V_e Y'_{ae}+V_f Y'_{af} \qquad (4.19)$$

$$I_{ya} = V_d Y_{p_1} \qquad (4.20)$$

$$I_{xa} = V_e(Y_{p_2}-Y_p) \qquad (4.21)$$

$$I_{za} = -V_c(Y_{p_2}-Y_p) \qquad (4.22)$$

Note that all inductive susceptances are negative quantities while capacitive susceptances are positive.

To solve for the recovery voltage V_a in equations (4.14) Gauss-Jordan elimination is used. Using R_n to represent

row (R) number (n), matrix (4.14) is diagonalized as follows:

By adding $\frac{Y_{p1}}{Y_{ra}} * R_1$ to R_2 and adding $\frac{Y_m}{Y_{s_2}} *(R_3+R_4)$ to

R_5 the coefficient matrix in (4.14) becomes:

$$\begin{vmatrix} Y_{ra} & -Y_{p1} & 0 & 0 & 0 \\ 0 & Y_{s_1}-\frac{Y_{p1}^2}{Y_{ra}} & 0 & 0 & -Y_m \\ 0 & 0 & Y_{s_2} & 0 & -Y_m \\ 0 & 0 & 0 & Y_{s_2} & -Y_m \\ 0 & -Y_m & 0 & 0 & Y_{a_1} \end{vmatrix} * \begin{vmatrix} V_a \\ V_y \\ V_x \\ V_z \\ V_T \end{vmatrix} = \begin{vmatrix} I_a \\ I_{ya}+\frac{Y_{p1}}{Y_{ra}} I_a \\ I_{xa} \\ I_{za} \\ \frac{Y_m}{Y_{s_2}} (I_{xa}+I_{za}) \end{vmatrix} \quad (4.23)$$

where $Y_{a_1} = Y_q - \frac{2Y_m^2}{Y_{s_2}}$ (4.24)

Adding $\frac{Y_m}{Y_{a_1}} * R_5$ to R_2 in (4.23) yields:

$$\begin{bmatrix} Y_{ra} & -Y_{p_1} & 0 & 0 & 0 \\ 0 & Y_{a_2} & 0 & 0 & 0 \\ 0 & 0 & Y_{s_2} & 0 & -Y_m \\ 0 & 0 & 0 & Y_{s_2} & -Y_m \\ 0 & -Y_m & 0 & 0 & Y_{a_1} \end{bmatrix} * \begin{bmatrix} V_a \\ V_y \\ V_x \\ V_z \\ V_T \end{bmatrix}$$

$$= \begin{bmatrix} I_a \\ I_{ya} + \frac{Y_{p_1}}{Y_{ra}} I_a + \frac{Y_m^2}{Y_{a_1} Y_{s_2}} (I_{xa} + I_{za}) \\ I_{xa} \\ I_{za} \\ \frac{Y_m}{Y_{s_2}} (I_{xa} + I_{za}) \end{bmatrix} \qquad (4.25)$$

where: $$Y_{a_2} = Y_{s_1} - \frac{Y_{p_1}^2}{Y_{ra}} - \frac{Y_m^2}{Y_{a_1}} \qquad (4.26)$$

Finally, adding $\frac{Y_{p_1}}{Y_{a_2}} * R_2$ to R_1 in (4.25) yields:

$$\begin{vmatrix} \overline{Y}_{ra} & 0 & 0 & 0 & 0 \\ 0 & Y_{a_2} & 0 & 0 & 0 \\ 0 & 0 & Y_{s_2} & 0 & -Y_m \\ 0 & 0 & 0 & Y_{s_2} & -Y_m \\ 0 & -Y_m & 0 & 0 & Y_{a_1} \end{vmatrix} * \begin{vmatrix} \overline{V}_a \\ V_y \\ V_x \\ V_z \\ V_T \end{vmatrix}$$

$$= \begin{vmatrix} I_a + \frac{Y_{p1}}{Y_{a_2}} \left| I_{ya} + \frac{Y_{p1}}{Y_{ra}} I_a + \frac{Y_m^2}{Y_{a_1} Y_{s_2}} (I_{xa} + I_{za}) \right| \\ I_{ya} + \frac{Y_{p1}}{Y_{ra}} I_a + \frac{Y_m^2}{Y_{a_1} Y_{s_2}} (I_{xa} + I_{za}) \\ I_{xa} \\ I_{za} \\ \frac{Y_m}{Y_{s_2}} (I_{xa} + I_{za}) \end{vmatrix} \quad (4.27)$$

From Equation (4.27) the capacitively coupled recovery voltage on the disconnected line 'a' is:

$$V_a = \frac{1}{Y_{ra}}\left|\bar{I}_a\left(1+\frac{Y_{pl}^2}{Y_{a_2}Y_{ra}}\right)+I_{ya}\frac{Y_{pl}}{Y_{a_2}} + \frac{Y_{pl}Y_m^2}{Y_{a_1}Y_{a_2}Y_{s_2}}(I_{xa}+\bar{I}_{za})\right| \quad (4.28)$$

The complex values of the parameters in equation (4.28) can be calculated using the prefault voltage sequence diagram shown in fig(19) for the sound phases. Thus, the voltages on the unfaulted lines are assumed to remain balanced after the faulted line is disconnected. This assumption does not hold for loaded conditions. However, for large systems, where six-phase transmission seems to find most of its applications, the unbalances are not very significant and hence the error in the calculations due to this assumption will be minimal. Moreover, the shunt compensation reactors are designed to minimize the capacitive coupling between the faulted line and the sound phases. This type of coupling is a function of the line voltage but not of its loading. Consequently, performing the calculations under the assumption of balanced postfault voltages simplifies the analysis and yields only tolerable error. Using fig(23), equation (4.19) yields:

$$I_a = M\angle 60^{\circ} * jY'_{ab} + M\angle 120^{\circ} * jY'_{ac} + M\angle 180^{\circ} * jY'_{ad} + M\angle -120^{\circ} * jY'_{ae} + M\angle -60^{\circ} * jY'_{af} \quad (4.29)$$

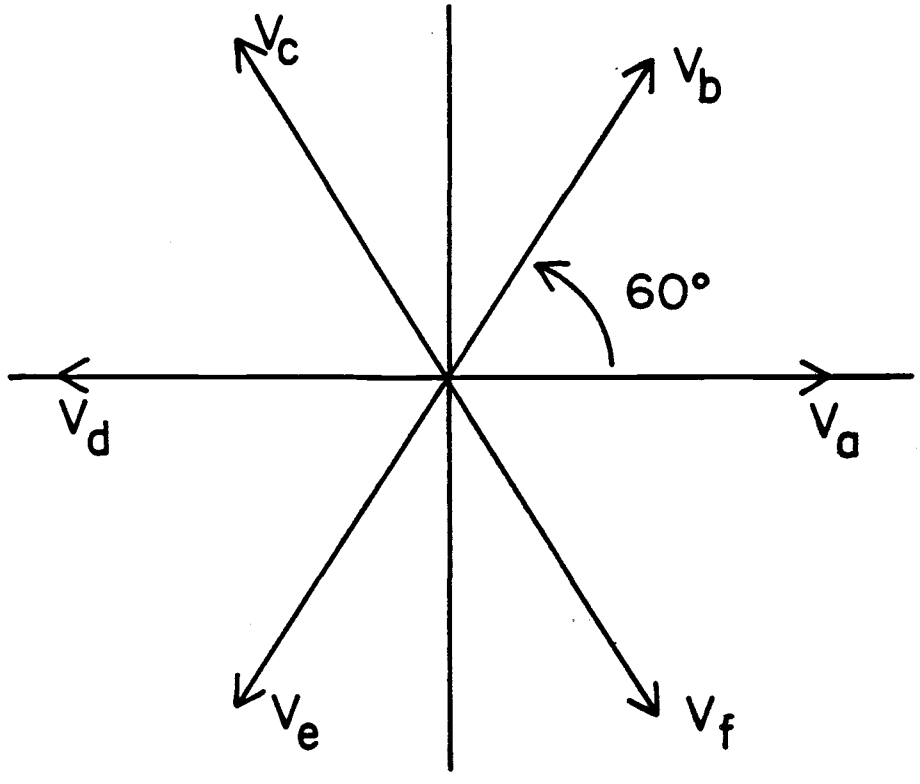

Fig(23) Six-phase voltages diagram.

Combining terms and simplifying produces:

$$I_a = M[j(Y'_{ae} - Y'_{ab})(\cos(-120)+j \sin(-120)) + j(Y'_{ac}-Y'_{af})$$

$$(\cos(120)+j \sin(120))+j Y'_{ad}(\cos(180)+j \sin(180))] \quad (4.30)$$

$$= -M\left|\underline{(Y'_{ae} - Y'_{ab}) \sin(-120) + (Y'_{ac} - Y'_{af}) \sin(120)}\right|$$

$$+ jM\left|\underline{(Y'_{ae} - Y'_{ab}) \cos(-120) + (Y'_{ac} - Y'_{af}) \cos(120) - Y'_{ad}}\right|$$

$$= M(I_{ar} + j I_{ax}), \quad (4.31)$$

where M is the magnitude of the system line-to-ground voltage. From equation (4.15)

$$Y_{ra} = j(Y'_{ag} + Y'_{ab} + Y'_{ac} + Y'_{ad} + Y'_{ae} + Y'_{af} + Y_{p1})$$

$$= j(Y'_{aa} + Y_{p1}) = jR_a \quad (4.32)$$

Y_{p1} is an inductive susceptance and hence it is an inherently negative quantity. From equations (4.17), (4.18), and (4.24),

$$Y_{a1} = j\left(3Y_m + Y_n - \frac{2 Y_m^2}{Y_p + Y_{p2} + Y_m}\right) = jQ_a \quad (4.33)$$

Also, from equations (4.16), (4.32), and (4.33),

$$Y_{a2} = j\left(2Y_{p1} + Y_m - \frac{Y_{p1}^2}{R_a} - \frac{Y_m^2}{Q_a}\right) = jP_a \quad (4.34)$$

Substituting from equations (4.16), (4.17), (4.20), (4.21), (4.22), and (4.31) - (4.34) into equation (4.28) yields:

$$V_a = \frac{M}{jR_a}\left[(I_{ar} + jI_{ax})\left(1 + \frac{Y_{p1}^2}{P_a R_a}\right) - j\frac{Y_{p1}^2}{P_a} + \frac{2Y_{p1}\, Y_m^2\, (Y_{p2}-Y_p)\sin(120)}{P_a\, Q_a\, (Y_p + Y_{p2} + Y_m)}\right]$$

$$= \frac{M}{R_a}\left[I_{ax}\left(1 + \frac{Y_{p1}^2}{P_a\, R_a}\right) - \frac{Y_{p1}^2}{P_a}\right]$$

$$-j\frac{M}{R_a}\left[I_{ar}\left(1+\frac{Y_{p1}^2}{P_a R_a}\right) + \frac{2Y_{p1}\, Y_m^2\, (Y_{p2}-Y_p)\sin(120)}{P_a Q_a (Y_p+Y_{p2}+Y_m)}\right]$$

$$= M\,(V_{ar} - jV_{ax})\,, \qquad (4.35)$$

where V_{ar} and V_{ax} are the per unit real and imaginary components of V_a, respectively. Equation (4.35) indicates that V_a can be calculated for any circuit voltage level by simply varying the system voltage magnitude (M). The capacitive component of the secondary arc current of line 'a' (I_{sa}) can be calculated in the same way as the recovery voltage (V_a). Assuming a worst case, where the arc path resistance is zero, an expression for I_{sa} similar to that of V_a in equation (4.28) can be derived by simply replacing the equivalent lumped capacitive susceptance from line 'a'

to ground (Y'_{ag}) in fig(22) with a short circuit and repeating the calculation process. The capacitively coupled secondary arc current I_{sa} is the total current from line 'a' to ground at the fault point. After simplification, the expression for I_{sa} comes out to be:

$$I_{sa} = I_a\left(1+\frac{Y_{p1}^2}{Y_{a_2}Y_{ra}}\right)+I_{ya}\frac{Y_{p1}}{Y_{a_2}} + \frac{Y_{p1}\,Y_m^2}{Y_{a_1}Y_{a_2}Y_{s_2}}(I_{xa}+I_{za}), \quad (4.36)$$

where all the parameters in equation (4.36) are as defined above for V_a. By substituting the expressions for the parameters in (4.36) I_{sa} becomes:

$$I_{sa} = M\left|(I_{ar}+jI_{ax})\left(1+\frac{Y_{p1}^2}{P_aR_a}\right)-j\frac{Y_{p1}^2}{P_a}+\frac{2Y_{p1}Y_m^2(Y_{p_2}-Y_p)\sin(120^\circ)}{P_aQ_a\,(Y_p+Y_{p_2}+Y_m)}\right|$$

$$= M\left|(I_{ar}\left(1+\frac{Y_{p1}^2}{P_aR_a}\right) + \frac{2Y_{p1}Y_m^2(Y_{p_2}-Y_p)\,\sin(120^\circ)}{P_aQ_a\,(Y_p+Y_{p_2}+Y_m)}\right|$$

$$+jM\left|I_{ax}\left(1+\frac{Y_{p1}^2}{P_a\,R_a}\right) - \frac{Y_{p1}^2}{P_a}\right|$$

$$= M\,[\,I_{sar} + j\,I_{sax}\,]\,, \quad (4.37)$$

where I_{sar} and I_{sax} represent the real and imaginary components of the secondary arc current on line 'a', (I_{sa}), repectively.

Because of line unbalance, the recovery voltages

and secondary arc currents are not the same on all lines. However, because of lines symmetry about the vertical axis of the tower as shown in fig(20), each two lines behave similarly. Thus, it is necessary to calculate only two voltages, V_f, and V_b, for completing the compensation reactor design. The compensation reactor parameters are then to be varied such as to minimize all the three different voltages, V_a, V_b, and V_f, at the same time.

To calcualte the capacitively coupled recovery voltage on line 'b', when it is disconnected at both ends, the procedure used above for line 'a' is to be followed. The result is:

$$V_b=\frac{1}{Y_{rb}}\left|\bar{I}_b\left(1+\frac{Y_p^2}{Y_{b_2}Y_{rb}}\right)+I_{xb}\,\frac{Y_p}{Y_{b_2}}+\frac{Y_p\,Y_m^2}{Y_{b_1}Y_{b_2}Y_{s_2}}\,\bar{I}_{zb}\right|, \quad (4.38)$$

where: $Y_{rb}= Y'_{bg}+Y'_{ab}+Y'_{bc}+Y'_{bd}+Y'_{be}+Y'_{bf}+Y_p= jR_b$ (4.39)

$$Y_{s_1} = 2Y_{p_1} + Y_m \quad (4.40)$$

$$Y_{s_2} = Y_p + Y_{p_2} + Y_m \quad (4.41)$$

$$Y_q = 3Y_m + Y_n \quad (4.42)$$

$$I_b= V_aY'_{ab}+ V_cY'_{bc}+ V_dY'_{bd}+ V_eY'_{be}+ V_fY'_{bf} \quad (4.43)$$

$$I_{xb} = V_e\, Y_{p_2} \quad (4.44)$$

$$I_{zb} = V_c\,(\,Y_p - Y_{p_2}) \quad (4.45)$$

$$Y_{b_1} = Y_q - \frac{Y_m^2}{Y_{s_2}} - \frac{Y_m^2}{Y_{s_1}} = j\,Q_b \qquad (4.46)$$

$$Y_{b_2} = Y_{s_2} - \frac{Y_p^2}{Y_{rb}} - \frac{Y_m^2}{Y_{b_1}} = j\,P_b \qquad (4.47)$$

Substituting for the parameters in equation (4.38) and using the voltage phasor diagram in fig(23) yields:

$$V_b = \frac{M}{jR_b}\left|\bar{}\right.(I_{br} + jI_{bx})\left(1+\frac{Y_p^2}{P_bR_b}\right)+j\,\frac{Y_p\,Y_{p_2}}{P_b}(\cos(-120)+j\sin(-120))$$

$$+j\,\frac{Y_p\,Y_m^2\,(Y_p - Y_{p_2})}{Q_b\,P_b(Y_p + Y_{p_2} + Y_m)}(\cos(120)+j\,\sin(120))\left.\bar{}\right|$$

$$= \frac{M}{R_b}\left|\bar{}\right. I_{bx}\left(1+\frac{Y_p^2}{P_bR_b}\right)+\frac{Y_pY_{p_2}}{P_b}\cos(-120)+\frac{Y_pY_m^2(Y_p-Y_{p_2})\cos(120)}{Q_bP_b(Y_p+Y_{p_2}+Y_m)}\left.\bar{}\right|$$

$$-j\frac{M}{R_b}\left|\bar{}\right. I_{br}\left(1+\frac{Y_p^2}{P_aR_b}\right)+\frac{Y_pY_{p_2}}{P_b}\sin(120)-\frac{Y_pY_m^2(Y_p-Y_{p_2})\sin(120)}{Q_bP_b(Y_p+Y_{p_2}+Y_m)}\left.\bar{}\right|$$

$$= M\left|\bar{}\right. V_{br} - j\,V_{bx}\left.\bar{}\right|\,, \qquad (4.48)$$

where

$$I_b = V_aY'_{ab} + V_cY'_{bc} + V_dY'_{bd} + V_eY'_{be} V_fY'_{bf}$$

$$= M \left| -jY'_{ab} - jY'_{bd} + j(Y'_{bc} - Y'_{bf})(\cos(120) + j \sin(120)) \right.$$

$$\left. + j\, Y'_{be}(\cos(-120) + j \sin(-120)) \right|$$

$$= -M \left| (Y'_{bc} - Y'_{bf})\sin(120) + Y'_{be}\sin(-120) \right|$$

$$+jM \left| -Y'_{ab} - Y'_{bd} + (Y'_{bc} - Y'_{bf})\cos(120) + Y'_{be}\cos(-120) \right|$$

$$= M \left| -I_{br} + j\, I_{bx} \right| \qquad (4.49)$$

In the same manner, as for line 'a', the capacitively coupled secondary arc current for line 'b', I_{sb}, can be calculated:

$$I_{sb} = M \left| (I_{br} + jI_{bx})\left(1 + \frac{Y_p^2}{P_b R_b}\right) + j\frac{Y_p\, Y_{p2}}{P_b}(\cos(-120) + j \sin(-120)) \right.$$

$$\left. + j\frac{Y_p Y_m^2 \,(Y_p - Y_{p2})}{Q_b P_b\,(Y_p + Y_{p2} + Y_m)}(\cos(120) + j \sin(120)) \right|$$

$$= M \left| I_{br}\left(1 + \frac{Y_p^2}{P_b R_b}\right) + \frac{Y_p Y_{p2}}{P_b} \sin(120) - \frac{Y_p Y_m^2 (Y_p - Y_{p2})\sin(120)}{Q_b P_b (Y_p + Y_{p2} + Y_m)} \right|$$

$$+jM \left| I_{bx}\left(1 + \frac{Y_p^2}{P_b R_b}\right) + \frac{Y_p Y_{p2}}{P_b} \cos(-120) + \frac{Y_p Y_m^2 (Y_p - Y_{p2})\cos(120)}{Q_b P_b (Y_p + Y_{p2} + Y_m)} \right|$$

$$= M \left| \bar{I}_{sbr} + j\, I_{sbx} \right| \qquad (4.50)$$

Similarly, the capacitive component of the recovery voltage on line 'f' is:

$$V_f = \frac{1}{jR_f} \left| \bar{I}_f \left(1 + \frac{Y_{p2}^2}{P_f R_f}\right) + I_{zf} \frac{Y_{p2}}{P_f} + I_{xf} \frac{Y_{p2}\, Y_m^2}{Q_f P_f Y_{s2}} \right|, \qquad (4.51)$$

where: Y_{s1}, Y_{s2}, Y_q are as defined above for line 'b',

and $$jR_f = Y_{rf} = Y'_{fg} + Y'_{af} + Y'_{bf} + Y'_{cf} + Y'_{df} + Y'_{ef} + Y_{p2} \qquad (4.52)$$

$$j P_f = Y_q - \frac{Y_m^2}{Y_{s2}} - \frac{Y_m^2}{Y_{s1}} = Y_{f1} \qquad (4.53)$$

$$jQ_f = Y_{s2} - \frac{Y_{p2}^2}{Y_{rf}} - \frac{Y_m^2}{Y_{f1}} = Y_{f2} \qquad (4.54)$$

$$I_f = V_a Y'_{af} + V_b Y'_{bf} + V_c Y'_{cf} + V_d Y'_{df} + V_e Y'_{ef}$$

$$= M[j(Y'_{af} - Y'_{df}) + j(Y'_{ef} - Y'_{bf})(\cos(-120) + j \sin(-120)) +$$

$$jY'_{cf}(\cos(120) + j \sin(120))]$$

$$= M[(Y'_{ef} - Y'_{bf}) \sin(120) - Y'_{cf} \sin(120)]$$

$$+ jM[Y'_{af} - Y'_{df} + (Y'_{ef} - Y'_{bf}) \cos(120) + Y'_{cf} \cos(120)]$$

$$= M[I_{fr} + j\, I_{fx}] \qquad (4.55)$$

$$I_{xf} = (Y_{p2} - Y_p) V_e = jM(Y_{p2} - Y_p)(\cos(+120) + j \sin(-120)) \qquad (4.56)$$

$$I_{zf} = V_c Y_p = jMY_p(\cos(120) + j \sin(120)) \qquad (4.57)$$

Substituting equations (4.52)-(4.57) into equation (4.51) yields:

$$V_f = \frac{M}{jR_f}\left[(I_{fr}+jI_{fx})\left(1+\frac{Y_{p2}^2}{P_f R_f}\right)+j\frac{Y_{p2}\,Y_p}{P_f}\,(\cos(120)+j\sin(120))\right.$$

$$\left.+j\frac{Y_{p2}\,Y_m^2(Y_{p2}-Y_p)}{Q_f\,P_f\,Y_{s_2}}\,(\cos(-120)+j\sin(-120))\right]$$

$$=\frac{M}{R_f}\left[I_{fx}\left(1+\frac{Y_p^2}{P_f R_f}\right)+\frac{Y_{p2}\,Y_p}{P_f}\cos(120)+\frac{Y_{p2}\,Y_m^2(Y_{p2}-Y_p)\cos(-120)}{Q_f\,P_f\,Y_{s_2}}\right]$$

$$-\frac{jM}{R_f}\left[I_{fr}\left(1+\frac{Y_p^2}{P_f R_f}\right)-\frac{Y_{p2}\,Y_p}{P_f}\sin(120)+\frac{Y_{p2}\,Y_m^2(Y_{p2}-Y_p)\sin(120)}{Q_f\,P_f\,Y_{s_2}}\right]$$

$$= M[V_{fr}- jV_{fx}] \qquad (4.58)$$

Also, the capacitively coupled secondary arc current on line 'f' can be calculated in the same way as I_{sa}. The results are:

$$I_{sf}=M\left[I_{fr}\left(1+\frac{Y_{p2}^2}{P_f R_f}\right)-\frac{Y_{p2}^2\,Y_p}{P_f}\sin(120)+\frac{Y_{p2}\,Y_m^2(Y_{p2}-Y_p)\sin(120)}{Q_f\,P_f\,Y_{s_2}}\right]$$

$$+jM\left[I_{fx}\left(1+\frac{Y_{p2}^2}{P_f R_f}\right)+\frac{Y_{p2}\,Y_p}{P_f}\cos(120)+\frac{Y_{p2}\,Y_m^2(Y_{p2}-Y_p)\cos(120)}{Q_f\,P_f\,Y_{s_2}}\right]$$

$$= M\,[I_{sfr}+ j\,I_{sfx}], \qquad (4.59)$$

Where I_{sfr} and I_{sfx} are the real and imaginary components

of the capacitively coupled secondary arc current of line 'f', respectively.

There are five parameters in the compensation reactor bank to be varied to minimize the three recovery voltages V_a, V_b, and V_f. In otherwords, three equations in five unknowns are to be solved for an optimum solution. It is almost impossible to perform these calculations by hand. Thus, a digital computer is necessary.

4.2.3 Optimization of the Compensation Scheme Parameters

The three capacitively coupled recovery voltage expressions, shown by equations (4.35), (4.48), and (4.58), and the corresponding secondary arc current expressions, given by equations (4.37), (4.50), and (4.59), are derived for separate cases. In each case, only one line is open while all other phases are carrying rated load current at normal operating voltage levels. Due to this and to the fact that the lines are not transposed, the various phase recovery voltages and secondary arc currents will behave independently for the three separate cases. Thus, if the shunt compensation scheme is designed to minimize the capacitive components of the recovery voltage and the secondary arc current on any particular phase, the recovery voltages and the secon-

dary arc currents on the other phases will not be necessarily minimized. The recovery voltage and the secondary arc current on a shunt compensated circuit can be very low on some lines while still at unacceptable higher values on the others when each of the lines is singly opened. Consequently, the compensation scheme is to be designed to satisfy the following requirements:

1. The recovery voltage on any line of the compensated circuit is less than the permissable upper limit. As mentioned above, a ten percent of normal circuit voltage can be tolerated as an upper limit on the recovery voltage.

2. The capacitive component of the secondary arc current of any phase is maintained below the 18 amp limit for circuits of less than 230 KV rated voltage, and below 35 amps for circuits of higher voltage ratings. These current limits, as mentioned above, will assure successful single-phase reclosure within 30 cycles.

3. The above two requirements can be satisfied, to a certain extent, with a wide range of shunt compensation scheme impedance values. However,

as the shunt compensation scheme impedance decreases, its steady state loading effect increases. Consequently, the steady state ratings of the reactors are increased and hence the cost of building such a scheme are increased. In addition to that, the system losses will increase. Thus, the best shunt compensation scheme is the one that satisfies requirements 1 and 2 above and has the highest impedance values possible. A shunt reactor steady state loading of less than 10% of the rated system current appears to be an acceptable limit[1].

A digital computer program called CMPLX has been written to evaluate the capacitively coupled recovery voltage and secondary arc current equations for various values of the compensation scheme parameters y_{p2}, y_{p1}, y_p, y_m, and y_n. The input to CMPLX consists of the line capacitance values and the range and number of intervals of each parameter. The program will automatically evaluate the recovery voltage and the secondary arc current equations of each line for all possible combinations of the various parameter values. The output of the program is a list of recovery voltage and secondary arc

[1]By personal communication with professor G.C. Alexander.

current values. In addition to that, the program will print out the parameter values that correspond to the set of minimum recovery voltages and those corresponding to the set of minimum secondary arc currents. Because the capacitive components of the recovery voltage and the secondary arc current of each line are related mainly through the line constants and the compensation reactor parameters, as shown in the expressions above, their minima will not necessarily be at the same set of parameter values. However, a compromise solution that satisfies the three compensation reactor requirements mentioned above can be found inbetween the two minima by inspection of program CMPLX's output. A flowchart of program CMPLX is shown in fig(24).

Program CMPLX is mainly a search program. It evaluates the capacitive components of the recovery voltages and the secondary arc currents for all possible combinations of the specified compensation scheme element values. The program then searches the output. When each one of the recovery voltages V_a, V_b, and V_f is less than 9% of the circuit voltage, the recovery voltages, secondary arc currents, and parameter values will be printed out.

Choosing the ranges of compensation scheme element values where minimum recovery voltages and secondary

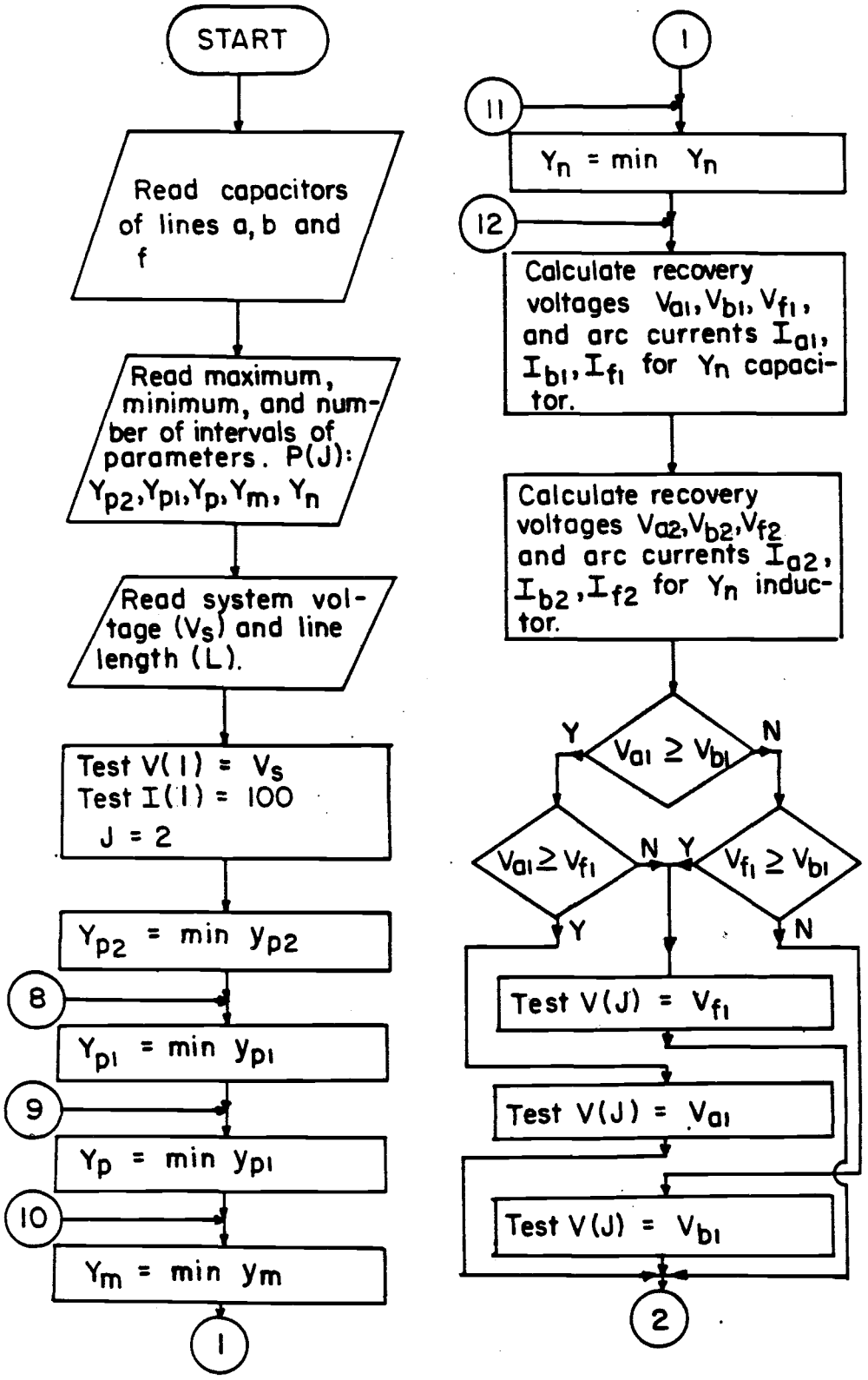

Fig(24) . A flowchart of program CMPLX.

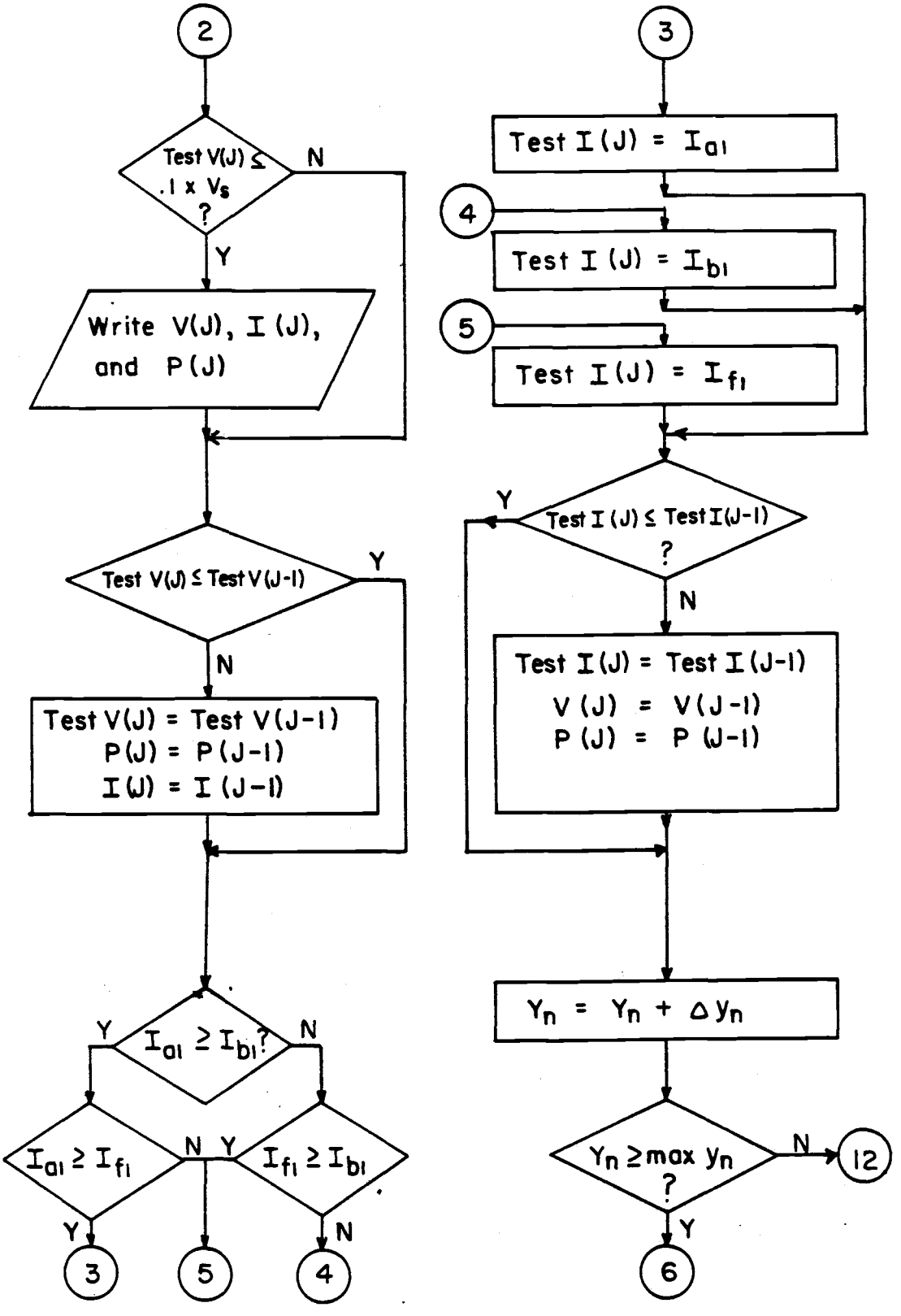

Fig(24) A flowchart of program CMPLX. (Continued)

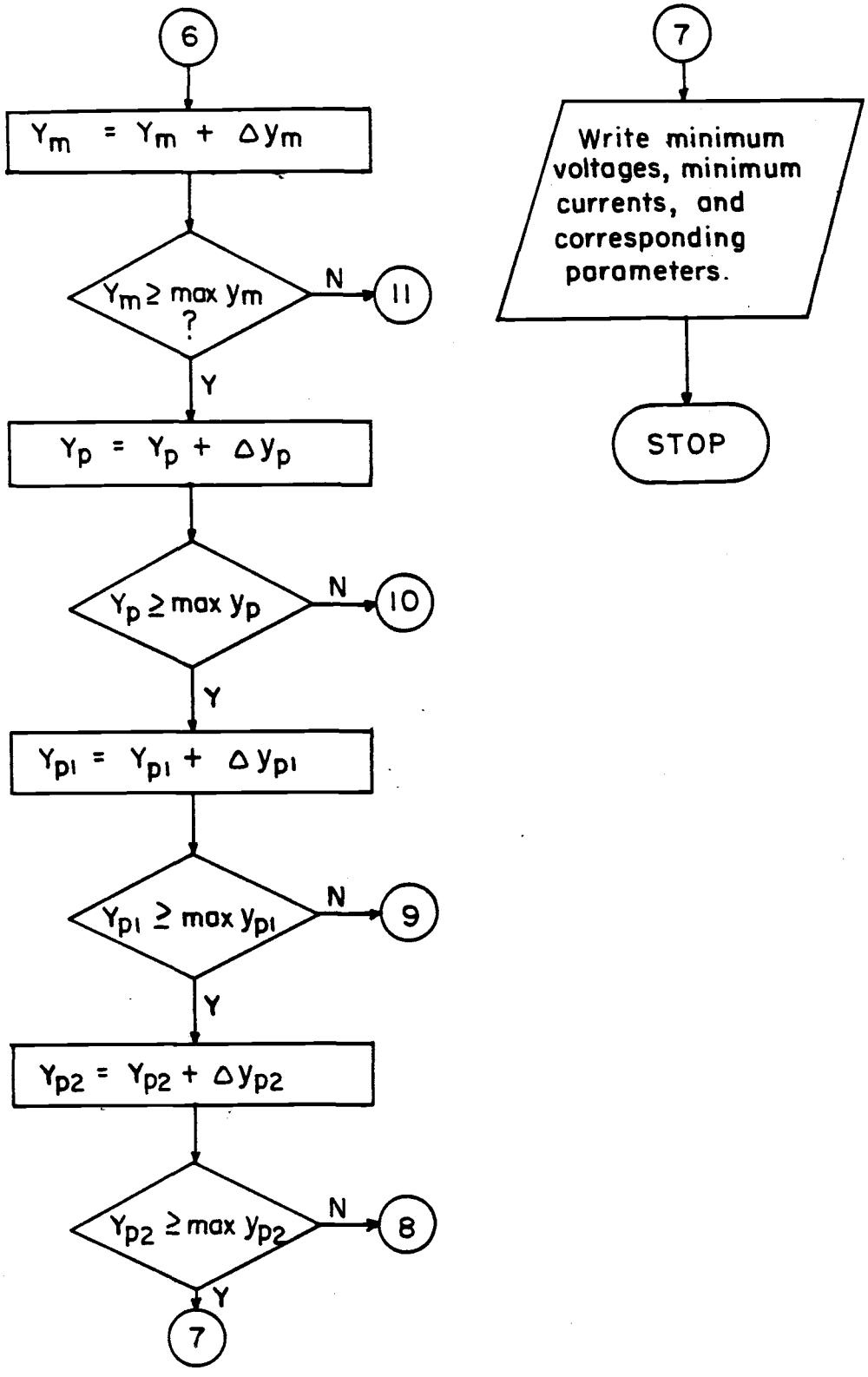

Fig(24) A flowchart of program CMPLX. (Continued)

arc currents will be found is not an easy task; especially when the system is unbalanced. The best way to do it is to start with wide ranges and large intervals. By inspecting the general pattern of CMPLX's output, it is possible to define smaller ranges where acceptable voltage and current values can be obtained. Sketching the recovery voltages and secondary arc currents versus the compensation scheme element values proves to be useful. Using the new determined ranges and increasing the number of intervals in each range will result in a precise solution.

There are some hints that are useful when first choosing the ranges of the compensation scheme element values. The maximum values of the phase reactor admittances Y_{P2}, Y_{P1}, and Y_P must satisfy requirement (3), as mentioned above. Of course, Y_{P2}, Y_{P1}, and Y_P are not equal, as mentioned before, but an upper limit on their values could be chosen the same. The minimum values of the admittances Y_{P2}, Y_{P1}, and Y_P can be chosen equal to the admittance of the smallest interline capacitance. This is a very conservative choice but it gives an absolute lower limit on the minimum of the compensation scheme admittances. This is because a capcitive circuit of tree form, similar to that of fig(38), will have capacitance values of the upper legs which are larger than

the capacitance values of the interline branches in the mesh circuit of fig(39).

To be more specific consider a balanced three--phase system similar to that shown in appendix A, for instance. The smallest branch in the mesh circuit, fig(39), is:

$$C_j \leq (2C_1 - C_0 - C_3)/6$$

For an equivalent capacitive circuit of tree form the upper leg will be:

$$C_p = C_1$$

which is much greater than C_j. This does not suggest that balanced system analysis applies to an unbalanced system, but it supports the above argument. The medium leg impedance (X_m) is a function of the system characteristics. For balanced systems, X_m takes values in the range of 100 ohms or less while for unbalanced systems it can take values in the range of 10 to 1000 ohms[2]. Test results, of which some were cited in chapter (2), and results obtained during this research indicated that the neutral leg admittance y_n usually has values in the range between 5 mmho and 0.1 mmho. For balanced systems, the range is between 5 mmho and 1 mmho.

The shunt compensation scheme is designed to minimize the effect of the capacitive coupling of the

---

[2]Reference [23] and test results of this research.

transmission lines. The scheme admittances are calculated using the line equivalent lumped capacitive admittances. In other words, the magnetic coupling and the effect of the line capacitance distribution are not taken into account in the reactor design. However, as mentioned at the beginning of this chapter, the limits set on the capacitive coupling are lower than the acceptable limits of the total coupling. This will allow enough margin to take these effects into account without exceeding the recovery voltage and the secondary arc current upper limits.

Primary simulation results obtained during this research indicate that the best shunt compensation scheme for a 200 mile long line is the one that has two reactor banks one at each end of the line. Each compensation reactor bank is designed to compensate a 100 mile section.

To test the performance of the design, the transmission system with the compensation reactors connected to it is simulated on a digital computer using the Electromagnetic Transient Program (EMTP) [40]. The transmission lines are represented in the EMTP input by their equivalent impedance and admittance matrices. The EMTP utilizes these matrices to construct the well-known transmission line voltage-current relations. It then solves the resulting system of equations by first diagonalizing

the coefficient matrices and then solves for the resulting uncoupled modes using single-line analysis in what is called the "mode domain". The solution is then transformed back to the phase domain. The transformation matrices used to transform the line equations from phase domain to mode domain and vice versa are to be provided by the user. Because the transmission lines are not transposed, these transformation matricies are complex. For fully transposed lines, these matrices have only real elements. The EMTP has subroutines that generate the transformation matrices for transposed and untransposed lines.

The test system to be simulated is shown in fig(25). The load can be taken into account by phase angle difference between sources at sending and receiving ends. Transformers are not included in the simulated system nor in the analysis because they are found to have no impact on the compensation reactor performance. This is because, in the case of a single-pole switching, the compensation reactors are switched with the disconnected line. On the contrary, the transformers are not to be switched with the line and hence their effect on the compensation is not significant. The transformers, if present, will draw some current and this, of course, will increase the line voltage drop. Under normal load

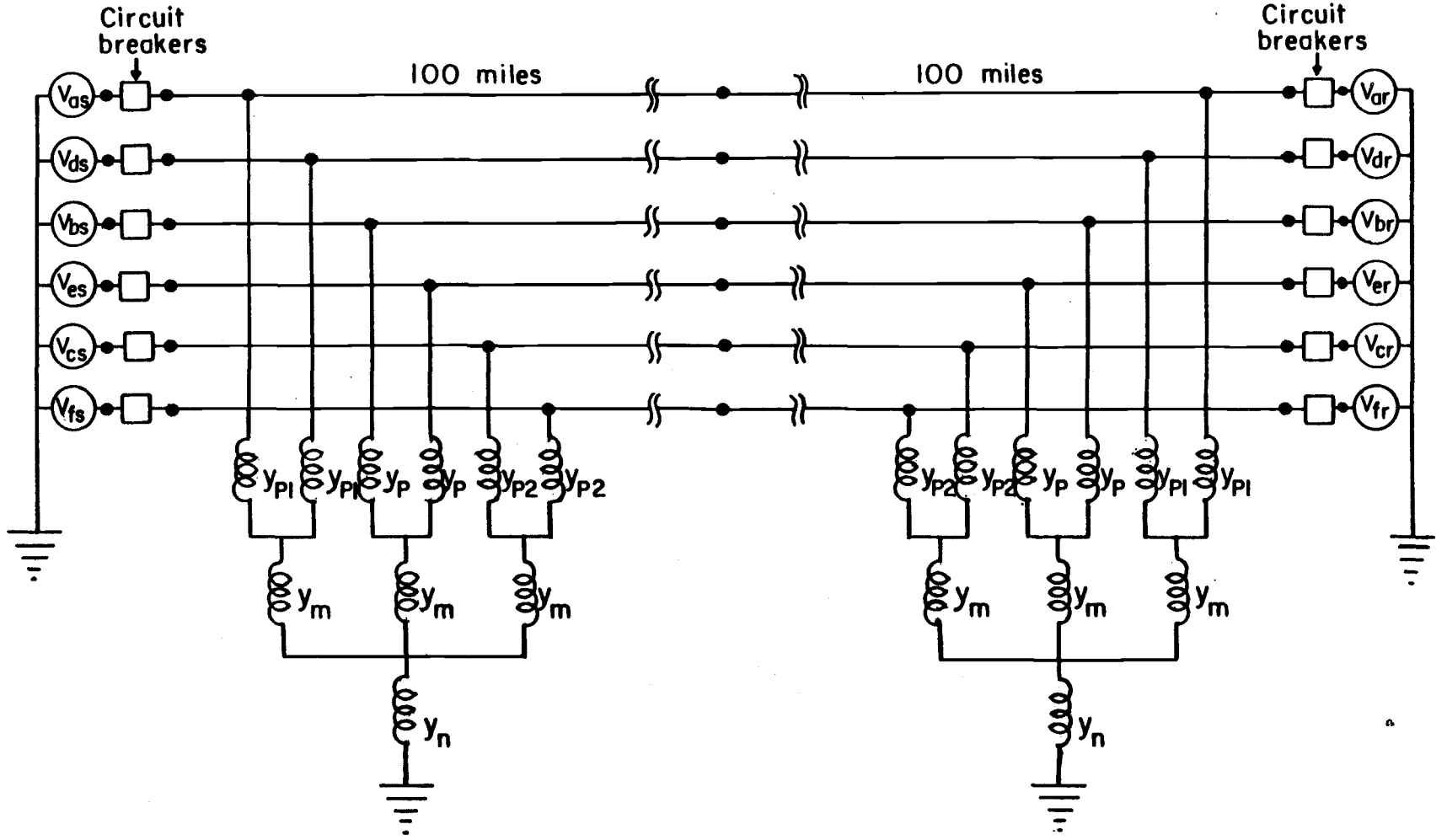

Fig(25) Connection diagram of the compensation reactors and the transmission system.

conditions the current drawn by the transformer is negligible compared to the load current and hence its effect on the line voltage drop is negligible.

The results obtained from the EMTP output include the capacitive as well as the inductive coupling and the line capacitance distribution effects.

4.3 Demonstration

Two existing transmission line data are used as a demonstration of the adequacy of the designed shunt compensation scheme to extinguish secondary arcs on six--phase transmission systems. The two lines have very different characteristics and operating voltage levels. One is rated at 735 KV and the other is rated at 230 KV. Thus, they provide a good idea of the compensation scheme performance under two extreme cases.

Results obtained using data for the above two lines show that the designed compensation scheme is very effective in reducing the recovery voltages on the disconnected lines. It demonstrates also that results obtained from the compensation design procedure are very close to the simulation results obtained using EMTP. The effects of the magnetic coupling and of the line capacitance distribution are shown to be negligible. The reactor design and testing procedures are discussed, and

some results are shown below for each line separately.

4.3.1 Line 'A'

This line was built and operated as a three-phase, double circuit, transmission line. When it is used for six-phase transmission, no change in the line configuration is needed. The line configuration is as shown in fig(26). It is described as follows:

Normal voltage	:424.4 KV, rms, phase-to-ground [735 KV, rms, phase-to-phase, (three-phase)]
Frequency	:60 Hz
Length	:200 miles
Configuration	:Stacked, fig(26)
Bundle conductors	:4 Chukar subconductors, 1.6 inch diameter, at corners of an 18 inch square

The analysis from now on is carried out for a 100 mile section, as mentioned above.

The line capacitances are shown in fig(27). There are 21 of them; but, because of symmetry, they have only 12 different values. It can be noticed that there is a large unbalance in the interphase capacitances. The strongest capacitive coupling exists between lines 'e' and 'f' which are the highest above ground. The positions

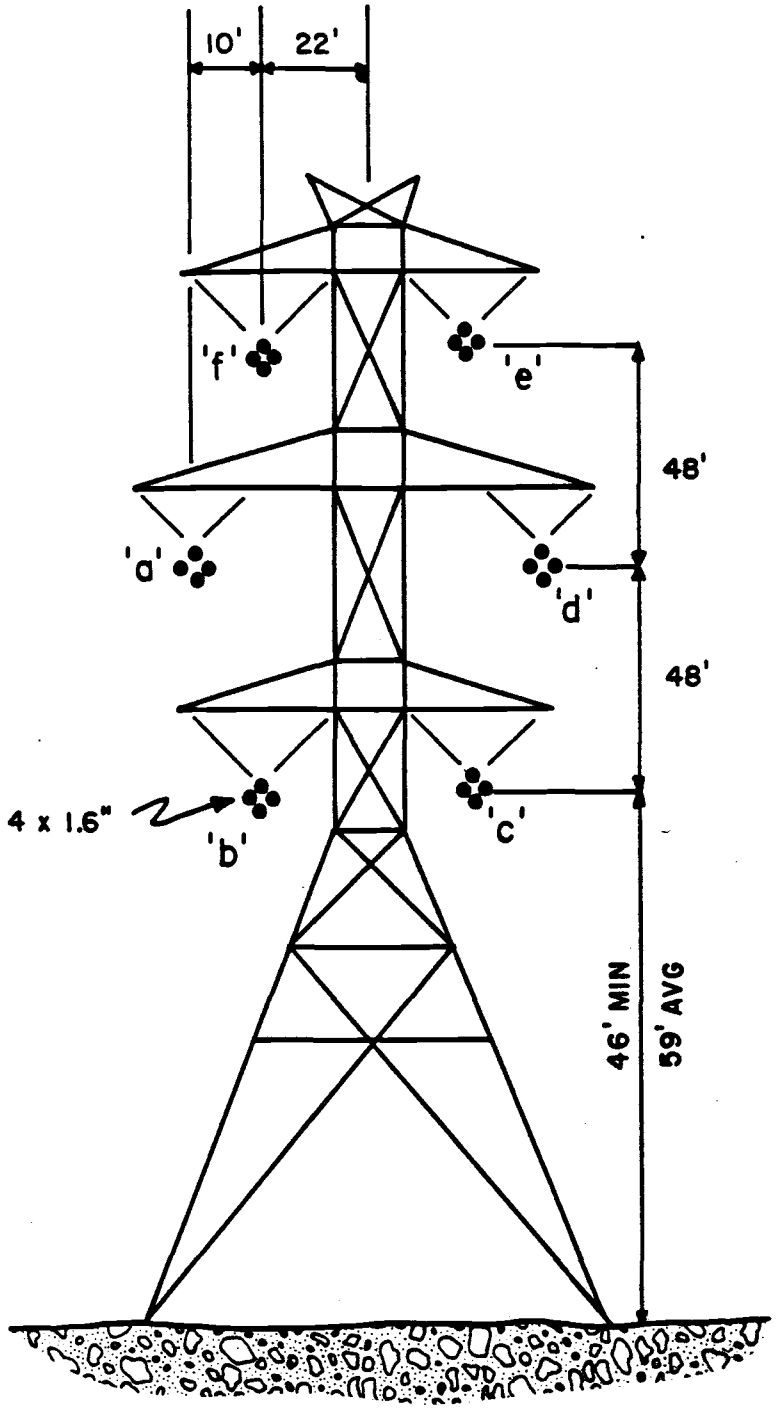

Fig(26) Tower for 424.4 KV lines.

	f	a	b	e	d	c
f	0.17871E-07					
a	-0.36076E-08	0.18631E-07				
b	-0.89486E-09	-0.30463E-08	0.19528E-07			
e	-0.43515E-08	-0.17732E-08	-0.63614E-09	0.17871E-07		
d	-0.17732E-08	-0.19938E-08	-0.13350E-08	-0.36076E-08	0.18631E-07	
c	-0.63614E-09	-0.13350E-08	-0.29771E-08	-0.89486E-09	-0.30463E-08	0.19528E-07

Fig(27) Capacitance matrix (Farad/mile) for the 424.4 KV line.

of lines 'b' and 'c' with respect to each other and to the other lines in the circuit are similar to those of 'e' and 'f'. Thus, one would expect the capacitive coupling between conductors 'e' and 'f' to be similar or very close to that of 'b' and 'c'. But as can be seen from fig(27) the capacitive coupling between conductors 'b' and 'c' is only about 68% of the capacitive coupling between conductors 'e' and 'f'. The only thing that seems to cause this difference in the interline capacitive coupling is the relative height above ground. For other line geometries where the difference between the conductor heights above ground is not too large, the interline capacitance unbalances might not be as significant as for this line.

The input to CMPLX consists of the self and mutual capacitance values of conductors 'a' 'b', and 'f', the maximum value, minimum value, and number of intervals of each of the compensation scheme components, and the system voltage (V_s). The outputs of CMPLX are the capacitively coupled recovery voltages V_a, V_b, and V_f, and the capacitive components of the secondary arc currents I_{sa}, I_{sb}, and I_{sf}, and the compensation scheme element values corresponding to these voltages and currents. A sample of CMPLX's output is shown in table(7). An interesting phenomena was observed for this line. The

Table(7) Sample of the output of program CMPLX for the 424.4 KV line. (Line length = 100 miles)

XP2 =	.0000E+00	.1700E+05	OHM	YP2 = 1/XP2 =	.0000E+00	-.5882E-04	MHO
XP1 =	.0000E+00	.2000E+05	OHM	YP1 = 1/XP1 =	.0000E+00	-.5000E-04	MHO
XP =	.0000E+00	.1200E+05	OHM	YP = 1/XP =	.0000E+00	-.8333E-04	MHO

	NEUTRAL LEG CAPACITOR			NEUTRAL LEG INDUCTOR		
	LINE A	LINE B	LINE F	LINE A	LINE B	LINE F
XM = 0.0 .10E+04 OHM						
YN = 0.0 -.40E-03 MHO						
VOLTAGES (%)	.646E+01	.601E+01	.671E+01	.533E+01	.853E+01	.163E+02
CURRENTS (A/VOLT)	.421E-04	.393E-04	.413E-04	.348E-04	.557E-04	.101E-03

XP2 =	.0000E+00	.8000E+04	OHM	YP2 = 1/XP2 =	.0000E+00	-.1250E-03	MHO
XP1 =	.0000E+00	.2000E+05	OHM	YP1 = 1/XP1 =	.0000E+00	-.5000E-04	MHO
XP =	.0000E+00	.6000E+04	OHM	YP = 1/XP =	.0000E+00	-.1667E-03	MHO

	NEUTRAL LEG CAPACITOR			NEUTRAL LEG INDUCTOR		
	LINE A	LINE B	LINE F	LINE A	LINE B	LINE F
XM = 0.0 .62E+03 OHM						
YN = 0.0 -.80E-03 MHO						
VOLTAGES (%)	.400E+01	.663E+01	.762E+01	.536E+01	.114E+02	.200E+02
CURRENTS (A/VOLT)	.261E-04	.377E-04	.418E-04	.349E-04	.647E-04	.110E-03

capacitively coupled recovery voltage V_f cannot be reduced to the desired limit of 0.09 V_s with Y_n as an inductor. When a capacitor (y'_n) is used in the neutral leg of the compensation bank instead of the reactor (y_n) it is possible to reduce all the voltages V_a, V_b, V_f to values less than 0.09 V_s. Plots for the voltages versus X_m for y_n inductor are shown in fig(28) for various parameter values. Similar plots for y_n replaced by an equivalent capacitive value are shown in figs(29), (30), and (31). The reason that V_f cannot be reduced to 0.09 V_s with y_n inductor is due to the large unbalance in its capacitor values. Because, as can be seen from fig(28), V_a, and V_b which have smaller capacitive unbalances are reduced to values less than 0.09 V_s. Not only that, but if the mutual capacitor C_{ef} was reduced by 25% the recovery voltage V_f would drop to values similar to those of V_a, and V_b.

From the plots in fig(28), it is obvious that when using an inductor in the neutral leg of the compensation bank, the recovery voltages vary little with X_m for various values of the other parameters. Also, it can be seen from the plots corresponding to line 'a' that for a balanced system the impedance X_m can be zero; that is, a short circuit. That is not possible for an unbalanced system like the

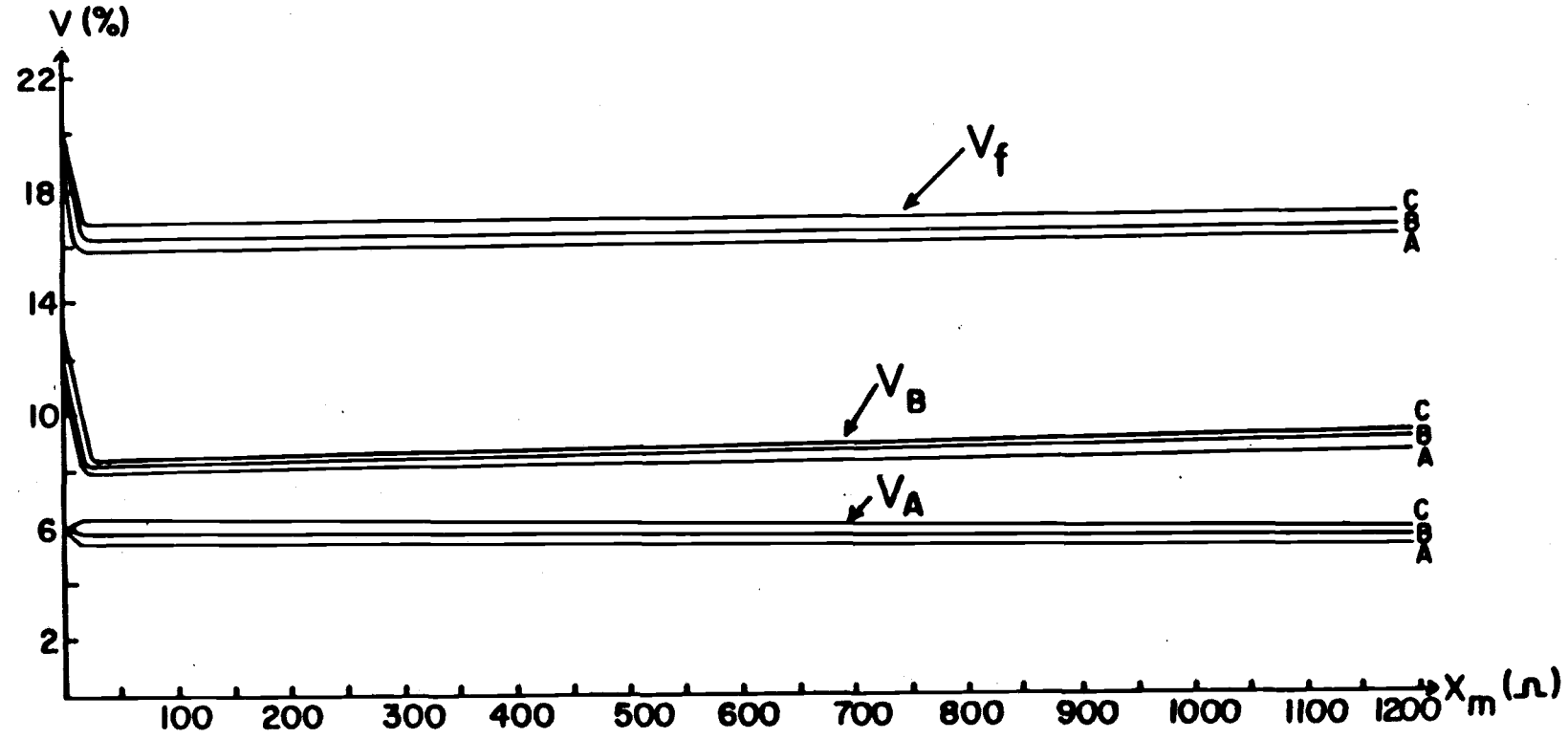

Fig(28) Recovery voltages(%) versus X_m(ohm) for y_n=-.5mmho
A: X_{p2} = 16.5kohm, X_{p1} = 16.5kohm, X_p = 13.5kohm
B: X_{p2} = 16.5kohm, X_{p1} = 16.5kohm, X_p = 10.5kohm
C: X_{p2} = 16.5kohm, X_{p1} = 16.5kohm, X_p = 7.5kohm

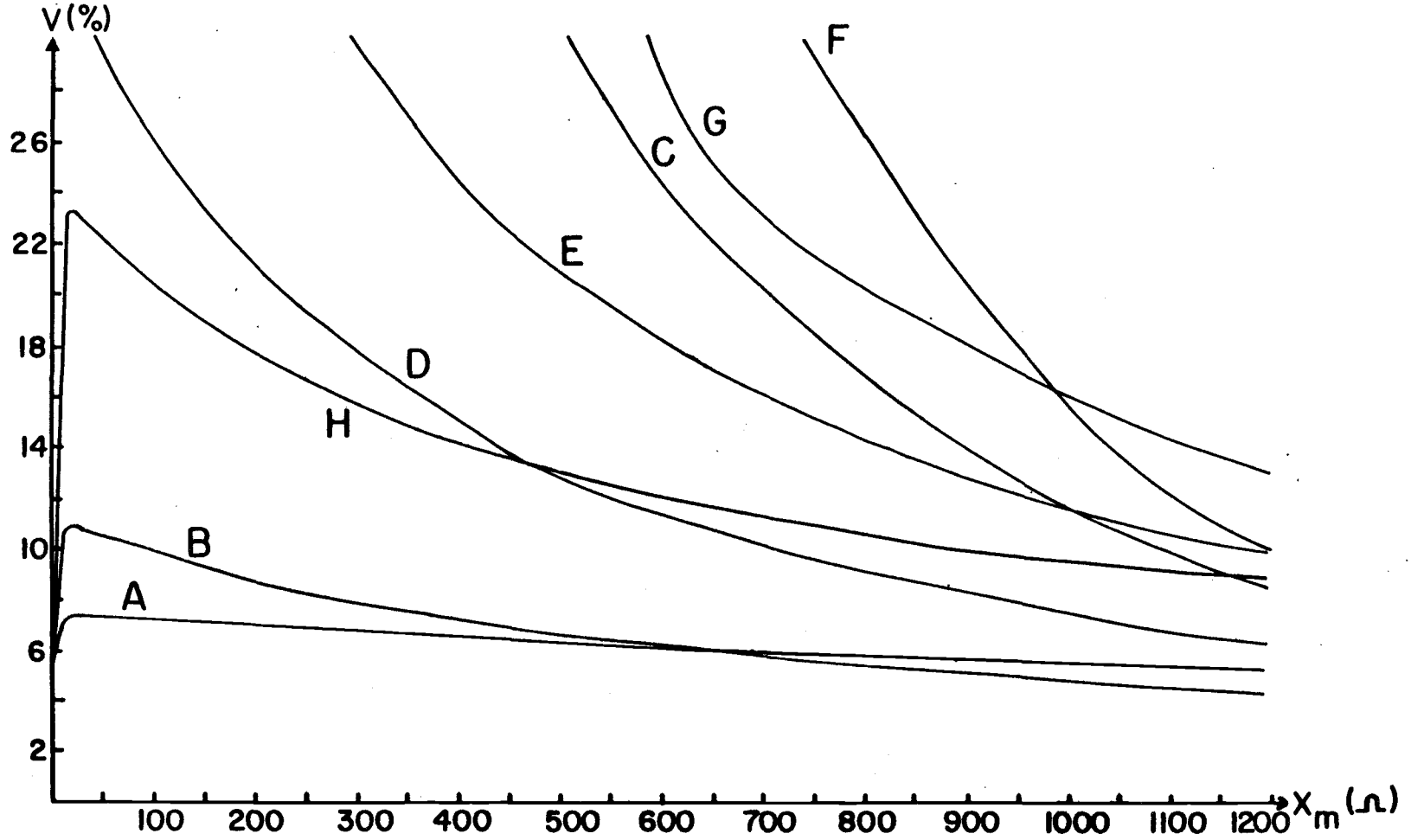

Fig(29) Recovery voltage of line 'a' V.S. X_m for y_n = j 0.5mmho. Parameters A-H are given in table (8).

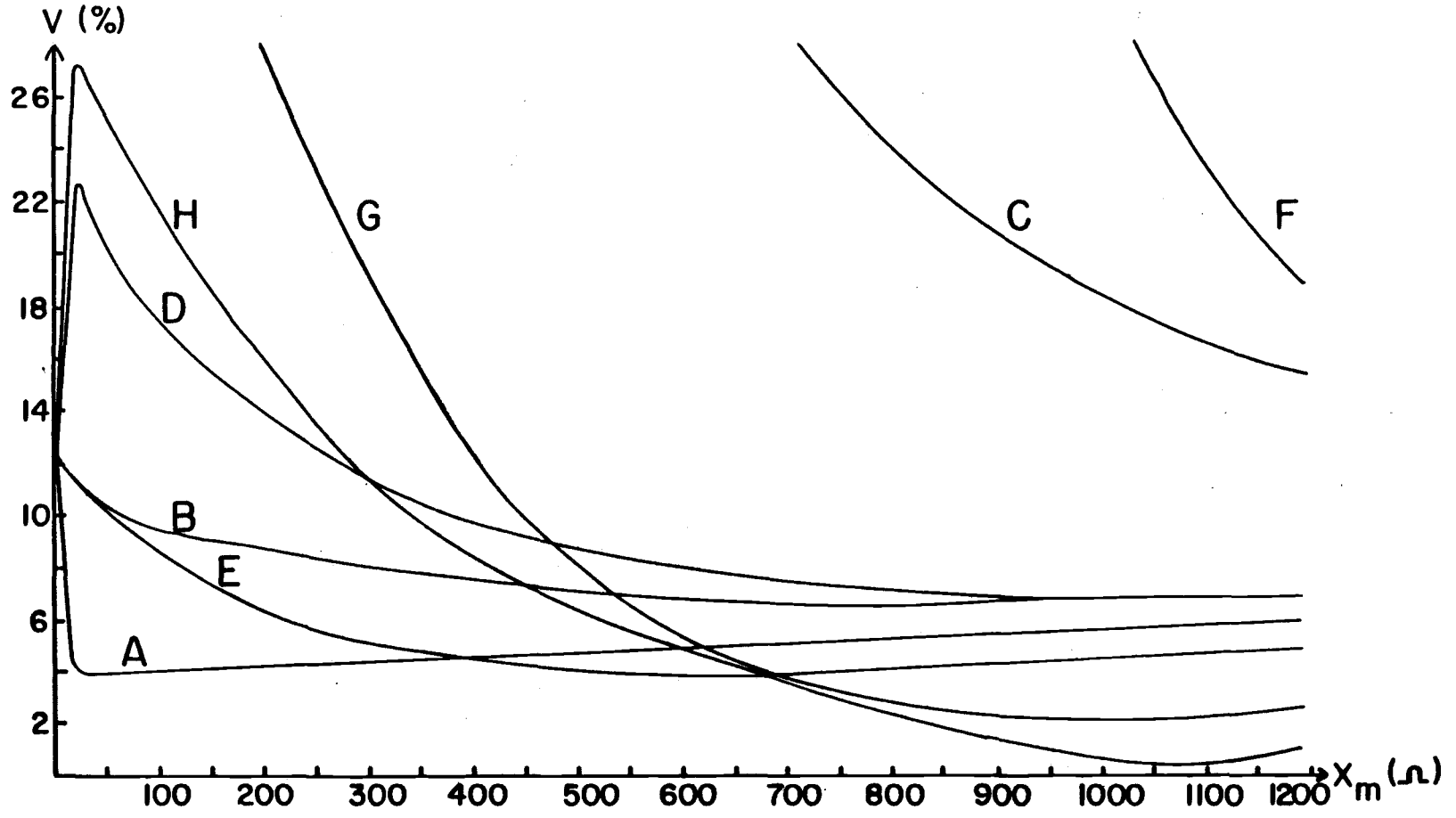

Fig(30) Recovery voltage of line 'b' V.s. X_m for Y_n = j 0.5mmho. Parameters A-H are given in table (8).

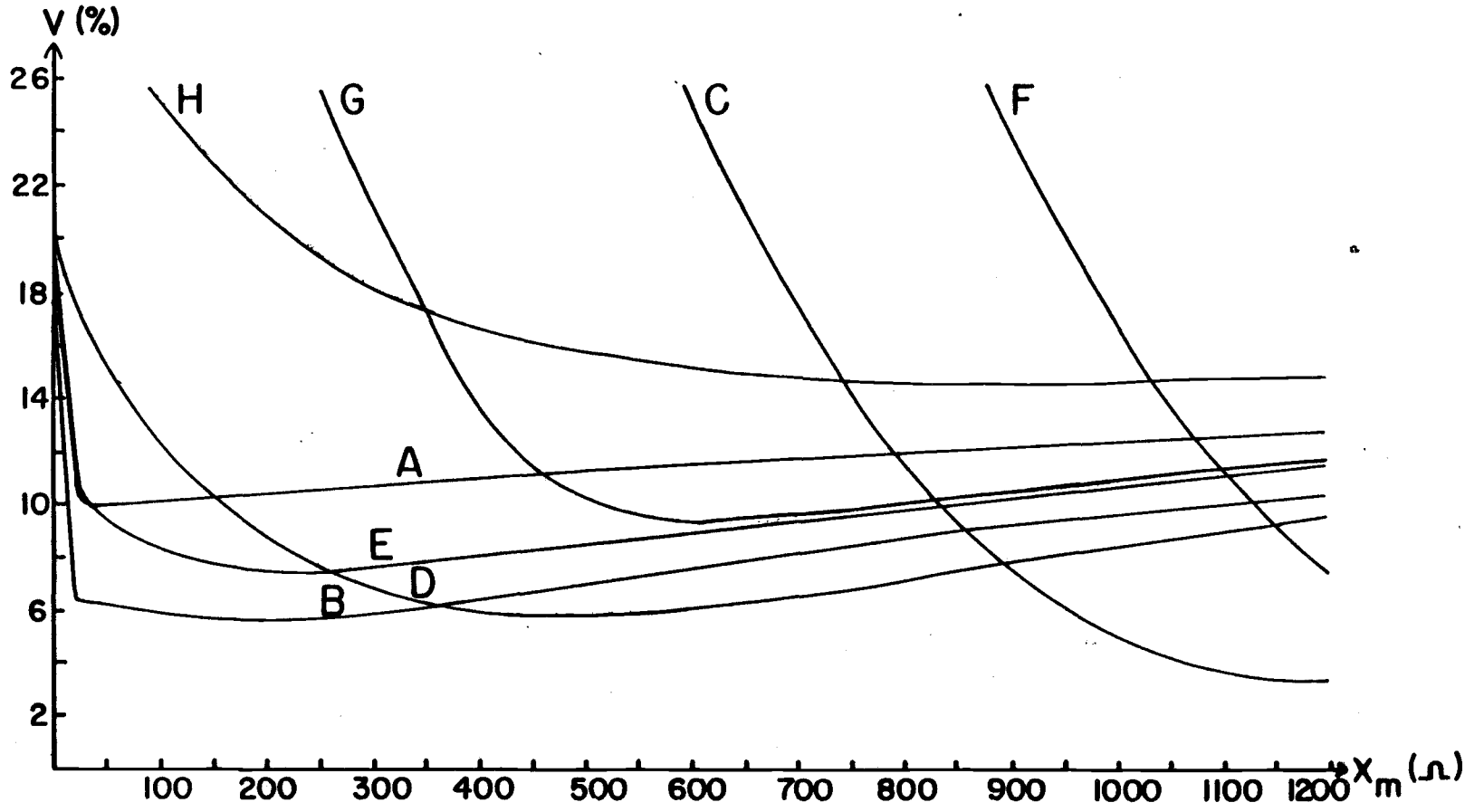

Fig(31) Recovery voltage of line (f) v.s. X_m for Y_n = j 0.5mmho. Parameters A-H are given in table (8).

Table (8) List of symbols for figs (29) - (31).

Symbol	X_{P2} (KΩ)	X_{P1} (KΩ)	X_P (KΩ)
A	16.5	16.5	13.5
B	16.5	16.5	10.5
C	16.5	16.5	7.5
D	16.5	13.5	10.5
E	16.5	10.5	13.5
F	13.5	16.5	7.5
G	13.5	10.5	13.5
H	10.5	16.5	13.5

one studied here as can be seen from the plots corresponding to V_b, and V_f in fig(28).

Comparing fig(29) with figs(30) and (31) indicates that with y_n capacitor X_m can still be replaced by a short circuit if the system capacitor unbalances are not too large. Also, figs(29) through (31) indicate that the recovery voltages vary widely with X_m when the compensation reactor's neutral leg is a capacitor. These figures show that a compromise solution of the recovery voltage equations which may not correspond to the minimum of either one can be obtained.

Program CMPLX searches for the optimum solutions of the capacitively coupled recovery voltage equations and secondary arc current equations as shown in fig(24). The optimum solution of the recovery voltage equations is the one with the least maximum value; that is, the set of voltages V_a, V_b, V_f for which the largest one is smaller than the largest value of any other solution set. The optimum solution of the secondary arc current equations is the set of currents I_a, I_b, and I_f for which the largest current is smaller than the largest value of any other set. Table(9) shows the optimum voltage and current solutions. The lowest portion of table(9) shows the recovery voltages and the secondary arc currents for the uncompensated system. Comparing the results

Table(9) Optimum Compensation Scheme Element Values for the 424.4 kV line. (Line length = 100 miles)

PART - 1 : VOLTAGE MINIMIZATION

THE LOWEST VOLTAGES ARE OBTAINED FOR

XP2 =	.0000E+00	.1700E+05	OHM
XP1 =	.0000E+00	.2000E+05	OHM
XP =	.0000E+00	.1200E+05	OHM
XM =	.0000E+00	.1020E+04	OHM
YN =	.0000E+00	.4000E-03	MHO

THE RECOVERY VOLTAGES ARE :

VA =	6.46 %
VB =	6.01 %
VF =	6.71 %

THE SECONDARY ARC CURRENTS ARE (AMP / VOLT OF INPUT) :

IA =	.421E-04
IB =	.393E-04
IF =	.413E-04

PART - 2 : CURRENT MINIMIZATION

THE LOWEST CURRENTS ARE OBTAINED FOR

XP2 =	.0000E+00	.8000E+04	OHM
XP1 =	.0000E+00	.1700E+05	OHM
XP =	.0000E+00	.6000E+04	OHM
XM =	.0000E+00	.6200E+03	OHM
YN =	.0000E+00	.8000E-03	MHO

THE SECONDARY ARC CURRENTS ARE (AMP / VOLT OF INPUT) :

IA =	.272E-04
IB =	.406E-04
IF =	.401E-04

THE RECOVERY VOLTAGES ARE :

VA =	4.23 %
VB =	7.13 %
VF =	7.30 %

PART - 3 : SYSTEM UNCOMPENSATED

THE RECOVERY VOLTAGES ARE :

VA =	4.79 %
VB =	6.66 %
VF =	13.72 %

THE SECONDARY ARC CURRENTS ARE (AMP / VOLT OF INPUT) :

IA =	.337E-04
IB =	.490E-04
IF =	.924E-04

---

in part(3) of table(9) with those in parts (1) and (2) shows the big improvement in the capacitively coupled recovery voltages and secondary arc currents achieved using the compensation bank with a capacitive neutral leg. It is obvious that for uncompensated, 424.4 KV, transmission lines a recovery voltage of more than 58.2 KV (13.7%) and a secondary arc current of more than 39.2 amps will be observed. If the shunt compensation scheme with capacitive neutral is used the maximum capacitively coupled recovery voltage will be 28.5 KV and the maximum capacitively coupled secondary arc current will be 17.8 amps. That is, a reduction of the capacitive components of the recovery voltage and the secondary arc current to values less than 50% of the values obtained for the uncompensated system.

The optimum impedance values of an all-inductive compensation scheme for this line are shown in table (10). It is obvious that using such a scheme will not reduce the recovery voltage nor the secondary arc current. Comparing the recovery voltage and the secondary arc current values in table (10) with those in part (3) of table (9) indicates that the uncompensated recovery voltage and secondary arc current values are lower than the corresponding values for the line with an all-inductive compensation scheme. Hence, such a scheme does

Table(10) Output of program CMPLX for the 424.4 KV line with an all-inductive compensation scheme. (line length = 100 miles)

THE LOWEST CURRENTS FOR AN ALL-INDUCTIVE COMPENSATION SCHEME ARE OBTAINED FOR :

XP2 =	.0000E+00	.8000E+04	OHM
XP1 =	.0000E+00	.2000E+05	OHM
XP =	.0000E+00	.1800E+05	OHM
XM =	.0000E+00	.6200E+03	OHM
YN =	.0000E+00	.0000E+00	MHO

THE SECONDARY ARC CURRENTS ARE (AMP / VOLT OF INPUT) :

IA =	.203E-04
IB =	.702E-04
IF =	.868E-04

THE RECOVERY VOLTAGES ARE :

VA =	3.12	%
VB =	10.31	%
VF =	15.82	%

---

not seem practical for this untransposed six-phase transmission line.

The effect of the line length is tested by running program CMPLX for a line length of 200 miles. The results are shown in table(11). These results in part(1) and part(2) of table(11) show that for system voltages greater than 420 KV it is not possible to reduce the capacitively coupled secondary arc current to less than the required 35 amp limit using the shunt compensation scheme. The shunt component of the recovery voltage could, however, still be reduced to less than the 10% system-voltage limit. Comparing tables(9) and (11) indicates that the capacitively coupled secondary arc current is proportional to the line length, while the corresponding component of the recovery voltage is independent of the line length. It is obvious, however, that the optimum shunt compensation reactor impedance values suitable for a 200 mile long line are less than those for a 100 mile long line but do not have the same proportionalities as the line length; that is, doubling the line length does not imply doubling the compensation reactor admittances. The results in tables(9) and (11) indicate, as mentioned above, that the best compensation scheme for a 200 mile long line is the one with a compensation reactor bank at each end. Each reactor bank is desig-

Table(11) Optimum Compensation Scheme Element Values for the 424.4 kV line (line length = 200 miles)

PART - 1 : VOLTAGE MINIMIZATION

THE LOWEST VOLTAGES ARE OBTAINED FOR

XP2 =	.0000E+00	.8000E+04	OHM
XP1 =	.0000E+00	.1800E+05	OHM
XP =	.0000E+00	.6000E+04	OHM
XM =	.0000E+00	.1220E+04	OHM
YN =	.0000E+00	.6000E-03	MHO

THE RECOVERY VOLTAGES ARE :

VA =	4.16 %
VB =	6.41 %
VF =	6.45 %

THE SECONDARY ARC CURRENTS ARE (AMP / VOLT OF INPUT) :

IA =	.562E-04
IB =	.838E-04
IF =	.789E-04

PART - 2 : CURRENT MINIMIZATION

THE LOWEST CURRENTS ARE OBTAINED FOR

XP2 =	.0000E+00	.8000E+04	OHM
XP1 =	.0000E+00	.1600E+05	OHM
XP =	.0000E+00	.6000E+04	OHM
XM =	.0000E+00	.2200E+03	OHM
YN =	.0000E+00	.8000E-03	MHO

THE SECONDARY ARC CURRENTS ARE (AMP / VOLT OF INPUT) :

IA =	.567E-04
IB =	.786E-04
IF =	.823E-04

THE RECOVERY VOLTAGES ARE :

VA =	4.22 %
VB =	6.02 %
VF =	6.73 %

PART - 3 : SYSTEM UNCOMPENSATED

THE RECOVERY VOLTAGES ARE :

VA =	4.79 %
VB =	6.66 %
VF =	13.72 %

THE SECONDARY ARC CURRENTS ARE (AMP / VOLT OF INPUT) :

IA =	.674E-04
IB =	.981E-04
IF =	.185E-03

---

ned to compensate for 100 mile section.

The results mentioned so far are obtained using a lumped model where the whole, or a section of, the transmission line is represented by its equivalent lumped capacitive impedance as shown in fig(22). It is obvious that the recovery voltage and secondary arc current values predicted by such a model do not correspond to values at any particular location along the line. But the objective is to determine whether or not the values predicted by the lumped equivalent model will constitute an upper limit on the actual values observed at any location along the line. In other words, the main task is to investigate how well the recovery voltage and the secondary arc current values predicted using the lumped model represent the actual values predicted for the distributed system. To perform this investigation, the same line studied above is represented by a distributed model as in fig(25) and simulated on a digital computer using the EMTP. The values obtained from the simulation are the steady-state, open-circuit voltage magnitudes at the middle and at the ends of the line, and the magnitude of the steady state short-circuit current at the fault location at the center of the line. These values are, of course, higher than the recovery voltage and the secondary arc current magnitudes expected for the physical line, as

mentioned in chapter (3); but they represent worst case limits on the recovery voltage and the secondary arc current values. Henceforth, the open-circuit voltage and the short-circuit current are taken to represent the recovery voltage and the secondary arc current, respectively.

An important thing to be emphasized here is that the lumped model does not take the effect of the line loading into account. Hence, the results predicted using the lumped equivalent capacitive model are to be compared mainly with the no-load simulation test results. In principle, in the no-load case, the voltage variations along the sound lines are small. Because the recovery voltage and the secondary arc current are mainly functions of the system voltage when the line is unloaded, their magnitudes along the disconnected line are almost constant. Moreover, the secondary arc current is too small to cause any appreciable voltage drop along the line. This is confirmed by the EMTP results. Thus, for a fixed line length, and with sources at or near both ends to assure balanced system voltages, the recovery voltage and the secondary arc current magnitudes can be assumed constant along the line. To simplify the comparisons between the lumped model and the distributed model only the worst cases are emphasized.

The results of the EMTP simulation tests are shown in tables(12) and (13) for a 200 mile long line. These tests were made with the line represented by its distributed equivalent impedance and admittance matrices, figs(27) and (32). Balanced Six-phase voltage sources of 424.4 KV (rms) were applied to each end of the line. In the first series of tests, the receiving-end voltage was set in phase with the sending-end voltage for simulating no-load conditions. In the second series of tests, full load conditions were simulated by making the phase difference between sending-end and receiving-end voltages equal to 34^{o}. In both tests SLG faults at the middle of the line were applied to line a, b, or f. The recovery voltages at the middle and at the ends of the disconnected line in addition to the secondary arc current are recorded in the tables. The third test series was made with all lines open at the receiving-end. The values recorded are the maximum and minimum overvoltages at the receiving-end. Tables(12) and (13) show the results for compensated and uncompensated cases. The simulated system with the compensation scheme connected to it is shown in fig(33).

Comparing the simulation results for the uncompensated line in the no-load tests, (series 1, table(12)), with the corresponding lumped model results shown in

Table(12) The EMTP simulation test results for the 424.4 kV, 200 mile long, untransposed six-phase transmission line.

Test Set #	Fault location at middle of:	Uncompensated			Compensated at both ends			Remarks
		Recovery voltage (KV)	Secondary arc current (amp)	Output impedance magnitude at fault point (kohm)	Recovery voltage (KV)	Secondary arc current (amp)	Output impedance magnitude at fault point (kohm)	
1	Line 'a'	17.30	25.59	0.676	26.81	34.89	0.768	System unloaded
	Line 'b'	22.20	35.03	0.634	12.59	15.40	0.818	
	Line 'f'	50.19	70.50	0.712	13.33	15.78	0.845	
2	Line 'a'	16.52	24.47	0.675	25.61	33.39	0.767	System loaded (Full-load current =2,000 amps)
	Line 'b'	21.20	33.50	0.633	12.04	14.70	0.819	
	Line 'f'	48.03	67.38	0.713	12.71	15.15	0.839	

Table(13) Open circuit voltages of the 424.4 KV line. Results obtained using the EMTP simulation.

Test Set #	Line Open	Open Circuit Voltage (Recovery voltage) (KV)						Remarks
		Line Uncompensated			Line Compensated at both ends			
		At Sending End	At Middle	At Receiving End	At Sending End	At Middle	At Receiving End	
1	'a' 'b' 'f'	20.10 21.92 53.01	17.30 22.21 50.24	20.10 21.92 53.01	25.49 10.52 16.71	26.81 12.59 13.33	25.54 10.52 16.71	System Unloaded
2	'a' 'b' 'f'	23.02 15.63 50.31	16.52 21.20 48.03	15.30 27.79 52.22	26.50 18.34 12.19	25.61 12.02 12.71	22.73 2.89 22.41	System loaded (Full load current = 2000 amps)
3	all lines are open at receiving end			480.2 448.6			462.2 456.8	Max. overvoltage Min. overvoltage

	f	a	b	e	d	c
f	0.98920E-01 0.10158E+01					
a	0.86813E-01 0.49996E+00	0.10166E+00 0.10124E+01				
b	0.88204E-01 0.41679E+00	0.89668E-01 0.49652E+00	0.10464E+00 0.10089E+01			
e	0.85448E-01 0.51480E+00	0.86776E-01 0.45297E+00	0.88179E-01 0.40524E+00	0.98920E-01 0.10158E+01		
d	0.86776E-01 0.45297E+00	0.88159E-01 0.46595E+00	0.89624E-01 0.44953E+00	0.86813E-01 0.49996E+00	0.10166E+00 0.10124E+01	
c	0.88179E-01 0.40524E+00	0.89624E-01 0.44953E+00	0.91161E-01 0.50792E+00	0.88204E-01 0.41679E+00	0.89668E-01 0.49652E+00	0.10464E+00 0.10089E+01

Fig(32). Impedance matrix (ohm/mile) for the 424.4 KV line.

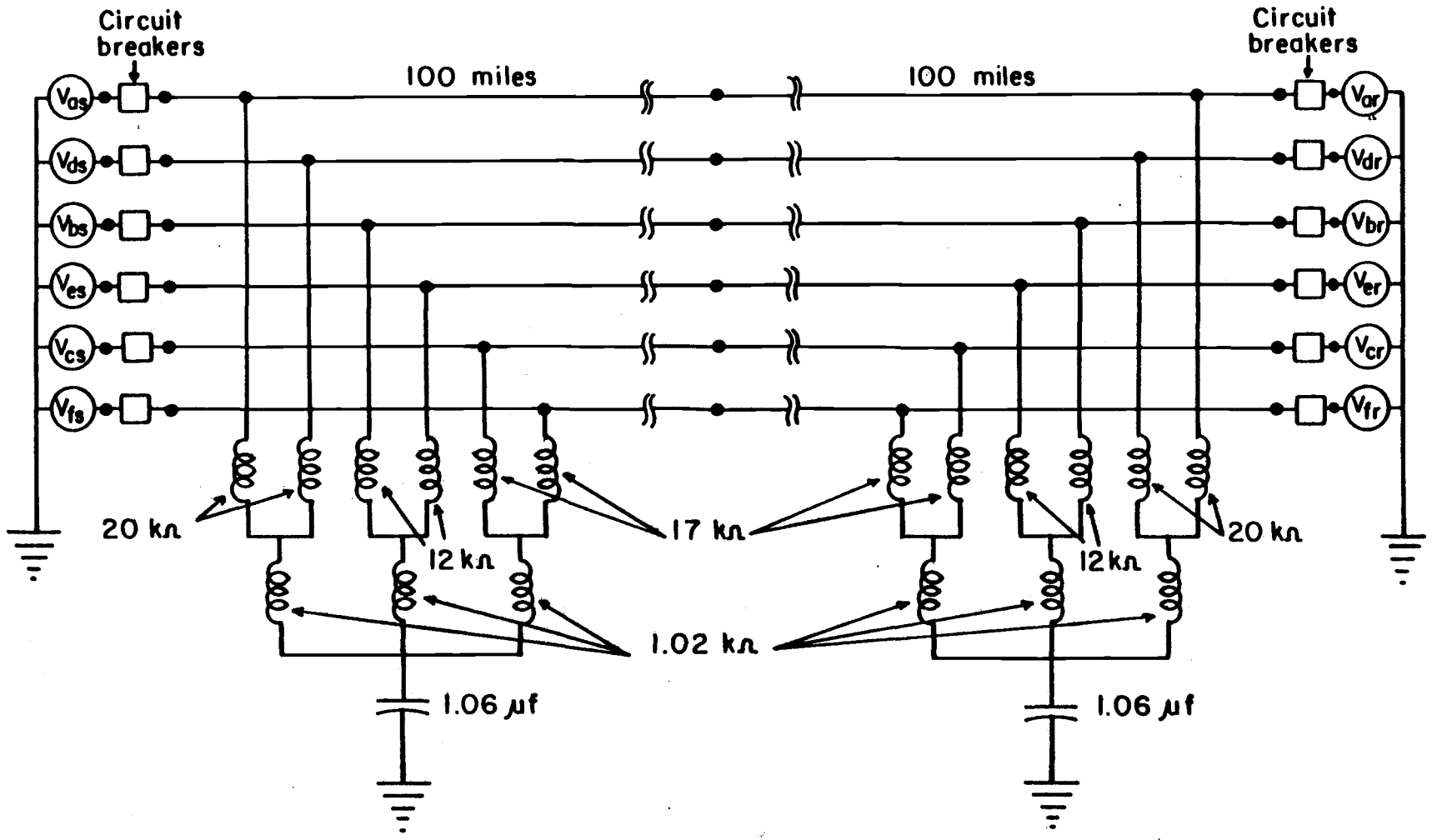

Fig(33) The simulated six-phase transmission lines with the compensation scheme connected at both ends.

part(3) of table(9), indicates that the actual simulation results are lower. From part(3) of table(9), the worst predicted recovery voltage of the 424.4 KV uncompensated line is 58.2 KV while the corresponding worst value in the first set of the simulation results shown in tables(12), and (13) is 53.0 KV. The secondary arc current values predicted by CMPLX using the lumped model, table(9), are for a 100 mile long line. To compare these values with the corresponding simulation results in table(12) one should keep in mind that the secondary arc current values shown in table(12) are for a SLG fault at the middle of a 200 mile long line. The secondary arc current magnitude at such a fault location is expected to be approximately double the magnitude of the secondary arc current of a 100 mile long line. The reason for this is the fact that the secondary arc current is almost linearly proportional to the line length. This can be seen by comparing the predicted results in tables(9) and (11). Hence, the predicted secondary arc current values shown in table (9) are to be compared with half the corresponding simulation result values shown in table(12). From part(3) of table(9), the worst predicted value of the secondary arc current is 39.2 amps, which is more than half the corresponding simulation result value, shown in the first test set of table(12), which

is 35.25 (=70.5/2) amps. The other predicted values in part(3) of table(9) are also higher than the corresponding values obtained from the simulation tests, tables(12), and (13).

The effectiveness of the compensation scheme in reducing the recovery voltage and the secondary arc current is depicted in the second part of the first simulation test series, tables(12), and (13). These results are obtained using the compensation scheme impedance values determined using CMPLX with results shown in part(1) of table(9). The results shown in the first simulation test series indicate that the conductor with the worst recovery voltage and secondary arc current values before compensation might not be the one with the worst values after compensation. Anyhow, the results in the first test series of tables(12), and (13) indicate that when the lines are compensated, the recovery voltage and the secondary arc current values are less than the values predicted by the preliminary design procedure, part(1) of table(9). The simulation and the predicted results also show that the worst recovery voltage and secondary arc current values for the compensated line are less than 50% of those for the uncompensated line.

The recovery voltage rate of rise K_r(KV/ms) is related to the secondary arc current I_s (amps rms) by K_r

= $0.2I_s$ as mentioned in section (4.1.1). Using this relationship, the simulation results indicate that the shunt compensation scheme will reduce the recovery voltage rate of rise from 14.1 KV/ms to 6.9 KV/ms. Comparing these values with the staged fault test results mentioned in chapter(3) indicates that the 14.1 KV/ms is above the average values for extinguishable arcs while the 6.9 KV/ms is below those values. Several sources indicate that an arc path of a length suitable for 500 KV application will experience an initial rate of rise of dielectric strength of about 10 to 12 KV/ms [30,31].

In the load tests (series 2, tables(12), and (13)), with and without compensation, the secondary arc current and the recovery voltage are almost the same as the values in the first test series for the no-load case. This shows that the capacitive coupling is more important than the inductive coupling for the line investigated. With shunt compensation, the maximum recovery voltage and the maximum secondary arc current are only about 50% of the corresponding uncompensated values.

Table(12) shows also the output impedance magnitude at the fault point. The output impedance magnitude is calculated by dividing the open circuit voltage by the short circuit current at the fault location.

The simulation results in tables(12), and (13) show

that, without the shunt compensation, the recovery voltages on some lines are above the tentative limits of 10% of system voltage, and the secondary arc currents are above the 40 amp limit. Thus, single-pole switching might not be successful for such a system. When the line is shunt compensated, the recovery voltages and the secondary arc currents are all below the acceptable upper limits. Hence, successful SPS application is highly expected. For lines longer than about 200 miles, the primary design procedure predicts that the recovery voltage will still be less than the tentative upper limit, but the secondary arc current might be higher than the 40 amp limit. This is because of the almost linear relationship between the secondary arc current and the line length mentioned above. The best way to overcome this problem appears to be adding sectionalizing switches and compensation banks along the line. The switches are to be placed so as to sectionalize the disconnected line in case of a SLG fault into two or more sections of about 200 miles long or less each. A line section longer than about 100 miles is to be compensated by two compensation banks, one at each end, as shown in fig(25). For sections of about 100 miles long or less, one compensation bank, placed at one end of the section, seems to be adequate. Thus, each section of the line is to

be compensated separately.

The third test series, table(13), shows the maximum and the minimum overvoltages on the lines in the case of six-phase switching at the receiving end. It is obvious that this shunt compensation reduces the maximum overvoltages from 13.15% of system voltage to 8.9%. To reduce the overvoltages by a greater amount, smaller shunt compensation impedance values are needed; because the more current the reactors draw, the lower the overvoltages are. However, as mentioned in section (4.2.3), the current drawn by the compensation reactors under steady state conditions should not exceed 5% of the system steady state load current. The shunt compensation reactors used in obtaining the results in tables(12) and (13) draw currents less than 2.6% of the system steady state load current. Thus, it would still be possible to reduce the impedance of the compensation reactors without violating requirement(3) of section (4.2.3). The shunt compensation impedance values used in obtaining the simulation results are predicted optimum values that minimize the recovery voltages and the secondary arc currents, as shown in part(1) of table(9). For the investigated line, they reduce the recovery voltage and the secondary arc current to values much smaller than the acceptable upper limits. Hence, by inspecting CMPLX's

output one can find smaller impedance values of the shunt compensation scheme that will result in more reduction of the transmission line overvoltages and still satisfy requirements 1,2, and 3 of section (4.2.3).

Simulation tests were also made to investigate the performance of the shunt compensation scheme with an inductive neutral leg. The first test was carried out by arbitrarily replacing the capacitive neutral leg of the compensation scheme used in the tests of tables(12) and (13) by an inductor of equal impedance magnitude. The recovery voltage (line 'f' open) was found to be very high, 62 KV. The second test was made by repeating test series (2) of table(12) for line 'f' using the optimum all-inductive shunt compensation scheme predicted using CMPLX with results shown in table(10). The recovery voltage from the simulation results was 58 KV and the secondary arc current was 68 amps. These results confirm the predicted results from the lumped model and indicate that a successful SPS is not expected when an all-inductive shunt compensation scheme is used.

An important conclusion to be derived from the above discussion is that the worst recovery voltage and secondary arc current values predicted using program CMPLX are higher than the corresponding values observed by runnning the simulation tests using EMTP. This can be

seen by comparing the predicted values in tables (9) and (10) with the simulation results mentioned above. The values may not have a one-to-one correspondence for the lines, but the results predicted by the preliminary design procedure using CMPLX provide an upper limit on the actual recovery voltage and secondary arc current values. Hence, it appears that CMPLX's output can be utilized as a safe design reference when designing a shunt compensation scheme. Moreover, because the weather conditions, such as winds and temperature, and the arc resistance which are important factors in reducing the recovery voltage and the secondary arc current are not taken into account during the preliminary design procedure development nor during the simulation test performance, the predicted recovery voltage and secondary arc current values are expected to be higher than the corresponding values to be seen on the actual system in practice. Hence, the reliability of the predicted values is assured.

4.3.2 Line 'B'

The second line to be investigated in this research is a 230 KV line. Its configuration is as shown in fig(34). It is described as follows:

Normal voltage : 138 KV, rms phase-to-ground.
[230 KV, rms, phase-to-phase (three phase)]

Frequency : 60 Hz

Length : 100 miles

Configuration : Stacked, fig(34)

Conductors per phase: One

The line capacitances are shown in fig(35). It is obvious that the system is unbalanced. The effect of height above ground can be noticed by comparing the two interline capacitors C_{ef} and C_{bc}. These two capacitors are geometrically identical but lines e and f are at a higher position above ground than lines b and c. Hence, C_{ef} is bigger than C_{bc}, but the difference between them is not as significant as in the case of Line 'A'.

Table (14) shows a sample of the output from CMPLX. The results in table (14) indicate that a compensation scheme with a capacitive neutral will perform better than an all-inductor bank. Table(15) shows the optimum compensation scheme element values and the corresponding capacitively coupled recovery voltages and secodnary

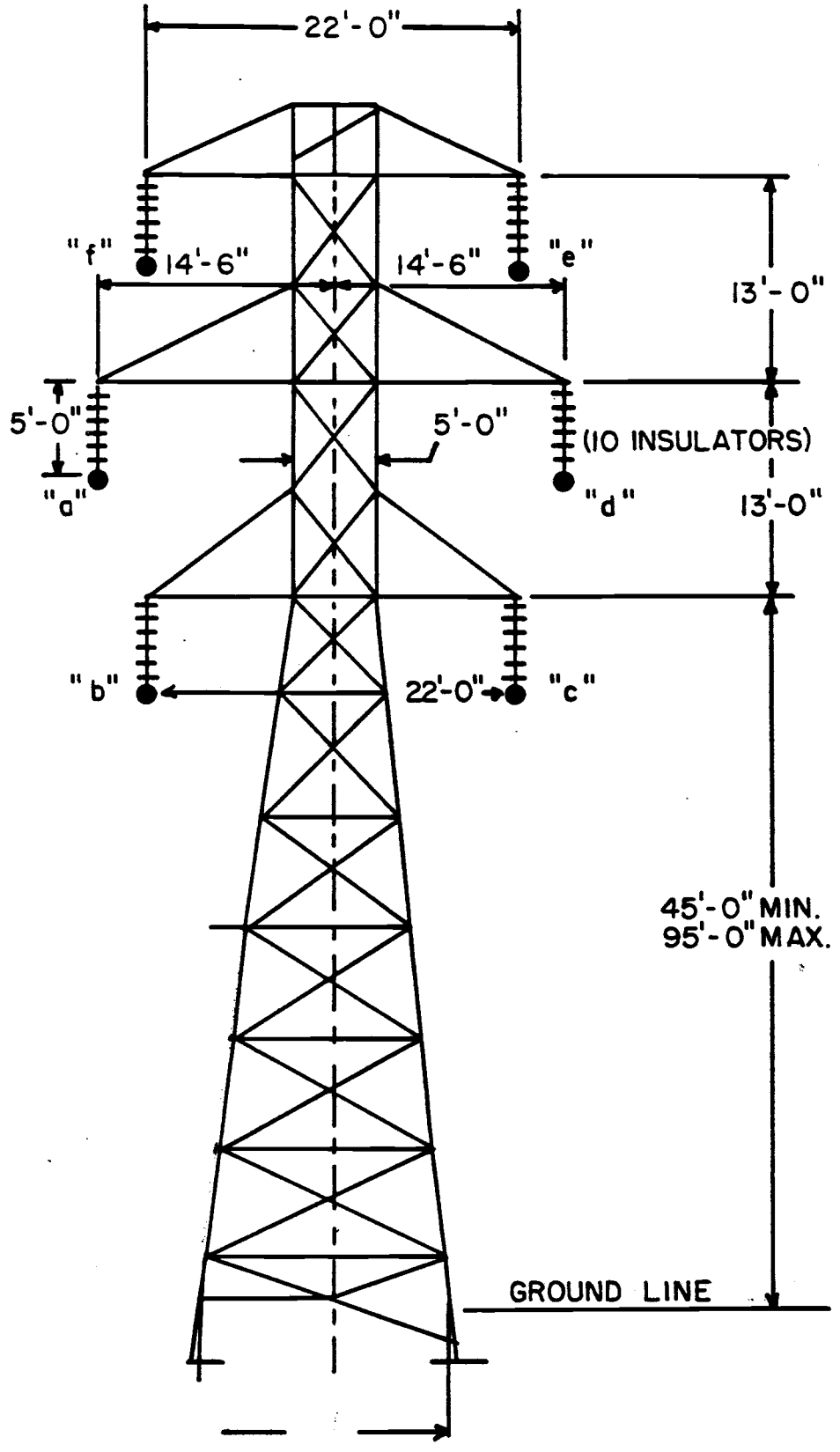

Fig(34) Tower for 138 KV transmission lines.

	f	a	b	e	d	c
f	0.13019E-07					
a	-0.28254E-08	0.13541E-07				
b	-0.12454E-08	-0.26820E-08	0.13350E-07			
e	-0.19288E-08	-0.11311E-08	-0.81716E-09	0.13019E-07		
d	-0.11311E-08	-0.96362E-09	-0.10009E-08	-0.28254E-08	0.13541E-07	
c	-0.81716E-09	-0.10009E-08	-0.16201E-08	-0.12454E-08	-0.26820E-08	0.13350E-07

Fig(35) Capacitance matrix (Farad/mile) for the 138 KV line.

Table(14) Sample of the output of program CMPLX for the 138 KV line. (Line length = 100 miles)

XP2 =	.0000E+00	.3300E+05	OHM	YP2 = 1/XP2 =	.0000E+00	-.3030E-04	MHO
XP1 =	.0000E+00	.1200E+05	OHM	YP1 = 1/XP1 =	.0000E+00	-.8333E-04	MHO
XP =	.0000E+00	.6000E+04	OHM	YP = 1/XP =	.0000E+00	-.1667E-03	MHO

	NEUTRAL LEG CAPACITOR			NEUTRAL LEG INDUCTOR		
	LINE A	LINE B	LINE F	LINE A	LINE B	LINE F
XM = 0.0 .42E+03 OHM						
YN = 0.0 -.13E-02 MHO						
VOLTAGES (%)	.614E+01	.838E+01	.824E+01	.881E+01	.146E+02	.798E+01
CURRENTS (A/VOLT)	.262E-04	.282E-04	.380E-04	.376E-04	.490E-04	.367E-04
XM = 0.0 .42E+03 OHM						
YN = 0.0 -.10E-02 MHO						
VOLTAGES (%)	.713E+01	.755E+01	.851E+01	.905E+01	.148E+02	.799E+01
CURRENTS (A/VOLT)	.305E-04	.254E-04	.392E-04	.387E-04	.499E-04	.368E-04
XM = 0.0 .20E+02 OHM						
YN = 0.0 -.15E-02 MHO						
VOLTAGES (%)	.557E+01	.853E+01	.814E+01	.834E+01	.150E+02	.778E+01
CURRENTS (A/VOLT)	.238E-04	.287E-04	.375E-04	.356E-04	.503E-04	.358E-04
XM = 0.0 .20E+02 OHM						
YN = 0.0 -.13E-02 MHO						
VOLTAGES (%)	.616E+01	.759E+01	.833E+01	.856E+01	.152E+02	.778E+01
CURRENTS (A/VOLT)	.263E-04	.256E-04	.383E-04	.365E-04	.512E-04	.358E-04
XM = 0.0 .20E+02 OHM						
YN = 0.0 -.10E-02 MHO						
VOLTAGES (%)	.822E+01	.752E+01	.879E+01	.883E+01	.155E+02	.779E+01
CURRENTS (A/VOLT)	.351E-04	.253E-04	.405E-04	.377E-04	.522E-04	.359E-04

Table(15) Optimum Compensation Scheme element values for the 138 KV line. (line length = 100 miles).

PART - 1 : VOLTAGE MINIMIZATION

THE LOWEST VOLTAGES ARE OBTAINED FOR

XP2 =	.0000E+00	.3300E+05	OHM
XP1 =	.0000E+00	.1200E+05	OHM
XP =	.0000E+00	.1400E+05	OHM
XM =	.0000E+00	.4200E+03	OHM
YN =	.0000E+00	.6000E-03	MHO

THE RECOVERY VOLTAGES ARE :

VA = 3.37 %
VB = 8.15 %
VF = 8.15 %

THE SECONDARY ARC CURRENTS ARE (AMP / VOLT OF INPUT) :

IA = .144E-04
IB = .352E-04
IF = .375E-04

PART - 2 : CURRENT MINIMIZATION

THE LOWEST CURRENTS ARE OBTAINED FOR

XP2 =	.0000E+00	.3300E+05	OHM
XP1 =	.0000E+00	.1200E+05	OHM
XP =	.0000E+00	.6000E+04	OHM
XM =	.0000E+00	.2000E+02	OHM
YN =	.0000E+00	.2600E-02	MHO

THE SECONDARY ARC CURRENTS ARE (AMP / VOLT OF INPUT) :

IA = .242E-04
IB = .363E-04
IF = .364E-04

THE RECOVERY VOLTAGES ARE :

VA = 5.68 %
VB = 10.78 %
VF = 7.90 %

PART - 3 : SYSTEM UNCOMPENSATED

THE RECOVERY VOLTAGES ARE :

VA = 5.63 %
VB = 8.62 %
VF = 7.31 %

THE SECONDARY ARC CURRENTS ARE (AMP / VOLT OF INPUT) :

IA = .287E-04
IB = .434E-04
IF = .359E-04

---

arc currents. In part(3) of table(15) the capacitive components of the recovery voltages and the secondary arc currents for the uncompensated line are shown. These values are already less than the desired limits. Thus, single-pole switching on this line will be successful without the use of a compensation scheme. Part(1) of table(15) shows that the compensation scheme will reduce the maximum value of the capacitively coupled secondary arc current by about 13.6% while the maximum value of the recovery voltage is reduced by only about 5%.

One may conclude from the results obtained for lines 'A' and 'B' that the shunt compensation scheme is essential mainly for EHV lines. For lines of rated voltage less than 230 KV, the SPS is expected to be successful without the neccessity to add shunt compensation. However, the reactors might still be needed to reduce the overvoltages on the lines in the case of six-pole switching.

For line 'B', the EMTP simulation test was not made because the test results of line 'A' proved that the EMTP simulation is not essential.

V. CONCLUSIONS AND FUTURE WORK

5.1 Conclusions

1. Capacitive coupling compensation using an unbalanced compensation scheme is investigated for untransposed n-phase transmission lines. A general method is developed to optimize the compensation bank element values in order to minimize the recovery voltage and the secondary arc current.

2. The design procedure developed in this research is simple and direct. No assumptions are made on the transmission line's geometry or arrangement on the tower. Thus, line transpositions and balance are not required. In addition to that, the design procedure requires only shunt compensation banks, but no extra capacitors are required to balance the interline capacitors as has been the case in previous design procedures.

3. A compensation scheme of tree form consisting of six-phase reactors, three middle reactors, and a capacitive neutral leg appears to be the most suitable scheme for compensating unbalanced, untransposed, six-phase transmission lines. An all-inductive compensation scheme of the same form does not appear to be feasible for unbalanced six-phase lines.

4. The designed compensation scheme is predicted to

effectively reduce the magnitude and rate of rise of the recovery voltage and the secondary arc current to values that will allow successful single-pole switching applications for unbalanced six-phase transmission lines. The design procedure and the simulation test results indicate that for a 200 mile long, 424.4 KV, six-phase transmission line, the recovery voltage is reduced from 53 KV to 26.8 KV, the recovery voltage rate of rise is reduced from 14.10 KV/msec. to 6.98 KV/msec., and the secondary arc current is reduced form 70.5 amps to 34.9 amps. In addition to that the receiving end overvoltages caused by six-pole switching are reduced substantially.

5. A single compensation bank at one end of the line appears to be adequate for lines less than about 100 miles long. For lines longer than about 100 miles but less than about 200 miles, two compensation banks are needed, one at each end. Each one of the compensation banks is designed to compensate a 100 mile section from one end. Lines longer than about 200 miles require sectionalizing switches in addition to the compensation banks. The switches will open to sectionalize the line into two or more sections after it is disconnected at both ends.

6. The recovery voltage and secondary arc current values predicted by the compensation design procedure provide

an upper limit on the maximum recovery voltage and secondary arc currents that might actually be observed on the line.

7. The shunt compensation scheme is proved necessary for successful SPS application to EHV lines. For systems of rated voltages less than about 230 KV the shunt compensation does not seem to be essential for successful SPS application. However, it might still be needed for reducing overvoltages due to six-pole switching.

8. The capacitive coupling is shown to be the dominant factor in deciding whether an arc will self extinguish or not. The inductive coupling seems to have negligible effect on the arc extinction for the lines investigated.

5.2 Future Work

The subject matter of this research was to develop a shunt compensation design procedure for six-phase transmission lines. Effort was directed toward making the procedure reliable, flexible, and easy to use. While proceeding through the work, new problems were discovered, as well as potential pursuits to improve the design procedure. Some of these were examined within the preceding parts of the research. Others are cited below as future work.

During this research, the system was assumed to

be in steady state. However, the power system behavior under transient conditions is important for establishing the system design levels. To complete the investigation, the transient secondary arc current and recovery voltage are to be studied and the adequacy of the shunt compensation under such conditions is to be tested.

As mentioned earlier in this research, only the worst case conditions of the secondary arc gap were estimated from previous staged fault test data. Upper limits on the secondary arc current and recovery voltage were established. The weather condition, arc resistance, and arc length were not precisely represented. To have more accurate results these factors should be studied, and a precise model of the air gap is to be constructed and simulated during the design procedure.

The compensation scheme found suitable for untransposed six-phase transmission lines during this research was composed of reactors and a capacitor in series. Thus, the system might resonate at a certain frequency. To investigate this, a frequency response of the transmission lines and the shunt compensation scheme should be obtained by finding the system response at a wide range of frequencies. If the resonance frequency is much higher than the power frequency, then its occurence is highly unexpected. If otherwise, some element impe-

dance values of the compensation scheme can be modified to avoid resonance in the frequency range close to the power frequency.

Simulation of the transmission lines and the compensation scheme is of great importance in the design stage, however, it does not take into account all factors needed to construct the system. Economic analysis and system feasibility investigation are also essential factors in the design stage. Economic analysis should consider number and sizes of compensation banks, sectionalizing switches if needed, relaying, and maintenance costs.

During the compensation scheme design procedure and during the simulation tests the transmission lines, the voltage sources and the compensation scheme are represented by equivalent mathematical models which cannot take into account all possible variations in the actual system elements. To obtain more accurate results staged fault tests are needed. This will provide more reliable data on the air gap characteristics, and the shunt compensation scheme performance and reliability.

Bibliography

[1] S.S. Venkata, and N.B. Bhatt, "Economic Analysis of Six-Phase power Transmission Systems", Paper presented at 1977 Midwest Power Symposium, West Virginia University, Morgantown, West Virginia, October 6-7, 1977.

[2] J.R. Stewart, and D.D. Wilson, "High-Phase Order Transmission - A Feasibility Analysis, Part I - Steady State Considerations", IEEE Transactions, PA&S, Vol. PAS-97, pp. 2300-2307, Nov./Dec. 1978.

[3] J.R. Stewart, and D.D. Wilson, "High-Phase Order Transmission - A Feasibility Analysis, Part II - Overvoltages and Insultation Requirements", IEEE Transactions PA&S, Vol. PAS-97, pp. 2308-2316, Nov./Dec. 1978.

[4] J.R. Stewart, and I.S. Grant, "High-Phase Order-Ready for Application", IEEE Transactions PA&S, Vol. PAS-101, pp. 1757-1767, June 1982.

[5] S.S. Venkata, W.C. Guyker, J. Kondragunta, N.K. Saini, and E.K. Stanek, "138-KV, Six-Phase Transmission System: Fault Analysis", IEEE Transactions PA&S, Vol. PAS-101, pp. 1203-1218, May 1982.

[6] Y.M. Luke, "Multiconductor Analysis: Part II - An Investigation of Faults on EHV Transmission Lines", IEEE Transactions PA&S, Vol. PAS-91, pp. 1113-1119, May/June 1972.

[7] K.D. Tran, and J. Robert, "Digital Simulation and Analysis of Surges on Polyphase Transmission Lines with Earth Return", IEEE Transactions PA&S, Vol. PAS-99, pp. 445-451, Mar./Apr. 1972.

[8] N.B. Bhatt, S.S. Venkata, W.C. Guyker, and W.H. Booth, "Six-Phase (Multi-Phase) Power Transmission Systems: Fault Analysis", IEEE Transactions PA&S, Vol. PAS-96, pp. 758-767, May/June 1977.

[9] J.L. Willems, "The Analysis of Interconnected Three-Phase and Polyphase Power Systems", IEEE PES Summer Meeting, Vancouver, B.C., Paper A-79-504-2, July 1979.

[10] S.M. Peeran, M. Al-Nema, and H.I. Zynal,

"Six-Phase Transmission Systems: Generalized Alpha-Beta-Zero Components and Fault Analysis", IEEE PES Winter Meeting, New York, Paper A-80-116-4, Feb. 1980.

[11] I.S. Grant, J.R. Stewart, D.D. Wilson, and T.F. Garrity, "High-Phase Order Transmission Line Research", Paper No. 220-02, CIGRE Symposium on Transmission Lines and the Environment, Stockholm, Sweden, June 1981.

[12] S.N. Tiwari, and L.P. Singh, "Mathematical Modelling and Analysis of Multi-Phase Systems", IEEE Transactions PA&S, Vol. PAS-101, pp. 1784-1793, June 1982.

[13] S.S. Venkata, W.C. Guyker, W.H. Booth, J. Kondragunta, N.B. Bhatt, and N.K. Saini, "EPPC - A Computer Program for Six-Phase Transmission Line Design", IEEE Transactions PA&S, Vol. PAS-101, pp. 1859-1869, July 1982.

[14] Y. Onogi, K. Isaka, A. Chiba, and Y. Okumoto, "A Method of Suppressing Fault Currents and Improving the Ground Level Electric Field in a Novel Six-Phase Power Transmission System", IEEE Transactions PA&S, Vol. PAS-102, pp. 870-880, April 1983.

[15] E.W. Kimbark, "Chart of Three Quantities Associated With Single-Pole Switching", IEEE Transactions, PA&S, Vol. PAS-94, pp. 388-395, Mar./Apr. 1975.

[16] E.W. Kimbark, "Selective-Pole Switching of Long Double-Circuit EHV Line", IEEE Transactions PA&S, Vol. PAS-95, pp. 219-230, Jan./Feb. 1976.

[17] R.M. Hasibar, A.C. Legate, J. Brunke, and W.G. Peterson, "The Application of High-Speed Grounding Switches for Single-Pole Reclosing on 500 KV power Systems", IEEE Transactions PA&S, Vol. PAS-100, pp. 1512-1515, Apr. 1981.

[18] L. Edwards, J.W. Chadwick, H.A. Riesch, and L.E. Smith, "Single-Pole Switching on TVA's Paradise-Davidson 500 KV Line: Design Concepts and Staged Fault Test Results", IEEE Transactions PA&S, Vol. PAS-90, pp. 2436-2450, Nov./Dec. 1971.

[19] N. Knudson, "Single-Phase Switching of Transmis-

sion Lines Using Reactors for Extinction of the Secondary Arc", Paper No. 310, CIGRE, Paris, France, pp. 1-11, 1962.

[20] E.W. Kimbark, "Suppresion of Ground Fault Arcs on Single-Pole Switched EHV Lines by Shunt Reactors", IEEE Transactions PA&S, pp. 408-413, Mar. 1964.

[21] H.A. Peterson, and N.V. Dravid, "A Method for Reducing Dead Time for Single-Phase Reclosing in EHV Transmission", IEEE Transactions PA&S, Vol. PAS-88, pp. 286-292, Apr. 1969.

[22] B.R. Shperling, A. Fakheri, B.J. Ware, "Compensation Scheme for Single-Pole Switching on Untransposed Transmission Lines", IEEE Transactions, PA&S, Vol. PAS-97, pp. 1421-1429, July/Aug. 1978.

[23] J.R. Stewart, and D.D. Wilson, Discussion of Reference [5], also shown in Reference [5], pp. 1215.

[24] J.J. Trainor, J.E. Hobson, and H.N. Muller, "High-Speed Single-Pole Reclosing", IEE Transactions, Vol. 61, pp. 81-87, Feb. 1942.

[25] R.B. Shipley, H.J. Holley, and D.W. Coleman, "Digital Analysis of Single-Pole Switching on EHV Lines", IEEE Transactions PA&S, Vol. PAS-87, pp. 1679-1686, Aug. 1968.

[26] S.J. Balser, P.C. Krause, "Single-Pole Switching - A Study of System Transients with Transposed and Untransposed Lines", IEEE PES Winter Meeting, New York, N.Y., Jan. 27 - Feb. 1, 1974.

[27] S.R. Lambert, V. Koschik, C.E. Wood, G. Worner, and R.G. Rocamora, "Long Line Single-Phase Switching Transients and Their Effect on Station Equipment", IEEE Transactions PA&S, Vol. PAS-97, pp. 857-865, May/June 1978.

[28] B.R. Shperling, and A. Fakheri, "Single-Phase Switching Parameters for Untransposed EHV Transmission Lines", IEEE Transactions PA&S, Vol. PAS-98, pp. 643-654, Mar./Apr. 1979.

[29] J.G. Kappenman, V. Koschik, F. Plourde, F.E. Hammerquist, W.E. Reid, and R.G. Rocamora, "The Existence and Control of Secondary Arc Harmonics in Long Line, Single-Phase Reclosing Applications",

IEEE PES Winter Meeting, New York, N.Y., Feb. 3-8, 1980.

[30] B.R. Shperling, A.J. Fakheri, C.H. Shih, and B.J. Ware, "Analysis of Single-Phase Switching Field Tests on the AEP 765 KV System", IEEE Transactions PA&S, Vol. PAS-100, pp. 1729-1735, Apr. 1981.

[31] J.G. Kappenman, G.A. Sweezy, V. Koschik, and K.K. Mustaphi, "Staged Fault Tests With Single-Phase Reclosing on the Winnipeg-Twin Cities 500 KV Interconnection", IEEE Transactions PA&S, Vol. PAS-101, pp. 662-673, Mar. 1982.

[32] J. Slepian, "Extinction of a Long A.C. Arc", AIEE Transactios PA&S, pp. 421-430, Jan. 1930.

[33] J.D. Cobine, "Gaseous Conductors-Theory and Engineering Applications", First Ed., McGraw Hill Book Company, Inc., N.Y., 1941.

[34] F.W. Crawford, and H. Edels, "The Reignition Voltage Characteristics of Freely Recovering Arcs", IEE Transactions, pp. 202-212, Apr. 1960.

[35] W.D. Kelham, "The Recovery of Electric Strength of an Arc-Discharge Column Following Rapid Interruption of the Current", IEE Transactions, pp. 321-334, Feb. 1954.

[36] G.D. McCann, J.E. Conner, and H.M. Ellis, "Dielectric-Recovery Characteristics of Power Arcs in Large Air Gaps", AIEE Transactions, PA&S, Vol. 69, pp. 616-625, Dec. 1949.

[37] Committee Report "Electromagnetic Effects of Overhead Transmission Lines - Practical Problems, Safeguards, and Methods of Calculation", IEEE Transactions PA&S, Vol. PAS-93, pp. 892-904, May/June 1974.

[38] F.R. Bergseth, Discussion of Reference [5], pp. 1215.

[39] J.R. Carson, "Wave Propagation in Overhead Wires with Ground Return", Bell System Technical Journal 5: 539-54, 1926.

[40] B.P.A. "Electromagnetic Transient Program (EMTP): Rule Book", B.P.A., Portland, Oregon, Apr. 1982.

[41] P.M. Anderson, "Analysis of Faulted Power Sys-

tems", First Ed., Iowa State University Press, Ames, Iowa, 1978.

[42] W.D. Stevenson, "Elements of Power System Analysis", Fourth Ed., McGraw-Hill Book Company, N.Y., 1982.

APPENDICES

APPENDIX - A

SHUNT COMPENSATION SCHEME FOR SINGLE-POLE SWITCHING ON THREE-PHASE TRANSMISSION LINES

A method by which the secondary arc current and the recovery voltage of a balanced three-phase transmission system could be reduced was presented for the first time by Knudson [19] in 1962, and Kimbark [20] in 1964. The main idea of the method was to neutralize the capacitive coupling between the faulted line and the sound phases using a lumped shunt inductive reactance equal and opposite to the capacitive reactance. Thus, a parallel resonance between the distributed shunt capacitance of one or more lines and the lumped shunt inductance is created. This resonant circuit decreases the capacitively coupled current and voltage on the faulted conductor due to voltages on the healthy conductors. Theoretically, in a lossless, parallel capacitance-inductance circuit, the net current can be made zero by proper tuning. Actually, the current does not become zero because of imperfect tuning, losses, and harmonics. However, the neutralized current is only about 10% of the unneutralized, capacitively-fed fault current [20].

A.1 REQUIRED SUSCEPTANCES FOR SHUNT COMPENSATION OF SINGLE-CIRCUIT LINE

The following method was developed by Kimbark [16] to calculate the susceptances of the reactors used for compensating balanced, transposed, three-phase, single circuit transmission lines. The most general equivalent circuit for the capacitances between lines a, b, c, and ground has a branch joining each pair of conductors, fig(36a). Assuming balanced lines, the equivalent circuit in fig(36a) can be replaced by the four-branched star circuit of fig(36b). The shunt reactors of figs(37a), and (37b) are analogous to the equivalent capacitance circuits of figs(36a), and (36b), respectively. These are to be used for compensating the line capacitances. Because the reactors are in parallel with the line capacitances, it is more convenient to express their values in terms of susceptance B than reactance X. Unprimed letters B and X will be used to denote inductive susceptance and reactance, and the corresponding primed letters B' and X' stand for the respective capacitive quantities. The requirements are:

1 - For fault suppression by neutralization of the interphase capacitances,

$$B_1 - B_0 = B_1' - B_0' = w(c_1 - c_0) = 2\pi f(c_1 - c_0), \qquad (A.1)$$

where the subscripts 1 and 0 denote positive and

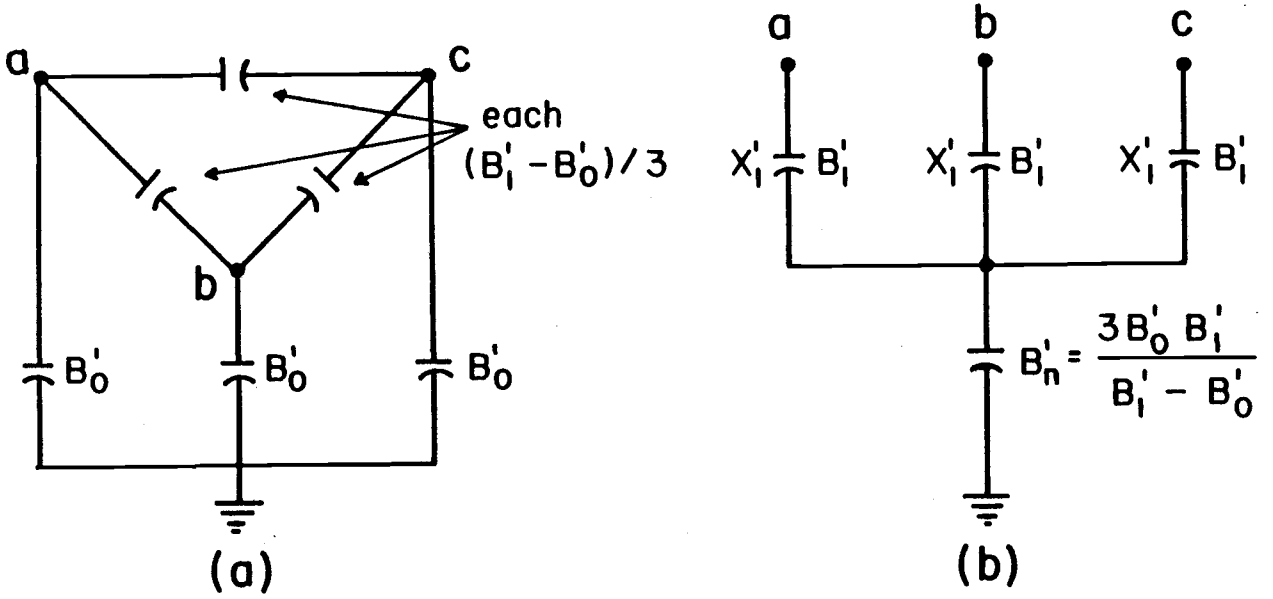

Fig(36) Equivalent circuits of the shunt capacitances of a three-phase transmission line.

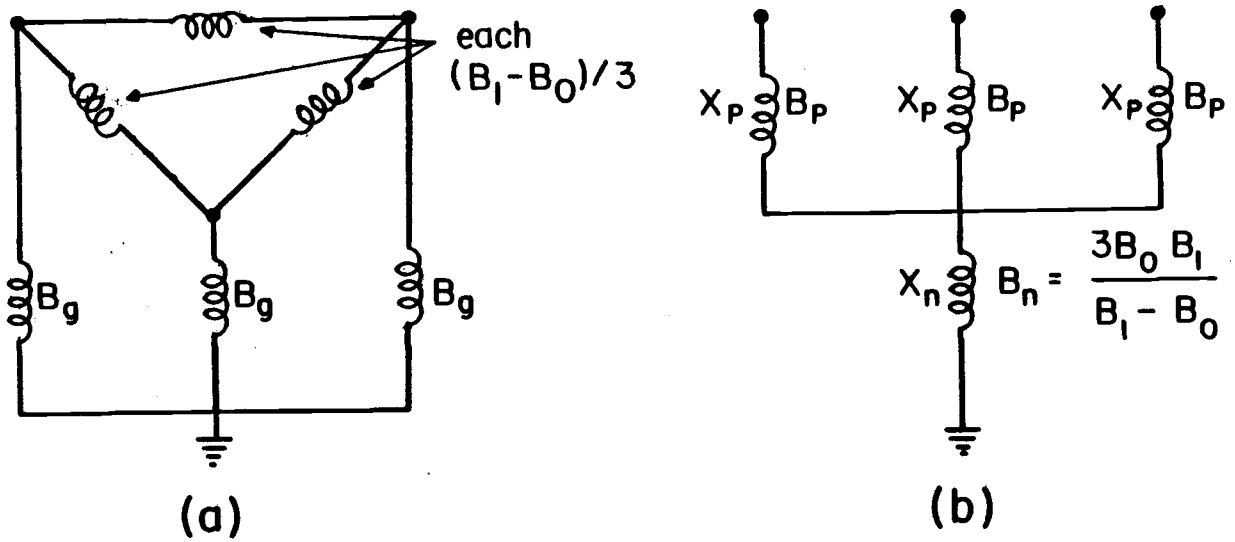

Fig(37) Possible connections of shunt reactors for fault suppression and compensation of charging current of a three-phase transmission line.

zero sequences, respectively.

2 - For shunt compensation of degree h,

$$B_1 = hB_1' = hwc_1 \tag{A.2}$$

From equations (A.1) and (A.2) it follows that

$$B_0 = B_0' - (1-h)B_1' \tag{A.3}$$

The required susceptances or reactances of the reators are found by using equations (A.1), (A.2), and (A.3) in conjunction with the appropriate pair of equations which follow. The susceptances of the reactors in fig(37b) in terms of zero and positive sequence susceptances are:

$$B_p = B_1 \tag{A.4}$$

$$B_n = \frac{3B_0 B_1}{B_1 - B_0} \tag{A.5}$$

and the corresponding reactances are:

$$X_p = X_1 \tag{A.6}$$

$$X_n = \frac{B_1 - B_0}{3B_0 B_1} \equiv \frac{X_0 - X_1}{3} \tag{A.7}$$

Equations (A.2) and (A.4) yield,

$$B_p = hB_1' = hwc_1 \tag{A.8}$$

While equations (A.2), (A.3), and (A.7) yield,

$$X_n = \frac{B_1' - B_0'}{3hB_1'(B_0' - (1-h)B_1')} \tag{A.9}$$

For 100% compensation h=1, and

$$B_p = B_1' \tag{A.10}$$

$$X_n = \frac{B_1' - B_0'}{3B_1' B_0'} = \frac{X_0' - X_1'}{3} = X_n' \tag{A.11}$$

Thus, the inductive susceptances can be expressed in terms of the equivalent lumped line capacitive susceptances for any degree of compensation; provided that the phase-to-phase capacitances are balanced. The phase--to-phase capacitances can be balanced either by transposition of the lines or by addition of lumped capacitors of proper values connected between the conductors.

A.2 REQUIRED SUSCEPTANCES FOR SHUNT COMPENSATION OF DOUBLE CIRCUIT LINE

The double circuit line has six phase-to-ground capcitances and fifteen interconductor capacitances which might all be different. Transposition could reduce the number of different values. However, a constraint is imposed on the transposition scheme of the double-circuit EHV line by the requirement that the six-conductors maintain the same relative positions [16].

Some of the symmetical polyphase circuits that might be used for the shunt inductive compensation of a double-circuit three-phase line are shown in fig(38). The most suitable circuit for compensating a double-cir-

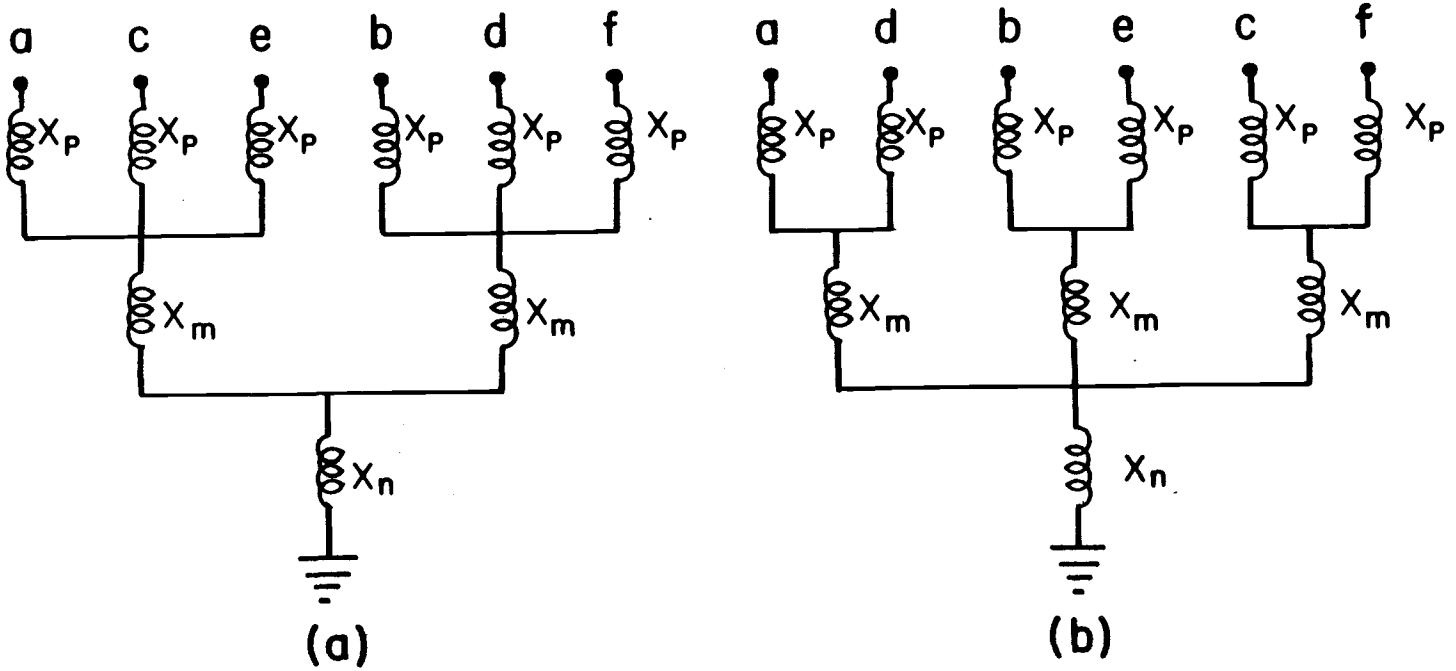

Fig(38) Six-terminal symmetrical polyphase circuits of tree form.

cuit line appears to be that shown in part b[16]. The balanced equivalent capacitance of a line in a double-circuit three-phase system is shown in fig(39). None of the compensating circuits have more than three different values of reactance, while there are four different values of capacitances to be compensated, fig(39). This suggests connecting lumped capacitors between like phases, which added to the distributed shunt capacitances between like phases, raise them to equality with the capacitances between unlike phases.

A method for computing the reactances of the compensating circuit of fig(38b) was developed by Kimbark [16]. In the derivation, it was found simpler to use symmetrical component analysis. The symmetrical components for a three-phase double-circuit line are defined as in fig(40). The symmetrical components of the shunt capacitive susceptances of the line are found by assuming a set of voltages of one sequence applied from conductor to ground, taking each sequence in turn. The currents in each branch of the mesh circuit from a particular terminal, say, phase a, fig(39), and their sum are written. For instance, for zero sequency, there are equal voltages V_0 from every phase to ground. Hence, there is no current in any branch except that from a to ground. Consequently,

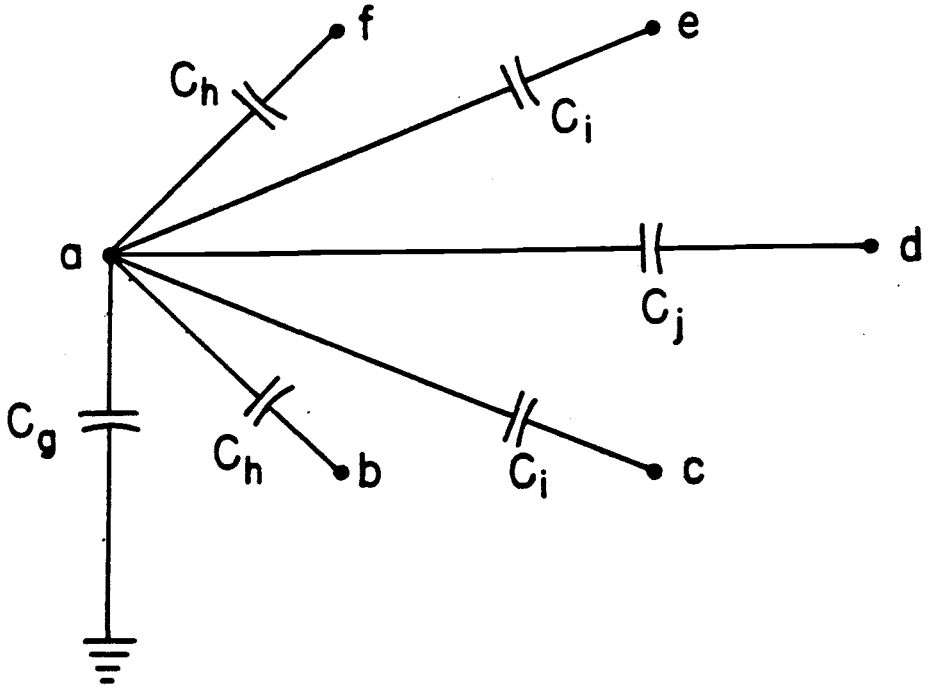

Fig(39) A six-phase transmission line capacitances connected to conductor a.

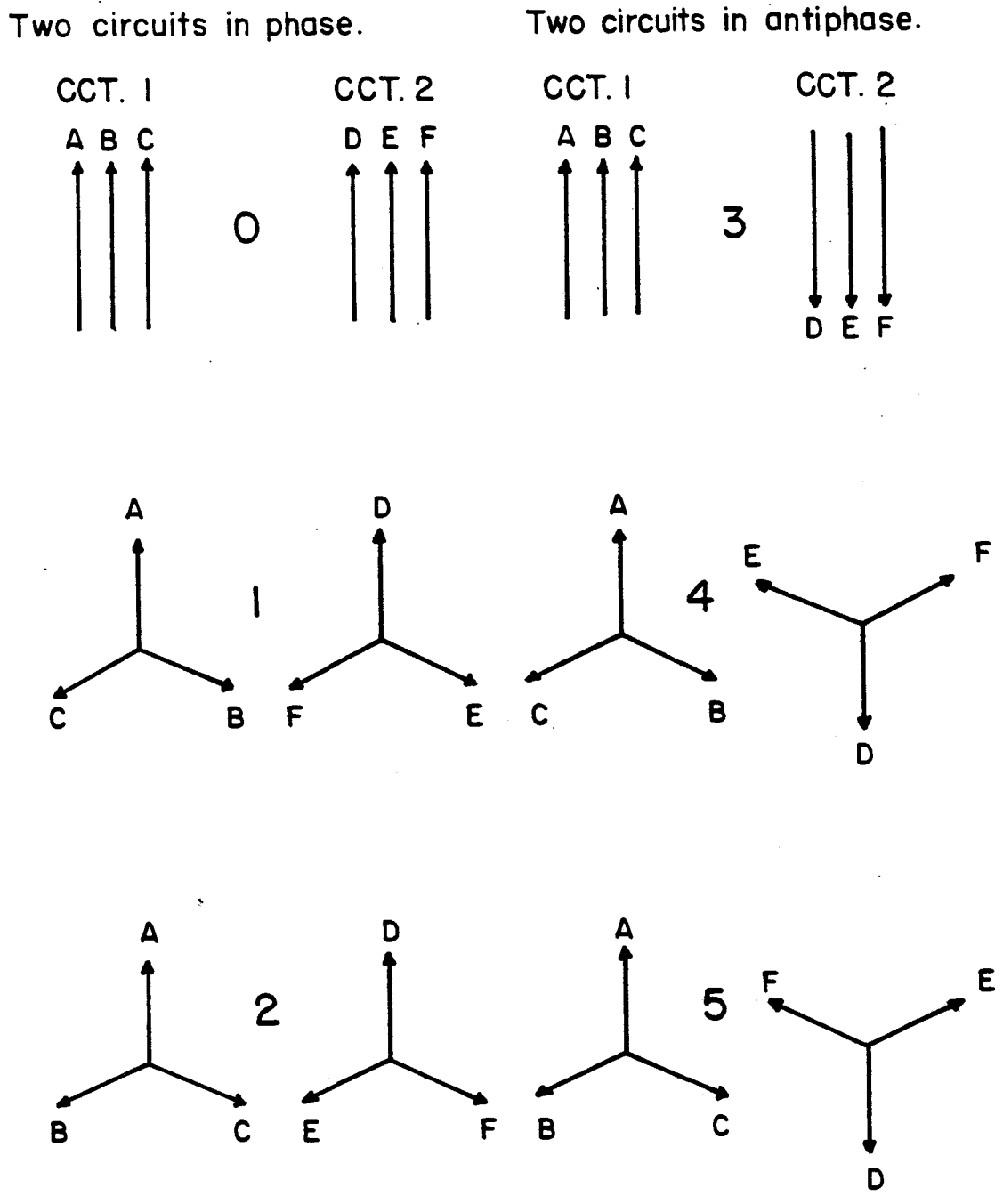

Fig(40) Phasor digrams for each of the six sequences of voltage or current in a double circuit three-phase lines.

$$B_{c_0} = B_{cg} \tag{A.12}$$

For positive-sequence the expression is:

$$B_{c_1} = B_{cg} + 3(B_{ch}+B_{ci}) \tag{A.13}$$

The third sequence is:

$$B_{c_3} = B_{cg} + 4B_{ci} + 2B_{cj} \tag{A.14}$$

For symmetrical circuits, sequences 1,2,4, and 5 have identical admittances or impedances. When lumped capacitors are connected in parallel with the capacitors between like phases so as to make $C_j = C_i$ then equation (A.14) becomes:

$$B_{c_3} = B_{cg} + 6B_{ci} \tag{A.15}$$

The inverse equations are:

$$B_{cg} = B_{c_0} \tag{A.16}$$

$$B_{ch} = (B_{c_3} - B_{c_0})/6 \tag{A.17}$$

$$B_{ci} = (2B_{c_1} - B_{c_0} - B_{c_3})/6 \tag{A.18}$$

The symmetrical components of the inductive reactances of the shunt tree circuit of fig(37b) can be found by a dual procedure of the procedure for finding the symmetrical components of the shunt capacitive susceptances. That is, a set of currents of a singel sequence is impressed on each terminal instead of a voltage, the resulting branch currents and voltage drops are found and the drops are summed from phase-to-ground. The results are:

$$X_{L1} = X_p \tag{A.19}$$

$$X_{L3} = X_p + 3X_m \tag{A.20}$$

$$X_{L0} = X_p + 3X_m + 6X_n \tag{A.21}$$

The inverse equations are:

$$X_p = X_{L1} \tag{A.22}$$

$$X_m = (X_{L3} - X_{L1})/3 \tag{A.23}$$

$$X_n = (X_{L0} - X_{L3})/6 \tag{A.24}$$

The required conditions of shunt compensation are:

1 - For the desired degree h_1 of positive shunt compensation:

$$B_{L1} = -h_1 B_{c1}, \tag{A.25}$$

where B_L represents inductive susceptance, and B_c represents capacitive susceptance.

2 - For obtaining complete compensation of the inter-phase capacitive susceptances of each circuit:

$$B_{Lh} = -B_{ch}, \tag{A.26}$$

and for the intercircuit susceptances:

$$B_{Li} = -B_{ci} \tag{A.27}$$

Where B_{Lh} and B_{Li} are the inductive susceptances of a mesh circuit equivalent to the desired tree circuit. Equations (A.26) and (A.27) can be expressed in terms of symmetrical components. By analogy with equations (A.17) and (A.18):

$$B_{Lh} = (B_{L3} - B_{L0})/6 \tag{A.28}$$

$$B_{Li} = (2B_{L1} - B_{L0} - B_{L3})/6 \tag{A.29}$$

substituting equations (A.17), (A.18), (A.25), (A.28), and (A.29) into equations (A.26) and (A.27) yield after clearing fractions:

$$B_{L3} - B_{L0} = -(B_{c_3} - B_{c_0}) \tag{A.30}$$

$$2h_1 B_{c_1} + B_{L3} + B_{L0} = 2B_{c_1} - B_{c_3} - B_{c_0} \tag{A.31}$$

Solving equations (A.30) and (A.31) for B_{L0} and B_{L3} yields:

$$B_{L0} = B_{c_1}(1-h_1) - B_{c_0} \tag{A.32}$$

$$B_{L3} = B_{c_1}(1-h_1) - B_{c_3} \tag{A.33}$$

While B_{L1} is given by equation (A.25).

By taking the reciprocal of equations (A.25), (A.32), and (A.33) and substituting into equations (A.22), (A.23), and (A.24) the reactances of the tree circuit can be obtained. It should be noted that these reactances depend upon the degree h_1 of positive-sequence shunt compensation. It should, also, be emphasized that this method works only for balanced, fully transposed systems. The main disadvantage of this method is the need to add lumped capacitors between the two circuits which can be bulky and expensive.

APPENDIX - B

CAPACITANCE CALCULATION METHOD

The transmission line capacitances are calculated by first constructing the potential coefficient matrix:

$$P = VQ^{-1} \quad \text{unit length/Farad} , \tag{B.1}$$

where V is the line voltage vector, and Q is the charge vector [41]. The elements of Q are the charges on the conductors per unit length. The ground effect is taken into account using the method of images. The coefficients of P are defined as:

$$P_{ij} = \frac{1}{2\pi\epsilon} \ln \frac{H_i}{r_i} \qquad i = j$$

$$= \frac{1}{2\pi\epsilon} \ln \frac{H_{ij}}{D_{ij}} \qquad i \neq j \tag{B.2}$$

where: r_i = the radius of conductor i

D_{ij} = Distance between conductors i and j

H_i = distance between conductor i and its image below ground

H_{ij} = distance between conductor i and the image of conductor j below ground.

P_{ij} = potential in volts assumed by conductor i due to linear charge on conductor j alone (of 1 coulomb/unit length) with all other charges zero.

Thus, each column of P is independent of all others depending only upon the geometry of the system. It is obvious from equation (B.2) that the matrix P is symmetric and all its coefficients are positive quantities since H_{ij} is greater than D_{ij}. Hence, P is nonsingular and has an inverse P^{-1}. Thus, from equation (B.1) one may compute

$$Q = CV \tag{B.3}$$

where

$$C = P^{-1} \tag{B.4}$$

where the elements of the matrix C are called the "capacitance coefficients" when referring to diagonal terms and "coefficients of electrostatic induction" when referring to off-diagonal terms. These coefficients are defined as [42]:

C_{ij} = the charge on conductor i (coulomb/unit length) due to the potential (one volt) on conductor j when all other conductors are short circuited.

All the off diagonal terms of C are positive quantities but have negative signs. This is due to the fact that the coefficients of P are all positive. Practically, this means applying a positive potential to one conductor induces a negative charge on the other conductors. The diagonal terms however, are all positive. The matrix C is also symmetric.

The EMTP Line Constants subroutine utilizes this method to calculate the line capacitance matrix. Its output is matrix C shown by equation (B.4).